**Data-driven design of fault diagnosis systems**

Von der Fakultät für Ingenieurwissenschaften der
Abteilung Elektrotechnik und Informationstechnik
der Universität Duisburg-Essen

zur Erlangung des akademischen Grades

**Doktor der Ingenieurwissenschaften**

genehmigte Dissertation

von

**Shen Yin**

aus

Harbin, V.R. China

1. Gutachter: Prof. -Ing. Steven X. Ding
2. Gutachter: Prof. Zidong Wang, Ph.D.
Tag der mündlichen Prüfung: 07. February 2012

# Acknowledgement

This work was done while the author was with the Institute for Automatic Control and Complex Systems (AKS) in the Faculty of Engineering at the University of Duisburg-Essen, Germany. I would like to give the most sincere thanks to Prof. Dr.-Ing. Steven X. Ding, my respectful mentor, who opened me the door to the scientific world. I am grateful forever for his influence on my research work and his great help in preparation of this work. My sincere appreciation must also go to Prof. Dr. Zidong Wang, Chair of Dynamical Systems and Computing from Brunel University, for his insightful discussion and constructive comments on the manuscript of this work.

Many thanks should go to wonderful colleagues from the institute who always offered great help during the days in Duisburg. Special thanks to Dr.-Ing. Ping Zhang, Dr.-Ing. Birgit Köppen-Seliger, Dr.-Ing. Bo Shen, Dipl.-Ing. Jonas Esch and Dipl.-Ing. Eberhard Goldschmidt for their valuable discussion and helpful subsections. I have extensively worked with Dr.-Ing. Amol Naik, M.Sc. Adel Haghani and M.Sc. Haiyang Hao. I wish them all the very best for their studies. My acknowledgement will be incomplete without thanking Mrs. Sabine Bay for her help in organizational responsibilities. I extend my gratitude towards Dipl.-Ing. Georg Nau, Dr.-Ing. Anderas de Moll, M.Sc. Jedsada Saijai, M.Sc. Waseem Damlakhi, M.Sc. Ali Abdo, M.Sc. Abdul Qayyum Khan, M.Sc. Shane Dominic, M.Sc. Wei Chen, M.Sc. Yulei Wang and M.Sc. Hao Luo for their timely suggestions, help and assistance.

Finally, I would like to dedicate this work to my parents for understanding and supporting me in whatever I decide to do - especially my wife, Cheng Yao, for her patience and love. Their unconditional support and unexplainable faith were the only reason for the completion of this work.

To my love *Cheng Yao*

# Contents

# Notation and symbols

### Abbreviations

| | |
|---|---|
| FD | Fault detection |
| FDI | Fault detection and isolation |
| FDIA | Fault detection, isolation, and analysis |
| LTI | Linear time invariant |
| FDF | Fault detection filter |
| DO | Diagnostic observer |
| MSPM | Multivariate statistical process monitoring |
| SIM | Subspace identification method |
| PCA | Principal component analysis |
| PCs | Principal components |
| PLS | Partial least squares |
| LVs | Latent variables |
| FDA | Fisher discriminant analysis |
| ICA | Independent component analysis |
| ICs | Independent components |
| SVD | Singular value decomposition |
| GLR | Generalized likelihood ratio |
| TPLS | Total projection to latent structure |
| DPM | Data projection method |
| FOP | First-order perturbation theory |
| TE | Tennessee Eastman |
| FBFP | Fed-batch fermentation penicillin |
| CSTH | Continuous stirred tank heater |

### Mathematical symbols

| | |
|---|---|
| $\| \ \|$ | 2-norm |
| $\hat{a}$ | Estimate of a |

| | |
|---|---|
| $\tilde{a}$ | Estimate error of a |
| $A^T$ | Transpose of A |
| $A^\perp$ | Orthogonal complement of A |
| $A^\dagger$ | Pseudo inverse of A |
| $\in$ | belongs to |
| $\mathcal{R}$ | Set of real numbers |
| $\mathcal{R}^m$ | Set of $m$-dimensional real vectors |
| $\mathcal{R}^{l\times m}$ | Set of $l \times m$ dimensional real matrices |
| $I_{m\times m}$ | $m \times m$ identity matrix |

**Control theoretical symbols**

| | |
|---|---|
| $n$ | System order |
| $k$ | Discrete time sample |
| $A$ | System matrix |
| $B$ | Input matrix |
| $C$ | Output matrix |
| $D$ | Feed-though matrix |
| $E_d$ | Disturbance matrix |
| $F_d$ | Disturbance feed-through matrix |
| $E_f$ | Process fault distribution matrix |
| $F_f$ | Sensor fault distribution matrix |
| $l$ | Number of inputs |
| $m$ | Number of outputs |
| $u$ | Input signal vector |
| $y$ | Output signal vector |
| $x$ | State variable vector |
| $w$ | Process noise vector |
| $v$ | Sensor noise vector |
| $d$ | Unknown disturbance vector |
| $f$ | Fault signal vector |
| $r$ | Residual signal vector |
| $\Gamma_s$ | Extended observability matrix |
| $\Gamma_s^\perp$ | Left null complement |
| $H_{u,s}$ | Input distribution matrix |
| $Y_f$ | Future output Hankel matrix |
| $U_f$ | Future input Hankel matrix |

| | |
|---|---|
| $Y_p$ | Past output Hankel matrix |
| $U_p$ | Past input Hankel matrix |
| $N$ | Length of sample size |
| $s$ | Order of parity vector |
| $\upsilon_s$ | Parity vector corresponding to output |
| $\beta_s$ | Parity vector corresponding to input |
| $L_z$ | Observer gain matrix |
| $Z$ | Process variable matrix |
| $U$ | Input matrix |
| $Y$ | Output matrix |
| $\beta$ | Number of principal components |
| $\gamma$ | Number of latent variables |
| $J_{th}$ | Threshold value for fault detection |

**Statistical symbols**

| | |
|---|---|
| $\Phi$ | Sample covariance matrix |
| $\chi^2$ | Chi-square distribution |
| $F$ | F distribution |
| $\mathcal{U}$ | Uniform distribution |
| $\mathcal{N}$ | Gaussian distribution |
| $\mathcal{E}$ | Mathematical Expectation |
| $\alpha$ | Confidence level |
| $T^2$ | T-square statistic |
| SPE | Squared prediction error |

# Abstract

Due to the increasing demands on system performance, production quality as well as economic operation, modern technical systems become more complicated and the automation degrees are significantly growing. To ensure the safety and reliability of such complicated processes, an effective fault diagnosis system is of prime importance in process industry nowadays. Although the model-based fault diagnosis theory has been well established, it is still difficult to establish mathematical model by means of the first principles for large-scale process.

On the other hand, a large amount of historical data from regular sensor measurements, event-logs and records are often available in such industrial processes. Motivated by this observation, it is of great interest to design fault diagnosis schemes only based on the available process data. Hence, development of efficient data-driven fault diagnosis schemes for different operating conditions is the primary objective of this thesis.

This thesis is firstly dedicated to the modifications on the standard multivariate statistical process monitoring approaches. The modified approaches are considerably simple, and most importantly, avoid the drawbacks of the standard techniques. As a result, the proposed approaches are able to provide enhanced fault diagnosis performance on the applications under stationary operating conditions.

The further study of this thesis focuses on developing reliable fault diagnosis schemes for dynamic processes under industrial operating conditions. Instead of identifying the entire process model, primary fault diagnosis can be efficiently realized by the identification of key components. Advanced design schemes like multiple residuals generator and state observer are also investigated to ensure high fault sensitivity performance.

For the large-scale processes involving changes, e.g. in operating regimes or in the manipulated variables, the recursive and adaptive techniques are studied to cope with such uncertainty issues. A novel data-driven adaptive scheme is proposed, whose stability and convergence rate are analytically proven. Compared to the standard techniques, this approach does not involve complicated on-line computation and produces consistent estimate of the unknown parameters.

To illustrate the effectiveness of the derived data-driven approaches, three industrial benchmark processes, i.e. the Tennessee Eastman chemical plant, the fed-batch fermen-

tation penicillin process and the continuously stirred tank heater, are finally considered in this thesis.

# 1 Introduction

Due to the increasing demands on system performance, production quality as well as economic operation, modern technical processes become more complicated and the automation degrees of such systems are significantly growing. The safety and reliability issues on the complicated processes receive more attention and become the most critical factors in process design nowadays. On the other hand, the complete reliance on human operators to deal with abnormal events has become increasingly difficult as shown by the following facts:

- It is claimed that about 70% of the industrial accidents are caused by human errors [106].
- Only the petrochemical industry in the US incurs approximately 20 billion dollars in annual losses due to process abnormalities [85]. Similar accidents cost the British 27 billion dollars in economic loss every year [68].
- The consequences of the accidents are not only performance degradation, economic loss but also more serious catastrophes such as the *Three Mile Island* and *Chernobyl* in nuclear industry.

Based on these observations, the integration of an automated fault diagnosis scheme is essential to ensure a reliable abnormal event management, which not only informs about process abnormalities in time but also makes further suitable actions to remove the undesirable influence from the process. Depending on the different operational constraints and requirements of the underlying applications, design of superior and robust fault diagnosis scheme has been an active research field in the control community during the past several decades. This chapter attempts to summarize some of the major developments in this field. The motivations and objectives of the thesis are also presented.

## 1.1 Basic concepts on fault diagnosis

**Faults** in process equipments, instructions or within the process can lead to an unpermitted deviation from the normal behavior of the plant and thus degrade overall system

performance. For instance, in an industrial chemical process, the faults are likely to occur in **sensors** (e.g. analyzer contamination, biased measurements), **actuators** (e.g., valves, pumps and pipes) and **process** itself (e.g. catalyst poisoning, heat exchanger fouling). A single fault can harm not only the functional components, but also the whole plant through the coupled control loops and feedback systems. To deal with such problems, a fault diagnosis system is desired to monitor the operating condition of the whole plant and achieve prompt detection and diagnosis of process malfunctions automatically. As pointed out in [21], the overall concept of fault diagnosis consists of the following three essential tasks:

**Fault detection:** detection of the occurrence of faults in the functional units of the process, which lead to the undesired or intolerable behavior of the whole system

**Fault isolation:** localization (classification) of different faults

**Fault analysis or identification:** determination of the type, magnitude and cause of the fault.

According to different performance requirements, a fault diagnosis system is called fault detection (FD) system, fault detection and isolation (FDI) system or fault detection, isolation, and analysis (FDIA) system.

In technical terms, the so-called **redundancy** plays a central role for a successful fault diagnosis [21]. The so-called **hardware redundancy** is one of the traditional ways to create system redundancy, in which the crucial components are reconstructed using the identical hardware. A fault can be directly detected and localized by the deviation between the output of actual hardware component and the one of its redundancy. Although an extremely reliable fault detection and isolation can be achieved, the application of hardware redundancy is only restricted to the case of a number of key components due to their higher cost involved in reconstruction. Associated with the concept of hardware redundancy, the so-called **software redundancy** or **analytical redundancy** is more efficient, whose basic idea is to replace the expensive hardware components by a model implemented in the software form in order to reconstruct the process behavior on-line. The fault detection is achieved by checking the so-called **residual**, which represents the difference between the measured process variables, e.g. output signals $y$, and their software redundancy $\hat{y}$, i.e.

$$\text{residual} = y - \hat{y}.$$

The basic model-based fault diagnosis scheme including **residual generation** and **residual evaluation** is represented by Fig. 1.1. In general, the model can be **quantita-**

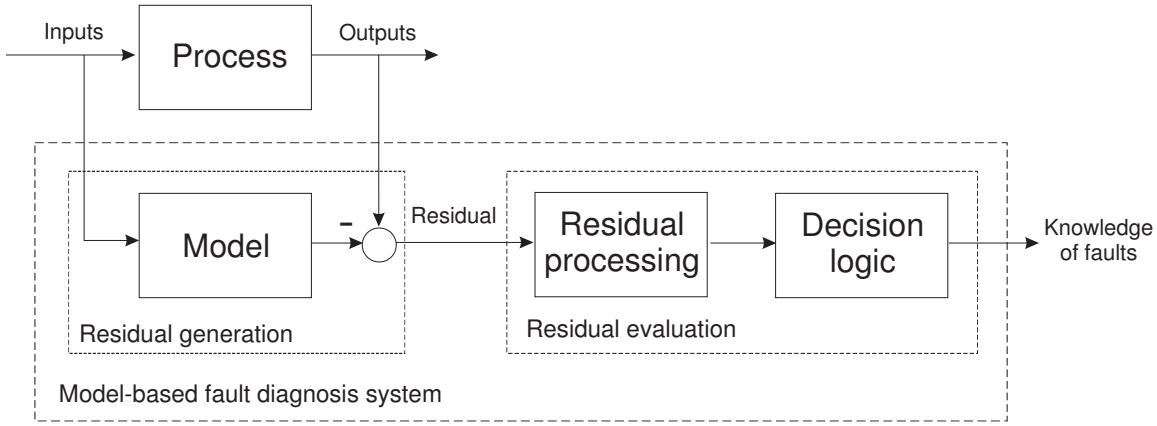


**Figure 1.1:** Basic model-based fault diagnosis scheme

**tive** (based on the first principles), **qualitative** (based on the if-then-else rules, decision trees etc.) or **process history data based** [106], [107], [108]:

**Quantitative model-based approach:** Most of the works on quantitative model-based approach are based on general input-output or state space model, which is usually developed based on the physics and mathematics knowledge of the process. From the 70s, observers and Kalman filtering theories have been widely used for residual generation in dynamic systems [2], [38], [39] [118]. The so-called parity relation has been firstly introduced in [117], whose basic idea is to check the parity relation of the model with available process input and output measurements. Further developments of this approach can be found in [17], [42], [43]. In addition, the so-called parameter estimation approach has been proposed to detect the unmeasurable parameter drift [52].

Based on these approaches, a large number of advanced fault diagnosis methods were developed to handle the issues of disturbances, model uncertainties, robust, optimization designs, etc. Nowadays, the quantitative model-based fault diagnosis techniques have been established into a well-founded theoretical framework and successfully demonstrated by a great number of applications in industrial processes and automatic control systems, see [8], [11], [21], [40], [53], [88], [98]. Reviews and analysis of current development of the quantitative model-based fault diagnosis techniques can be found in [27], [50], [106], [112], [115], [131].

**Qualitative model-based approach:** Unlike quantitative model, in which the relationships between inputs and outputs of the process are described in terms of mathematical functions, the relationships in qualitative model are expressed by qualitative functions centered around different units of the process. Based on such a qualitative

model, any fault diagnostic strategy requires a knowledge base, which contains a large set of if-then-else rules that mimics the cognitive behavior of a human expert. In addition, an efficient search mechanism shall also be included to make final decision from given facts. The qualitative models are suitable to be utilized on large-scale processes which are difficult to be modeled based on the first principals. On the other hand, since the knowledge base does not have a fundamental understanding of the physics of underlying process, it is difficult to update or accommodate in case that new conditions are encountered. More detailed discussion on qualitative approach can be found in [107] and the references therein.

**Data-driven approach:** In contrast to model-based approach, which requires reliable *a priori* quantitative or qualitative knowledge about the process, the data-driven approach makes use of this information from the huge amount of process history data [108]. Since most of the data-driven approaches assume that the process data have certain probability density functions, they are sometimes also called statistical process monitoring methods. The univariate control chart may be the earliest statistical approach based on *a priori* knowledge of process measurement distributions [97] and has been widely used for quality control in earlier industrial applications.

In modern large-scale industrial applications, many important final product quality variables are measured off-line and thus are only available on an hourly or daily basis. To effectively monitor process operating performance, all the information contained in the large number of process measurements shall be utilized. The so-called multivariate control charts based on multivariate statistical process monitoring methods like principal component analysis [34], [37], [63], [90], [130] and partial least squares [49], [79] have been proposed to treat these situations. The major advantage of the multivariate statistical methods lies in their ability to handle large numbers of highly correlated variables. Most importantly, instead of checking the information contained in all the measured variables simultaneously, process monitoring can be achieved by using several two- or three-dimensional control charts that retain all the variability information within the process data.

Parallel to statistical process monitoring methods, Basseville and Nikiforov [4] summarized a series of change detection algorithms depending on the available probability density function. In addition, a neural network is also a form of parametric data-driven approach which is widely used in practice [56], [62], [113], [114].

Notice that it is difficult to establish quantitative model for large-scale process industry by means of the first principles. On the other hand, the modern process is typical

dynamic process with different operating regimes, which can not be directly treated by the basic statistical approaches. Therefore, the extension and combination of the advantages of model-based and data-driven techniques have nowadays gained more attention to accommodate large-scale and complex process. A straightforward way to achieve this purpose is to utilize the process history data for model identification and based on it, the well-established model-based techniques can be used to design efficient fault diagnosis system.

## 1.2 Motivation and objective

As discussed in the last section, an efficient way to design a fault diagnosis system for complex industrial process begins with the large amount of process data. Moreover, it is necessary to consider following important issues in the practical situations:

- The basic statistical data-driven approaches have the simplest forms and less restrictive requirements on the design and engineering efforts. However, due to some limitations of these approaches, the necessary modifications are essential to achieve better performance on the applications under stationary operating conditions.
- In case that the basic conditions can not be satisfactorily met in the industrial environment, some of these methods may suffer a considerable loss in fault diagnosis performance. The novel method, which combines the advantages of aforementioned fault diagnosis approaches, shall be developed under industrial operating conditions.
- Due to the limited computation power and memory storage in real-time compute systems, the fault diagnosis system must be efficiently designed with minimal computation and storage requirements. In addition, the design procedure shall be simplified so that no special knowledge about the process and control theory is needed for the application engineers.

A reasonable assumption for industrial process monitoring is that the knowledge about the quantitative or qualitative model of the process under consideration is unknown *a priori*. Based on the available process data, the main objective of this thesis is to design efficient fault diagnosis schemes according to operating conditions of the underlying process. More specifically, the goals of this thesis are stated as follows:

- Only based on the available process data, develop efficient data-driven approaches for monitoring the process under stationary operating conditions. The proposed approaches shall be simple, and most importantly, avoid the drawbacks of the standard techniques.

- On the applications under industrial operating conditions, develop reliable fault diagnosis scheme for dynamic processes. Instead of identifying the entire process model, primary fault diagnosis shall be realized with the identification of key components. It is also desirable to investigate the advanced design schemes in order to ensure high fault sensitivity performance.

- In practice, since the process parameters are likely to vary around their nominal values, the fault diagnosis system must have scope for possible adaptation. The adaptive design scheme shall consider on-line storage and computation constraints, and most importantly, possess desired performance on stability and convergence rate.

- The developed data-driven fault diagnosis approaches must be demonstrated on industrial benchmark plants, which should be good approximations of complex industrial processes under different operating conditions.

The data sets used for fault diagnosis system design can be obtained from either available process logs or experimental tests. In case that a process simulator is available, the data generated from such simulations are also useful. In this thesis, three well-known industrial benchmark processes are utilized to evaluate the effectiveness of the proposed approaches for fault diagnosis purpose.

## 1.3 Outline of the thesis

This thesis is organized as follows. Chapter 2 includes preliminaries of fault diagnosis techniques with technical systems notations, which serve as fundamental basis in forthcoming chapters. The basic model-based approaches like parity space and diagnostic observer are firstly introduced in this chapter. The subspace identification method is also discussed therein. The most popular multivariate statistical process monitoring approaches like principal component analysis and partial least squares, are finally reviewed. Based on it, the modifications of these basic statistical approaches are introduced in Chapter 3 and 4.

In Chapter 3, the modifications on principal component analysis based fault diagnosis technique are discussed. A new test statistic is firstly proposed, which delivers an optimal fault detection performance and is considerably less complicated than the standard one. The further study is dedicated to the analysis of fault sensitivity. The fault identification issue is finally discussed in the proposed framework.

Chapter 4 begins with the partial least squares based fault diagnosis technique. A new approach is proposed to overcome the drawbacks of the standard approach. The associated

computation cost for the proposed approach is considerably lower, and most importantly, the novel approach provides a clear interpretation of the correlation model. Based on this approach, a fault detection scheme is then developed, in which only two test statistics are used for monitoring input measurement space that offers further efficiency compared to the existing methods. An algorithm for fault identification is finally presented in this chapter.

In Chapter 5, a subspace aided data-driven approach is presented to achieve fault detection in dynamic processes under industrial operating conditions. The study is dedicated to extending the single residual generation scheme to multiple case in order to ensure the high sensitivity to the faults. The proposed multiple diagnostic observers can also be utilized to construct state observer for the process monitoring and control purposes.

Chapter 6 mainly discusses the uncertainty issue in industrial applications. Two recursive algorithms for subspace tracking are firstly proposed. Both algorithms avoid repeated calculations of standard singular value decomposition and provide approximate result in an efficient way. The further study is dedicated to developing a data-driven adaptive diagnostic observer based residual generation scheme, whose stability and convergence rate can be analytically proven.

Chapter 7 illustrates the applications of the algorithms developed in Chapters 3-6. For this task, three well-known industrial benchmark processes, i.e. Tennessee Eastman process, fed batch fermentation penicillin process and continuously stirred tank heater, are considered to simulate their behaviors under different operating conditions. The experiments are carried out under scenarios involving different types of faults existing in the industrial processes. For simplicity in reading, the organization of chapters is also shown in Fig. 1.2 on the following page. This thesis ends with the conclusions and the discussion on future work.

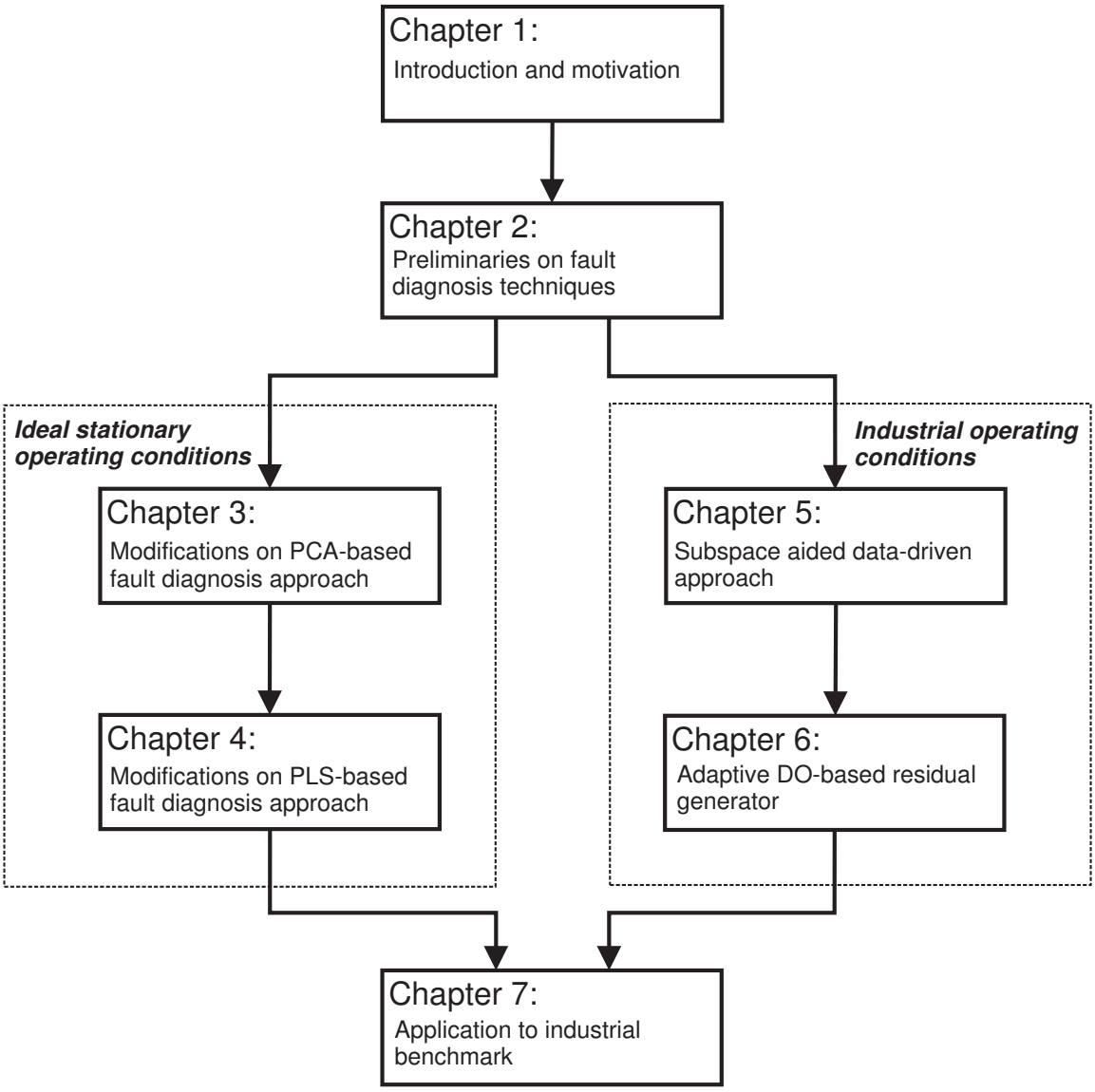


**Figure 1.2:** Organization of chapters

# 2 Fault diagnosis techniques

As discussed in Chapter 1, the basic idea of fault diagnosis is to generate the output redundancy through a "model" which is able to offer precise behavior of process under consideration. Any significant deviation between the actual measurement and the redundancy generated by process model should sufficiently indicate the existence of abnormal situation. Due to the high cost to achieve hardware redundancy, the most efficient way for a successful fault diagnosis is to create the redundancy analytically.

During the last two decades, the model-based fault diagnosis schemes are intensively studied. Since the majority of these approaches involve rigorous development of process models based on the first principles, later identification technique that extracts transfer function [77] or state space model becomes a necessary step prior to the design. For this purpose, subspace identification methods that identify the complete state space matrices have been successfully implemented [36], [91], [105].

Parallel to the aforementioned techniques, the data-driven approaches, which extract necessary information through large amount of process data, are currently receiving considerably increasing attention both in application and in research domains. Thanks to their simple forms and less requirements on the design and engineering efforts, the data-driven methods become more popular in many industry sectors, especially for large-scale industrial applications [96].

The objective of this chapter is to summarize the preliminaries of the fault diagnosis techniques, which serve as the fundamentals of this thesis.

## 2.1 Description of technical systems

According to the process dynamics and modeling aims, technical processes can be described by different system model types, among which the linear time invariant (LTI) system is the mostly used one and assumed as a good starting point for modeling and design phase. The standard form of the state space representation of a discrete time LTI

system is given by

$$x(k+1) = Ax(k) + Bu(k),\ x(0) = x_0, \tag{2.1}$$
$$y(k) = Cx(k) + Du(k) \tag{2.2}$$

where $x \in \mathcal{R}^n$ is the state vector, $x_0$ is the initial condition of the system, $u \in \mathcal{R}^l$ is the input vector and $y \in \mathcal{R}^m$ is the output vector. System matrices $A, B, C$ and $D$ are real constant matrices with appropriate dimensions. Considering that the subsequent study mainly focuses on data-driven design of fault diagnosis systems based on sampled process measurements, the state space model is defined only in the discrete time LTI framework.

In order to describe the deterministic disturbances, an additional input vector $d \in \mathcal{R}^{k_d}$ is integrated into Eqs.(2.1)-(2.2) as follows:

$$x(k+1) = Ax(k) + Bu(k) + E_d d(k), \tag{2.3}$$
$$y(k) = Cx(k) + Du(k) + F_d d(k) \tag{2.4}$$

where $E_d$ and $F_d$ are disturbance distribution matrices of compatible dimensions. If the process is corrupted by stochastic noises, e.g. process and measurement noises, the state space representation becomes

$$x(k+1) = Ax(k) + Bu(k) + w(k), \tag{2.5}$$
$$y(k) = Cx(k) + Du(k) + v(k) \tag{2.6}$$

where the stochastic disturbance signals $w \in \mathcal{R}^n, v \in \mathcal{R}^m$ are often white noise sequences with known mean and covariance matrix.

In order to model the faults in technical systems, the system model in Eqs.(2.1)-(2.2) can be extended to incorporate them as:

$$x(k+1) = Ax(k) + Bu(k) + E_f f(k), \tag{2.7}$$
$$y(k) = Cx(k) + Du(k) + F_f f(k) \tag{2.8}$$

where $f \in \mathcal{R}^{k_f}$ is the fault vector to be detected and $E_f, F_f$ are fault distribution matrices of appropriate dimensions. Generally, the system faults can be divided into three categories according to their locations, i.e. sensor fault, actuator fault and process fault, which can be modeled by choosing proper values of $E_f$ and $F_f$. Depending on the way how they affect the system dynamics, the faults are either additive or multiplicative changes in the parameters. In case of multiplicative fault, $f(k)$ is a function of the state and input variables of the system and may affect the system stability.

## 2.2 Model-based fault diagnosis techniques

Model-based techniques have been remarkably developed since 80's and their efficiency for detecting faults has been demonstrated by a great number of applications in industrial processes and automatic control systems. Among the existing model-based fault diagnosis schemes, the so-called observer-based and parity relation based methods, which are developed in the framework of well-established modern control theory, have received much attention during last two decades. Brief introductions of the related topics will be included in this section.

### 2.2.1 Fault detection filter

Fault detection filter (FDF) is the first kind of observer-based residual generator for FDI purpose proposed in [6], [59]. The core of an FDF is a full order state observer described by

$$\begin{aligned} \hat{x}(k+1) &= A\hat{x}(k) + Bu(k) + L(y(k) - \hat{y}(k)), && (2.9) \\ \hat{y}(k) &= C\hat{x}(k) + Du(k) && (2.10) \end{aligned}$$

where the matrix $L$ is the so-called observer gain. By introducing the estimation error of state variable, $e = x - \hat{x}$, the observer gain matrix $L$ is chosen such that $A - LC$ is stable, i.e. the estimation error asymptotically goes to zero

$$\begin{aligned} e(k+1) &= (A - LC)e(k), && (2.11) \\ r(k) &= Ce(k) && (2.12) \end{aligned}$$

where $r$ is the residual signal and defined as $r(k) = y(k) - \hat{y}(k)$. The selection of the observer gain matrix $L$ is crucial to improve the performance of estimation. For FDI purpose, in order to increase the sensitivity to faults and the robustness against disturbances, the residual generator can also be extended to

$$r(k) = V(y(k) - \hat{y}(k)) \tag{2.13}$$

where $V$ is the so-called post-filter and, by a suitable selection, is helpful to obtain significant characteristics of faults. Thus, the design of the FDF lies in the optimal selection of the observer gain matrix and the post-filter $V$. Notice that FDF is a full order observer. A reduced order observer may provide the same performance with less on-line computation cost. For this purpose, the so-called diagnostic observer will be introduced in the next subsection.

### 2.2.2 Diagnostic observer

The diagnostic observer (DO) is one of the mostly used model-based residual generators. The core of a DO is a reduced order Luenberger type (output) observer that is described by

$$\begin{aligned} z(k+1) &= A_z z(k) + B_z u(k) + L_z y(k), & (2.14)\\ \hat{y}(k) &= \bar{c}_z z(k) + \bar{d}_z u(k) + \bar{g}_z y(k) & (2.15) \end{aligned}$$

where $z \in \mathcal{R}^s$, $s$ denotes the order of the observer and it can be equal or lower than system order $n$. The matrices $A_z, B_z, L_z, \bar{c}_z, \bar{d}_z$ and $\bar{g}_z$ together with a matrix, $T \in \mathcal{R}^{s\times n}$, have to solve the Luenberger equations,

- $A_z$ is stable
- $TA - A_z T = L_z C,\ B_z = TB - L_z D$
- $C = \bar{c}_z T + \bar{g}_z C,\ \bar{d}_z = -\bar{g}_z D + D$

under which, system described by Eqs.(2.14) -(2.15) achieves an unbiased estimation for output, i.e. $\lim_{k\to\infty}(y(k) - \hat{y}(k)) = 0$. Introducing the error vector $e = Tx - z$, the observer error dynamics become

$$\begin{aligned} e(k+1) &= A_z e(k), & (2.16)\\ y(k) - \hat{y}(k) &= \bar{c}_z e(k). & (2.17) \end{aligned}$$

To increase the design degrees of freedom, the residual vector is defined as Eq.(2.13). Then, it turns out

$$\begin{aligned} z(k+1) &= A_z z(k) + B_z u(k) + L_z y(k), & (2.18)\\ r(k) &= g_z y(k) - c_z z(k) - d_z u(k) & (2.19) \end{aligned}$$

where $g_z = V(I - \bar{g}_z)$, $c_z = V\bar{c}_z$ and $d_z = V\bar{d}_z$. For residual generation, the third condition in Luenberger equations shall be replaced by

$$VC - g_z T = 0,\ d_z = VD.$$

According to the discussion in the last subsection, the FDF design lies in the optimal selection of an observer gain matrix and a post-filter. The problem of DO design is to solve the Luenberger equations. Compared with FDF scheme, DO leads to a reduced order residual generator with less on-line computation.

### 2.2.3 Parity space approach

Parallel to the observer-based residual generation approaches, the so-called parity space approach has been proposed by Chow and Willsky [17] in the early 80's and serves as one of the simplest ways for FDI. Based on the state space model, the parity relation, instead of an observer, is used for residual generation. Suppose that the system described by Eqs.(2.1)-(2.2) is observable and $rank(C) = m$. The system can be recursively expressed as follows:

$$\begin{aligned} y(k-s+1) &= Cx(k-s+1) + Du(k-s+1), \\ y(k-s+2) &= Cx(k-s+2) + Du(k-s+2) \\ &= CAx(k-s+1) + CBu(k-s+1) + Du(k-s+2), \end{aligned}$$

and so on. Repeating this procedure yields:

$$y(k) = CA^{s-1}x(k-s+1) + CA^{s-2}Bu(k-s+1) + \cdots + CBu(k-1) + Du(k). \quad (2.20)$$

Introducing the following notations for input and output data

$$y_s(k) = \begin{bmatrix} y\,(k-s+1) \\ y\,(k-s+2) \\ \vdots \\ y\,(k) \end{bmatrix} \in \mathcal{R}^{sm},\ u_s(k) = \begin{bmatrix} u\,(k-s+1) \\ u\,(k-s+2) \\ \vdots \\ u\,(k) \end{bmatrix} \in \mathcal{R}^{sl},$$

the system can be rewritten into the following compact form

$$y_s(k) = \Gamma_s x(k-s+1) + H_{u,s}u_s(k) \quad (2.21)$$

where

$$\Gamma_s = \begin{bmatrix} C \\ CA \\ \vdots \\ CA^{s-1} \end{bmatrix} \in \mathcal{R}^{sm\times n},\ H_{u,s} = \begin{bmatrix} D & 0 & \cdots & 0 \\ CB & D & \cdots & 0 \\ \vdots & \vdots & \ddots & \vdots \\ CA^{s-2}B & \cdots & CB & D \end{bmatrix}.$$

Eq.(2.21) is the so-called parity relation, which describes the input and output relationship with the past state variable $x(k-s+1)$.

Assume that $(C, A)$ is observable, for $s > n$, the following rank condition holds:

$$rank\,(\Gamma_s) = n \quad (2.22)$$

which ensures that there exists at least a row vector $v_s(\neq 0) \in \mathcal{R}^{1\times sm}$ such that

$$v_s\Gamma_s = 0. \quad (2.23)$$

The vectors satisfying Eq.(2.23) are termed as parity vectors, whose set

$$P_s = \{v_s | v_s \Gamma_s = 0\} \tag{2.24}$$

is called the parity space of the $s$-th order.

Consequently, a parity relation based residual generator can be constructed as

$$r(k) = v_s(y_s(k) - H_{u,s}u_s(k)). \tag{2.25}$$

In case that the system is corrupted by faults and disturbances, it follows that

$$y_s(k) = \Gamma_s x(k-s+1) + H_{u,s}u_s(k) + H_{f,s}f_s(k) + H_{d,s}d_s(k) \tag{2.26}$$

where

$$f_s(k) = \begin{bmatrix} f(k-s+1) \\ f(k-s+2) \\ \vdots \\ f(k) \end{bmatrix}, \; H_{f,s} = \begin{bmatrix} F_f & O & \cdots & O \\ CE_f & F_f & \ddots & \vdots \\ \vdots & \ddots & \ddots & O \\ CA^{s-2}E_f & CA^{s-3}E_f & \cdots & F_f \end{bmatrix},$$

$$d_s(k) = \begin{bmatrix} d(k-s+1) \\ d(k-s+2) \\ \vdots \\ d(k) \end{bmatrix}, \; H_{d,s} = \begin{bmatrix} F_d & O & \cdots & O \\ CE_d & F_d & \ddots & \vdots \\ \vdots & \ddots & \ddots & O \\ CA^{s-2}E_d & CA^{s-3}E_d & \cdots & F_d \end{bmatrix}.$$

Thus, residual signal presented in Eq.(2.25) becomes

$$r(k) = v_s \left( H_{d,s}d_s(k) + H_{f,s}f_s(k) \right). \tag{2.27}$$

The design of parity relation based residual generator can be achieved in a straightforward manner. The only parameter to be designed is the parity vector. On the other hand, the implementation form of Eq.(2.25), which not only includes the temporal but also the past input and output data, is not ideal for on-line realization. Based on the research on the characterization of parity space and Luenberger equations, Ding et al. [22] revealed interesting interconnections between DO and parity space.

### 2.2.4 Interconnections between DO and parity space

Although the implementation forms of DO and parity space based residual generators are different, the one-to-one mapping between these two approaches has been proposed by Ding et al. [22], which reveals that all design approaches based on parity space can be

used to design DO-based residual generators, and vice-versa. In this subsection, a brief explanation of these connections will be introduced.

Given a parity vector $v_s = \begin{bmatrix} v_{s,0} & v_{s,1} & \cdots & v_{s,s-1} \end{bmatrix}$ of the system described by Eqs.(2.1)-(2.2), the matrices $A_z, B_z, L_z, g_z, c_z$ and $T$ can be obtained as

$$
\begin{aligned}
A_z &= \begin{bmatrix} 0 & 0 & \cdots & 0 & 0 \\ 1 & 0 & \ddots & \vdots & 0 \\ \vdots & \ddots & \ddots & 0 & \vdots \\ 0 & 0 & \cdots & 1 & 0 \end{bmatrix}, \; L_z = - \begin{bmatrix} v_{s,0} \\ v_{s,1} \\ \vdots \\ v_{s,s-2} \end{bmatrix}, \\
B_z &= \begin{bmatrix} v_{s,0} & v_{s,1} & \cdots & v_{s,s-1} \\ v_{s,1} & \cdots & v_{s,s-1} & 0 \\ \vdots & \iddots & 0 & 0 \\ v_{s,s-1} & 0 & \cdots & 0 \end{bmatrix} \begin{bmatrix} D \\ CB \\ CAB \\ \vdots \\ CA^{s-2}B \end{bmatrix}, \\
T &= \begin{bmatrix} v_{s,1} & v_{s,2} & \cdots & v_{s,s-2} & v_{s,s-1} \\ v_{s,2} & v_{s,3} & \cdots & v_{s,s-1} & 0 \\ \vdots & \cdots & \cdots & \vdots & \vdots \\ v_{s,s-1} & 0 & \cdots & \cdots & 0 \end{bmatrix} \begin{bmatrix} C \\ CA \\ \vdots \\ CA^{s-2} \end{bmatrix}, \\
c_z &= \begin{bmatrix} 0 & \cdots & 0 & 1 \end{bmatrix}, \; g_z = v_{s,s-1}.
\end{aligned}
$$

On the other hand, given system model of Eqs.(2.1)-(2.2) and DO-based residual generator from Eqs.(2.18)-(2.19), then the vector $v_s$ with

$$
v_{s,s-1} = g_z, \; \begin{bmatrix} v_{s,0} \\ v_{s,1} \\ \vdots \\ v_{s,s-2} \end{bmatrix} = -L_z \tag{2.28}
$$

belongs to the parity space. The above one-to-one relationship indicates that the selection of a parity vector is equivalent to the selection of parameters in DO. Since the parity space approach is characterized by its simple mathematical formulation, a strategy of *parity space design, observer-based implementation* has been widely applied in industry to ensure a numerically stable and less complicated observer-based on-line implementation.

## 2.3 Subspace identification method

Since the majority of observer and parity space based residual generators involve rigorous development of state space models, which are generally hard to obtain based on the first

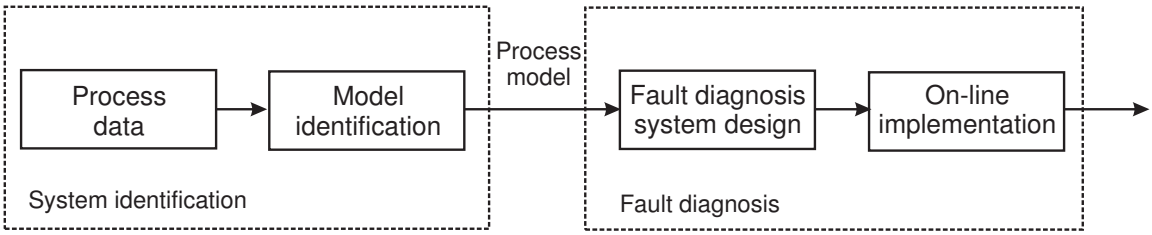


**Figure 2.1:** Design of model-based fault diagnosis system

principles in practice, the system identification becomes a necessary step prior to the design [77]. Especially, the subspace identification method (SIM) has recently drawn much attention due to its numerical simplicity and stability. Based on it, the state space model can be directly extracted for the purpose of prediction, control and fault diagnosis. From the application point of view, the procedure from the process history data to the final implementation of a model-based fault diagnosis system consists of three steps: (a) model identification, (b) fault diagnosis system design, and (c) on-line implementation, as schematically sketched in Fig. 2.1.

Based on the study of several subspace identification algorithms [67], [104], [109], it is possible to interpret them as singular value decomposition (SVD) task with different weighting [19]. A typical subspace identification algorithm includes two steps: (a) identification of the extended observability matrix $\Gamma_s$ and $H_{u,s}$, and (b) calculation of system matrices $A, B, C$ and $D$. In order to understand subspace identification algorithm, a brief procedure for deterministic case identification will be introduced in this section.

Considering a discrete LTI system described by Eqs.(2.1)-(2.2), for $N \gg s > n$, the extended state space model can be obtained according to Eq.(2.21)

$$Y_p = \Gamma_s X + H_{u,s} U_p \tag{2.29}$$

with block Hankel matrices

$$\begin{aligned} Y_p &= \left[ \begin{array}{cccc} y_s(k) & y_s(k+1) & \cdots & y_s(k+N-1) \end{array} \right] \in \mathcal{R}^{sm \times N}, \\ U_p &= \left[ \begin{array}{cccc} u_s(k) & u_s(k+1) & \cdots & u_s(k+N-1) \end{array} \right] \in \mathcal{R}^{sl \times N}, \\ X &= \left[ \begin{array}{cccc} x(k-s+1) & x(k-s+2) & \cdots & x(k-s+N) \end{array} \right] \in \mathcal{R}^{n \times N}. \end{aligned}$$

Introducing $Z_p^T = \begin{bmatrix} Y_p^T & U_p^T \end{bmatrix}$, the SVD of $Z_p$ leads to

$$Z_p = \begin{bmatrix} U_1 & U_2 \end{bmatrix} \begin{bmatrix} \Lambda_1 & O \\ O & \Lambda_2 \end{bmatrix} \begin{bmatrix} V_1^T \\ V_2^T \end{bmatrix} \tag{2.30}$$

where $\Lambda_2$ contains $sm - n$ zero singular values under the assumption that the persistent excitation condition is satisfied [110]. Straightforwardly, it follows that

$$U_2 = \begin{bmatrix} U_{2,y} \\ U_{2,u} \end{bmatrix} = \begin{bmatrix} (\Gamma_s^{\perp})^T \\ -H_{u,s}^T (\Gamma_s^{\perp})^T \end{bmatrix} \tag{2.31}$$

which indicates that

$$\Gamma_s = (U_{2,y}^T)^{\perp}, \tag{2.32}$$

$$-U_{2,y}^T H_{u,s} = U_{2,u}^T. \tag{2.33}$$

According to Eqs.(2.32)-(2.33), the extended observability matrix $\Gamma_s$ and the block triangular Toeplitz matrix $H_{u,s}$ can be simply extracted and the system matrices $A, B, C$ and $D$ are then identified with the help of the least square method.

## 2.4 Multivariate statistical process monitoring

In contrast to model-based approaches, in which the quantitative model is known *a priori*, the so-called multivariate statistical process monitoring (MSPM) methods are dependent on large amount of historical data to describe the variability of the process. The most attractive features of MSPM techniques are easy design and operational simplicity, which make MSPM more popular in many industrial sectors, especially for detecting the abnormality in large-scale industrial applications [13], [96].

Generally, the basic idea of MSPM techniques is to provide a concise set of statistics that describes the desired process behavior without direct presentation of huge amount of raw process data to process engineers. Compared to the univariate methods, which only monitor the magnitude and variation of single variable, the reliability and robustness against plant-wide disturbances have been significantly improved. In this section, the basic MSPM methods, including principal component analysis and partial least squares, will be briefly introduced in the form of off-line design and on-line implementation algorithms.

### 2.4.1 Principal component analysis

Principal component analysis (PCA) is a basic method in the framework of MSPM and originally serves as a dimensionality reduction technique that preserves the significant

variability information in the original data set. Since 80's, PCA has been successfully applied in numerous areas including data compression, image processing, feature extraction, pattern recognition and process monitoring [54], [58]. Due to its simplicity and efficiency in handling huge amount of process data, PCA is recognized as a powerful multivariate statistical tool and widely used in the process industry for fault detection and diagnosis [25], [55], [90], [92], [108].

The off-line design procedure of PCA-based process monitoring scheme is based on the training data, which can be obtained either from the process or from a simulation platform that can replicate the desired process behavior. Given a process with $N$ samples of $m$ measured variables, the training data set is firstly collected and normalized to zero mean (often scaled to unit variance). Finally, the preprocessed training data is denoted by

$$Z = \begin{bmatrix} z_1^T \\ z_2^T \\ \vdots \\ z_N^T \end{bmatrix} = \begin{bmatrix} z_{11} & z_{21} & \cdots & z_{1m} \\ z_{21} & z_{22} & \cdots & z_{2m} \\ \vdots & \vdots & \ddots & \vdots \\ z_{N1} & z_{N2} & \cdots & z_{Nm} \end{bmatrix} \in \mathcal{R}^{N \times m}. \tag{2.34}$$

The sample covariance matrix of $Z$ can be written as

$$\Phi = \frac{1}{N-1} Z^T Z. \tag{2.35}$$

In order to extract the significant variability information, an SVD is performed on the sample covariance matrix, i.e.

$$\frac{1}{N-1} Z^T Z = P \Lambda P^T \tag{2.36}$$

where $\Lambda = diag\left(\lambda_1, \ldots, \lambda_m\right)$ with $\lambda_1 \geq \ldots \geq \lambda_m \geq 0$. By the nature of singular values, it is possible to divide $P$ and $\Lambda$ into

$$\Lambda = \begin{bmatrix} \Lambda_{pc} & 0 \\ 0 & \Lambda_{res} \end{bmatrix}, \; P = \begin{bmatrix} P_{pc} & P_{res} \end{bmatrix},$$

respectively, where $P_{pc} \in \mathcal{R}^{m \times \beta}$ consists of the singular vectors corresponding to the $\beta$ largest singular values in $\Lambda_{pc}$ and $P_{res} \in \mathcal{R}^{m \times (m-\beta)}$ is related to the $m-\beta$ smallest singular values in $\Lambda_{res}$. $\beta$ is the number of principal components (PCs), which can be determined by a certain criterion in [103]. As a result, the original $m$-dimensional measurement $z$ is projected onto two orthogonal subspaces

$$\hat{z} = P_{pc} P_{pc}^T z \in S_p \equiv \text{Span}\left\{P_{pc}\right\}, \tag{2.37}$$

$$\tilde{z} = P_{res} P_{res}^T z \in S_r \equiv \text{Span}\left\{P_{pc}\right\}^{\perp} \tag{2.38}$$

where Span $\{P_{pc}\}$ is defined as the set of all linear combinations of the columns in $P_{pc}$. Span $\{P_{pc}\}^{\perp}$ is the orthogonal complement of Span $\{P_{pc}\}$. In order to detect the abnormal changes in the both subspaces, the squared prediction error (SPE) [55] and $T^2$ statistic [102] are computed for on-line implementation. Based on the on-line normalized measurement sample $z$, the SPE and $T^2$ statistics are

$$\begin{aligned} \text{SPE} &= z^T P_{res} P_{res}^T z, && (2.39) \\ T^2 &= z^T P_{pc} \Lambda_{pc}^{-1} P_{pc}^T z. && (2.40) \end{aligned}$$

The thresholds can be calculated for a given confidence level $\alpha$:

$$\begin{aligned} J_{th,SPE} &= \theta_1 \left( \frac{c_\alpha \sqrt{2\theta_2 h_0^2}}{\theta_1} + 1 + \frac{\theta_2 h_0 \left(h_0 - 1\right)}{\theta_1^2} \right)^{1/h_0}, && (2.41) \\ J_{th,T^2} &= \frac{\beta \left(N^2 - 1\right)}{N \left(N - \beta\right)} F_\alpha \left(\beta, N - \beta\right) && (2.42) \end{aligned}$$

where $c_\alpha$ is the normal deviate corresponding to the upper $1-\alpha$ percentile, $F\left(\beta, N-\beta\right)$ stands for $F$-distribution with $\beta$, $N-\beta$ degrees of freedom and

$$\begin{aligned} h_0 &= 1 - \frac{2\theta_1 \theta_3}{3\theta_2^2}, \\ \theta_i &= \sum_{j=\beta+1}^{m} \left(\lambda_j\right)^i, \; i = 1, 2, 3. \end{aligned}$$

Consequently, the fault detection logic follows

$$\text{SPE} \leq J_{th,SPE} \text{ and } T^2 \leq J_{th,T^2} \Longrightarrow \text{fault free, otherwise faulty.}$$

Notice that the basic assumption for applying PCA to process monitoring is that the measurement variables follow multivariate Gaussian distribution. In addition, the normalization procedure gives same weighting for measurement variables, in which the input and output relationship has not been considered. However, the correlation between input and output variables may offer additional advantages for prediction and fault diagnosis. To this aim, another popular MSPM method, i.e. partial least squares will be introduced in the next subsection.

### 2.4.2 Partial least squares

Besides PCA, partial least squares (PLS) is another popular method in MSPM framework and widely used for model building, fault detection and diagnosis [61], [64], [119]. The original idea behind PLS is to predict output variables using the on-line observation of

process inputs with the help of identified correlation model. For the purpose of process monitoring, PLS approach is aiming to detect the faults in input measurements which are mostly related to the output variables. The final outputs in process industry are always termed as product quality variables and generally can not be measured on-line.

Similar to PCA, the off-line design procedure of PLS-based process monitoring scheme is based on the training data with process input and output information. Given a normalized data matrix $U$ which records $N$ samples of $l$ process input variables, and $Y$ consisting of $N$ samples of $m$ normalized outputs

$$U = \begin{bmatrix} u_1^T \\ u_2^T \\ \vdots \\ u_N^T \end{bmatrix} \in \mathcal{R}^{N\times l},\ Y = \begin{bmatrix} y_1^T \\ y_2^T \\ \vdots \\ y_N^T \end{bmatrix} \in \mathcal{R}^{N\times m},$$

$u_i \in \mathcal{R}^l$, $y_i \in \mathcal{R}^m$, for $i = 1, \ldots, N$, then PLS involves projection of $U$ and $Y$ onto a low dimensional space defined by the so-called latent variables (LVs),

$$T = \begin{bmatrix} t_1 & t_2 & \cdots & t_\gamma \end{bmatrix} \in \mathcal{R}^{N\times\gamma}$$

such that the correlation model between $U$ and $Y$ becomes

$$U = TP^T + \tilde{U} = \hat{U} + \tilde{U}, \tag{2.43}$$

$$Y = TQ^T + E_y = UM + E_y \tag{2.44}$$

where $\gamma$ is the number of LVs and $P \in \mathcal{R}^{l\times\gamma}, Q \in \mathcal{R}^{m\times\gamma}$ are loading matrices of $U$ and $Y$, respectively. $M \in \mathcal{R}^{l\times m}$ is the coefficient matrix. $\hat{U} = TP^T$ is highly correlated with $Y$. $\tilde{U}$ and $E_y$ are residual subspaces and assumed to be uncorrelated with $Y$ and $U$, respectively. From the correlation model presented by Eqs.(2.43)-(2.44), the matrix $T$ and coefficient matrix $M$ can be calculated as

$$T = UR, \tag{2.45}$$

$$M = RQ^T \tag{2.46}$$

where $P^TR = R^TP = I_{\gamma\times\gamma}$ and $R \in \mathcal{R}^{l\times\gamma}$. The basic PLS algorithm, which is implemented with the so-called nonlinear iterative partial least squares algorithm (NIPALS), has been summarized in [18], [48], [49].

According to the correlation with outputs, PLS projects input measurement onto the following two subspaces

$$\hat{u} = PR^Tu \in S_{\hat{u}} \equiv \text{Span}\left\{P\right\}, \tag{2.47}$$

$$\tilde{u} = \left(I_{l\times l} - PR^T\right)u \in S_{\tilde{u}} \equiv \text{Span}\left\{R\right\}^\perp. \tag{2.48}$$

**NIPALS Algorithm:**

- Collect and normalize the input and output data
- Perform the following iterative computations $\gamma$ times:

$$(w_i^*, q_i^*) = \arg \max_{\|w_i\|=1, \|q_i\|=1} w_i^T U_i^T Y q_i,\ U_1 = U,$$
$$t_i = U_i w_i^*,\ p_i = \frac{U_i^T t_i}{\|t_i\|^2},\ U_{i+1} = U_i - t_i p_i^T,$$
$$r_1 = w_1^*,\ r_i = \prod_{j=1}^{i-1} \left(I_{n\times n} - w_j^* p_j^T\right) w_i^*,\ i > 1$$

  where $i = 1, \cdots, \gamma$, $\gamma$ is determined by applying a known criterion, e.g. leave-N-out cross validation [120].

- Compute matrices $P$, $Q$, $R$, $T$ and $M$ as follows:

$$P = \left[\begin{array}{ccc} p_1 & \cdots & p_\gamma \end{array}\right],\ T = \left[\begin{array}{ccc} t_1 & \cdots & t_\gamma \end{array}\right],$$
$$Q = \left[\begin{array}{ccc} q_1 & \cdots & q_\gamma \end{array}\right],\ R = \left[\begin{array}{ccc} r_1 & \cdots & r_\gamma \end{array}\right],$$
$$M = RQ^T.$$

Hence, fault detection can be achieved using suitable test statistics based on the above two subspaces. The $T^2$ and SPE statistics are popularly used to detect changes in $\hat{u}$ and $\tilde{u}$, i.e.

$$T^2 = u^T R \left(\frac{T^T T}{N-1}\right)^{-1} R^T u, \tag{2.49}$$
$$\text{SPE} = \|\tilde{u}\|^2 = \left\|\left(I_{l\times l} - PR^T\right) u\right\|^2. \tag{2.50}$$

Under a given confidence level $\alpha$, the threshold for fault detection can be calculated as:

$$J_{th,T^2} = \frac{\gamma\left(N^2-1\right)}{N\left(N-\gamma\right)} F_\alpha\left(\gamma, N-\gamma\right), \tag{2.51}$$
$$J_{th,SPE} = g\chi_\alpha^2(h) \tag{2.52}$$

where $g\chi^2(h)$ is the $\chi^2$-distribution with scaling factors $g = S/2\mu$ and $h = 2\mu^2/S$. $\mu$ and $S$ are sample mean and variance of SPE statistic [86], [102].

The PLS-based process monitoring scheme is also based on the assumption that process measurements follow multivariate Gaussian distribution. The geometric interpretation of PLS approach has been recently proposed in [74].

### 2.4.3 Recent developments on MSPM

PCA and PLS are the most widely accepted data-driven process monitoring methods in MSPM framework. The standard PCA and PLS algorithms require that the process is linear and static. The dynamic PCA (DPCA) and dynamic PLS (DPLS) are natural extensions of the both methods to deal with process dynamics, which can be roughly expressed in terms of the serial correlations of process variables [16], [66]. In order to cope with the nonlinearity issue, the kernel-based approaches are also intensively studied these days [15], [71].

The other MSPM techniques like fisher discriminant analysis (FDA) and independent component analysis (ICA), are also frequently used in industrial applications. FDA is a dimensionality reduction technique and has been well studied in the fields of multivariate statistic and pattern classification [33], [81]. Due to its ability to discriminate among classes of data, FDA is recognized as an efficient tool for fault classification [12], [14], [46]. In addition, by defining an additional class of data to represent normal operating conditions, FDA can also be applied for fault detection purpose [13]. For ICA approach, the basic idea is to find out the hidden statistically independent components (ICs) from the observed data. ICA approach is originally proposed to solve the signal processing as well as blind source separation problems [44], [51], [73]. Recently, ICA has been applied for process monitoring, especially for the process measurements with non-Gaussian distributions [60], [72], [70], [133]. Compared with PCA and PLS, the calculation involved in ICA is more complicated. However, it is worthy of further discussion whether the independence between the latent variables could bring additional advantage for the evaluation stage. Although more sophisticated variants of these methods have been recently proposed to deal with different issues in industrial processes, a simple method without complicated computations is still of great interest from the application viewpoint in order to reduce the design and engineering efforts.

## 2.5 Concluding remarks

This chapter offers a brief introduction to the major developments and basic concepts of fault diagnosis techniques, which include model-based and data-driven MSPM approaches. Depending on the availability of system model, the model-based techniques, such as FDF, DO and parity space approach, as well as their interconnections are discussed in detail. Since the process model is hard to be established in practice, the subspace model identification techniques can be applied to extract the model from process data.

In the second part of this chapter, the data-driven MSPM approaches are briefly in-

troduced with the help of PCA and PLS. Compared with model-based techniques, the data-driven MSPM approaches try to extract a concise set of statistics from huge amount of process data and hence receive more attention in large-scale process industry nowadays.

Based on the experiences from industrial and research projects, it is observed that some modifications on basic MSPM approaches are often helpful to improve the process monitoring performance under ideal stationary operating conditions. Moreover, alternative solutions, which combine the advantages of model-based and MSPM techniques, will lead to additional improvements on their applicability, capacity and efficiency for industrial applications. These issues will be discussed in the next four chapters.

# 3 Modifications on PCA-based approach

The efficiency of PCA-based fault diagnosis scheme lies in its ability to compress a huge amount of process data and extract the meaningful information within. From application point of view, the PCA-based fault diagnosis technique is suitable for the processes with little or no a *priori* knowledge about their mathematical models. Several extensions of standard PCA approach have been developed to deal with parameter variations [35], [76] and industrial batch processes [10], [57], [71], [123]. Although more sophisticated variants of PCA are proposed, some basic issues of PCA, such as the original idea, test statistics and their sensitivities to the faults, have not been paid enough attention in research study.

It is well-known that the original idea behind PCA is to reduce the dimension of a data set, while retaining significant variability information. However, for fault diagnosis, PCA offers no reduction from the computation point of view since the data should be projected onto the both subspaces as shown in Eqs.(2.37)-(2.38). In this sense, the core of the PCA-based approach consists in a numerically reliable implementation of the test statistics for fault detection, which is mainly achieved based on the SVD. To achieve optimal fault detection performance, the thresholds of related test statistics shall be delivered by suitable methods.

In the present work, a new test statistic is firstly proposed. In comparison with the SPE index, the threshold setting associate with the new statistic is considerably less complicated than the one given in Eq.(2.41). The further study is dedicated to the analysis of fault sensitivity. The fault identification issue is finally solved in the proposed framework [25], [126].

## 3.1 Problem formulation

The basic assumption on PCA-based fault diagnosis method is that the process variables follow multivariate Gaussian distribution. Without loss of generality, the measurement vector can be described as $z \sim \mathcal{N}(0, \Phi)$ due to the mean center procedure. The projections of $z$ onto $P_{pc}$ and $P_{res}$ are shown in Eqs.(2.37)-(2.38) such that $z = \hat{z} + \tilde{z}$ with $P_{pc}^T z \sim$

$\mathcal{N}(0, \Lambda_{pc})$ and $P_{res}^T z \sim \mathcal{N}(0, \Lambda_{res})$. In order to simplify the following study, throughout this thesis, it is assumed that the sample number $N$ is large enough so that the $\chi^2$-distribution can be adopted instead of $F$-distribution. The threshold for $T^2$ statistic can be calculated as

$$J_{th,T^2} = \chi_\alpha^2(\beta) \tag{3.1}$$

where $\alpha$ is confidence level and $\beta$ is number of PCs. A natural way to monitor the subspace spanned by $P_{res}$ is to use the so-called Hawkin's statistic

$$T_H^2 = z^T P_{res} \Lambda_{res}^{-1} P_{res}^T z \tag{3.2}$$

which is, however, less utilized in practice due to the drawback with the possible ill-conditioning $\Lambda_{res}$ when some of the singular values of $\lambda_{\beta+1}, \ldots, \lambda_m$ are very close to zero. To solve the problem, the SPE statistic [55] in the form of Eq.(2.39) is proposed with the threshold given in Eq.(2.41), which is derived from statistical approximation with complicated computation.

For process monitoring, the offset and scaling faults are the two types of faults which are mostly considered both in the academic study and practical application. Given a measurement sample $z$, the offset and scaling faults can be formulated as follows:

$$z_f = z + f, \ f \neq 0, \tag{3.3}$$

$$z_F = Fz, \ F \neq I \tag{3.4}$$

where $f \in \mathcal{R}^m$ and $F \in \mathcal{R}^{m \times m}$ are constant fault vector and matrix, respectively. Although a successful application of the PCA-based fault diagnosis method depends on the suitable test statistics for both subspaces, their sensitivities for detecting both types of faults have not been analytically studied. To complete the entire fault diagnosis scheme, the fault identification issue shall be finally taken into consideration. Based on the above observations, this chapter mainly focuses on the following topics:

- Propose suitable test statistic and threshold to monitoring subspace spanned by $P_{res}$,
- Analyze the sensitivity of related test statistic to the fault and,
- Develop an effective fault identification algorithm.

## 3.2 On the test statistic

The test statistic plays an important role in PCA-based fault diagnosis technique. Under given probability density function of the considered variable, the test statistic is utilized to

detect the change within. The likelihood ratio methods [4] are popularly used in practice for the purpose of change detection. Some essentials are introduced in the next subsection.

### 3.2.1 Generalized likelihood ratio

Given the system model

$$y = \varepsilon + \theta,\ \theta = \begin{cases} \theta_0, & \text{no change} \\ \theta_1, & \text{change} \end{cases}$$

where $y, \theta, \varepsilon \in \mathcal{R}^m$, $\varepsilon \sim \mathcal{N}(0, \Sigma)$ and $\theta$ is a constant vector. The probability density function of Gaussian vector $y$ is defined by

$$p_{\theta,\Sigma}(y) = \frac{1}{\sqrt{(2\pi)^m \det(\Sigma)}} e^{-\frac{1}{2}(y-\theta)^T \Sigma^{-1}(y-\theta)}.$$

The log likelihood ratio for given vector $y$ satisfies

$$s(y) = \ln \frac{p_{\theta_1}(y)}{p_{\theta_0}(y)} = \frac{1}{2}\left[(y-\theta_0)^T\Sigma^{-1}(y-\theta_0) - (y-\theta_1)^T\Sigma^{-1}(y-\theta_1)\right].$$

The basic idea of likelihood ratio method can be clearly seen from the following decision rule

$$s(y) = \begin{cases} < 0, & \theta = \theta_0 \text{ is accepted} \\ > 0, & \theta = \theta_1 \text{ is accepted} \end{cases}.$$

In statistical framework, $s(y) > 0$ means $p_{\theta_1}(y) > p_{\theta_0}(y)$, i.e. given $y$, the probability of $\theta = \theta_1$ is higher than the one of $\theta = \theta_0$. Under the assumption that $\theta_0 = 0$ and $N$ samples of $y$, i.e., $y_1, \ldots, y_N$, are available, the likelihood ratio is defined by

$$\begin{aligned} S_1^N &= \frac{1}{2}\left[\sum_{k=1}^N y_k^T\Sigma^{-1}y_k - \sum_{k=1}^N (y_k-\theta_1)^T\Sigma^{-1}(y_k-\theta_1)\right] \\ &= \frac{1}{2}\left[\sum_{k=1}^N y_k^T\Sigma^{-1}y_k - \sum_{k=1}^N y_k^T\Sigma^{-1}y_k - N\left(\theta_1^T\Sigma^{-1}\theta_1 - \frac{2\theta_1^T\Sigma^{-1}}{N}\sum_{k=1}^N y_k\right)\right] \\ &= \frac{1}{2}\left[N\bar{y}^T\Sigma^{-1}\bar{y} - N(\bar{y}-\theta_1)^T\Sigma^{-1}(\bar{y}-\theta_1)\right] \end{aligned} \tag{3.5}$$

where $\bar{y} = \frac{1}{N}\sum_{k=1}^N y_k$. Generally, $\theta_1$ is unknown in practice. In order to detect the change in $\theta$, the so-called generalized likelihood ratio (GLR) is developed. The basic idea of GLR is to estimate $\theta_1$ with maximum likelihood estimation. The maximum likelihood estimate of $\theta_1$ is achieved if the likelihood ratio described in Eq.(3.5) is maximized, which leads to the solution of the following optimization problem

$$\hat{\theta}_1 = \arg\max_{\theta_1} S_1^N = \bar{y} \Longrightarrow \max_{\theta_1} S_1^N = \frac{N}{2}\bar{y}\Sigma^{-1}\bar{y}^T.$$

It is of practical interest to notice that the maximum likelihood estimate of $\theta_1$ is the estimate of the mean value of $y$ based on the available samples. Since $\bar{y} \sim \mathcal{N}(0, \Sigma/N)$, it is obvious that $N\bar{y}\Sigma^{-1}\bar{y}^T$ follows $\chi^2$-distribution. Therefore, given a confidence level $\alpha$, the following algorithm can be used for GLR-based change detection.

**GLR-based change detection algorithm:**

- Determine $\chi_\alpha(m)$ using the table of $\chi^2$-distribution with $m$ degrees of freedom under confidence interval $\alpha$
- Set threshold $J_{th} = \chi_\alpha(m)$
- Define testing statistic

$$J = N\bar{y}\Sigma^{-1}\bar{y}^T \tag{3.6}$$

  with $\bar{y} = \frac{1}{N}\sum_{k=1}^{N} y_k$

- Define detection logic

$$J = \begin{cases} < J_{th}, \text{no change} \\ > J_{th}, \text{a change is detected} \end{cases}.$$

### 3.2.2 An alternative test statistic

The PCA approach decomposes the measurement space into the so-called principal component subspace and residual subspace, which are spanned by $P_{pc}$ and $P_{res}$, respectively. Since a fault may appear in one of these subspaces, projections of $z$ onto both $P_{pc}$ and $P_{res}$ presented by Eqs.(2.37)-(2.38) should be applied for the fault detection purpose. Note that $T^2$ and SPE statistics are of quadratic forms associated with $\hat{z}$ and $\tilde{z}$, respectively. For a fixed sample number $N$, the GLR test statistic given by Eq.(3.6) leads to an optimal fault detection performance. It is evident that the $T^2$ index is exact GLR test statistic with $N = 1$ and thus delivers an optimal fault detection performance for the principal component subspace.

For the residual subspace, the Hawkin's statistic of Eq.(3.2) can not be directly utilized due to the possible ill-conditioning of $\Lambda_{res}$. To avoid this difficulty and also to make use of easy $\chi^2$-distribution table, an alternative statistic is introduced below.
Let

$$\Xi = diag\left(\frac{\lambda_m}{\lambda_{\beta+1}}, \cdots, \frac{\lambda_m}{\lambda_{m-1}}, 1\right) \in \mathcal{R}^{(m-\beta)\times(m-\beta)}.$$

It turns out that

$$\Xi^{1/2} P_{res}^T z \sim \mathcal{N}\left(0, \lambda_m I_{(m-\beta)\times(m-\beta)}\right)$$

and

$$z^T P_{res} \Xi P_{res}^T z = \lambda_m z^T P_{res} \Lambda_{res}^{-1} P_{res}^T z.$$

An alternative statistic and the associated threshold are proposed under given confidence level $\alpha$

$$T_{new}^2 = z^T P_{res} \Xi P_{res}^T z, \tag{3.7}$$

$$J_{th,T_{new}^2} = \lambda_m \chi_\alpha^2 (m-\beta) \tag{3.8}$$

which deliver an optimal fault detection performance in the residual subspace.

It is necessary to point out that

- the new statistic $T_{new}^2$ is equivalent to Hawkin's statistic $T_H^2$ but without the numerical problem,
- unlike the conventional SPE statistic, whose threshold is derived by statistical approximation, the new statistic $T_{new}^2$ follows $\chi^2$-distribution and the associate threshold can be exactly determined by using the $\chi^2$-distribution table, and
- the computation given in Eq.(3.8) is considerably less complicated than the one of conventional SPE threshold.

Since the principal component subspace and residual subspace are mutually orthogonal, the fault occurred in one of them can not be detected by the test statistic developed for the other subspace. In order to ensure high fault detectability, the so-called combined index [90], [92], which makes simultaneously use of both statistics, is generally formulated as

$$T_c^2 = \beta_1 T^2 + \beta_2 T_{res}^2 \tag{3.9}$$

with known constants $\beta_1, \beta_2 > 0$. Rewrite Eq.(3.9) into

$$T_c^2 = z^T P \Psi P^T z$$

where

$$\Psi = \begin{bmatrix} \beta_1 \Lambda_{pc}^{-1} & 0 \\ 0 & \beta_2 Q \end{bmatrix}, \; Q = \begin{cases} \Lambda_{res}^{-1}, & T_{res}^2 = T_H^2 \\ I, & T_{res}^2 = \text{SPE} \\ \Xi, & T_{res}^2 = T_{new}^2 \end{cases}.$$

Considering that $P^T z \sim \mathcal{N}(0, \Lambda)$, $z^T P \Lambda^{-1} P^T z \sim \chi^2(m)$, it is reasonable to introduce the following combined statistic to avoid possible difficulty with the computation of $\Lambda^{-1}$

$$T^2_{comb} = z^T P \bar{\Xi} P^T z \text{ with } \bar{\Xi} = diag\left(\frac{\lambda_m}{\lambda_1}, \cdots, \frac{\lambda_m}{\lambda_{m-1}}, 1\right) \tag{3.10}$$

which is a combined index $T^2_{comb} = \lambda_m(T^2 + T^2_H)$. For a given confidence level $\alpha$, the threshold of $T^2_{comb}$ is given by

$$J_{th,comb} = \lambda_m \chi^2_\alpha(m). \tag{3.11}$$

The combined index can also be interpreted as a weighted quadratic form of the observation projection $P^T z$. It is interesting to notice that the direction coupled with a stronger variance is less weighted, while the direction with a weaker variance has a stronger weighting.

In the extreme case that the sample covariance matrix $\Phi$ is singular, an SVD yields

$$\Phi = \frac{1}{N-1} Z^T Z = \begin{bmatrix} P & P_\perp \end{bmatrix} \begin{bmatrix} \Lambda & 0 \\ 0 & 0 \end{bmatrix} \begin{bmatrix} P^T \\ P^T_\perp \end{bmatrix}.$$

As a result, the fault detection can be achieved by using the combined index in Eq.(3.10) with the associated threshold Eq.(3.11) and the parity checking

$$P^T_\perp z = 0. \tag{3.12}$$

The corresponding detection logic is

$$T^2_{comb} \leq J_{th,comb} \text{ and (3.12) is true} \implies \text{fault free, otherwise a fault is detected.}$$

## 3.3 Fault sensitivity analysis

In this section, the fault sensitivity of the related test statistic will be analyzed. Recalling the offset and scaling faults defined in Eqs.(3.3)-(3.4), the scaling fault can also be formulated as a special kind of offset fault in case of

$$f = F - I_{m\times m} z.$$

Therefore, in the sequent study of fault sensitivity analysis, the general form of fault is considered as

$$z_f = z + f.$$

Since $T^2_H$, $T^2_{new}$ and SPE are equivalent to represent test statistic for residual subspace, in the following analysis $T^2_{res}$ is formulated by $T^2_H$ to simplify the notation. Similarly, $T^2_{comb}$ represents the combined index $T^2_c$.

### 3.3.1 Comparison between $T^2$ and $T^2_{res}$ statistics

According to the nature of fault, two cases are considered as follows.

- *Fault occurs in $P_{pc}$ or $P_{res}$.* In this case, the $T^2$ and $T^2_{res}$ statistics are only sensitive to the faults which can be decomposed into subspaces spanned by $P_{pc}$ and $P_{res}$, respectively. Since the principal component subspace and residual subspace are mutually orthogonal, if a fault occurs only in $P_{pc}$ (or $P_{res}$), the $T^2_{res}$ (or $T^2$) statistic will never detect the fault regardless of its magnitude.

- *Fault has the similar influences on both subspaces.* Since the covariance matrices of $P^T_{pc}z$ and $P^T_{res}z$ are, respectively, $\Lambda_{pc}$ and $\Lambda_{res}$, and furthermore $\lambda_{min}(\Lambda_{pc}) = \lambda_\beta \gg \lambda_{max}(\Lambda_{res}) = \lambda_{\beta+1}$, the $T^2_{res}$ statistic may be more sensitive to the fault than $T^2$ statistic. To demonstrate it, the fault sensitivity of related test statistic will be analytically studied in this subsection.

For a confidence level $\alpha$, it follows that

$$\begin{aligned}\max_{z\in\mathcal{N}(0,\Phi)} \left(z^T P_{res}\Lambda^{-1}_{res}P^T_{res}z\right) &\le J_{th,T^2_H} = \mathcal{X}^2_\alpha(m-\beta),\\ \max_{z\in\mathcal{N}(0,\Phi)} \left(z^T P_{pc}\Lambda^{-1}_{pc}P^T_{pc}z\right) &\le J_{th,T^2} = \mathcal{X}^2_\alpha(\beta).\end{aligned}$$

Thus, if a fault $f$ causes

$$\left(f^T P_{res}P^T_{res}f\right)^{1/2} > 2\lambda^{1/2}_{\beta+1}J^{1/2}_{th,T^2_H} = 2\lambda^{1/2}_{\beta+1}\left(\mathcal{X}^2_\alpha(m-\beta)\right)^{1/2}, \tag{3.13}$$

it becomes

$$\begin{aligned}\left(z^T_f P_{res}\Lambda^{-1}_{res}P^T_{res}z_f\right)^{1/2} &\ge \left(f^T P_{res}\Lambda^{-1}_{res}P^T_{res}f\right)^{1/2} - \left(z^T P_{res}\Lambda^{-1}_{res}P^T_{res}z\right)^{1/2}\\ &\ge \lambda^{-1/2}_{\beta+1}\left(f^T P_{res}P^T_{res}f\right)^{1/2} - J^{1/2}_{th,T^2_H}\\ &> J^{1/2}_{th,T^2_H}\end{aligned}$$

which means this fault can be detected with the confidence level $\alpha$. Note that Eq.(3.13) is a sufficient condition under that a fault can be detected by $T^2_H$. On the other hand, it is obvious that

$$\begin{aligned}\mathcal{E}\left(T^2\right) &= \mathcal{E}\left(z^T_f P_{pc}\Lambda^{-1}_{pc}P^T_{pc}z_f\right)\\ &= \mathcal{E}\left(z^T P_{pc}\Lambda^{-1}_{pc}P^T_{pc}z\right) + f^T P_{pc}\Lambda^{-1}_{pc}P^T_{pc}f\\ &\le \mathcal{E}\left(z^T P_{pc}\Lambda^{-1}_{pc}P^T_{pc}z\right) + \lambda^{-1}_\beta f^T P_{pc}P^T_{pc}f\\ &= \beta + \frac{\lambda_{\beta+1}f^T P_{pc}P^T_{pc}f\cdot\lambda^{-1}_{\beta+1}f^T P_{res}P^T_{res}f}{\lambda_\beta f^T P_{res}P^T_{res}f}.\end{aligned}$$

According to Eq.(3.13), it is known that

$$\begin{aligned} \lambda_{\beta+1}^{-1} f^T P_{res} P_{res}^T f &= 4J_{th,T_H^2} + \delta, && (3.14) \\ \left(f^T P_{res} P_{res}^T f\right)^{1/2} &> 2\lambda_{\beta+1}^{1/2} J_{th,T_H^2}^{1/2} && (3.15) \end{aligned}$$

with $\delta > 0$. In case that the fault has similar influence on the both subspaces, i.e.

$$f^T P_{pc} P_{pc}^T f \approx f^T P_{res} P_{res}^T f, \tag{3.16}$$

it turns out

$$\mathcal{E}\left(z_f^T P_{pc} \Lambda_{pc}^{-1} P_{pc}^T z_f\right) \leq \beta + \frac{\lambda_{\beta+1}\left(4\chi_\alpha^2(m-\beta) + \delta\right)}{\lambda_\beta}.$$

In case

$$\frac{\lambda_{\beta+1}}{\lambda_\beta} \leq \frac{\mathcal{X}_\alpha^2(\beta) - \beta}{4\mathcal{X}_\alpha^2(m-\beta) + \delta}, \tag{3.17}$$

it follows that

$$\mathcal{E}\left(z_f^T P_{pc} \Lambda_{pc}^{-1} P_{pc}^T z_f\right) \leq \mathcal{X}_\alpha^2(\beta) = J_{th,T^2} \tag{3.18}$$

which indicates that $f$ is expectably undetected by the $T^2$ statistic under condition in Eq.(3.17), although it is detectable using the Hawkin's $T_H^2$ statistic. Since generally $4\mathcal{X}_\alpha^2(m-\beta)$ and $\mathcal{X}_\alpha^2(\beta) - \beta$ are comparable and the singular values $\lambda_\beta \gg \lambda_{\beta+1}$, the condition Eq.(3.17) is a general condition and easy to satisfy.

The previous analysis reveals that $T_{res}^2$ is more sensitive to the fault than the $T^2$ statistic when the fault has the same influence on both subspaces.

### 3.3.2 On the combined index

In this subsection, the sensitivity of combined index will be analyzed. It is straightforward that, for a fault occurred in $P_{pc}$, it will cause same change in $T^2$ and $T_c^2$. Note that the threshold of $T_c^2$ can be calculated by $\chi_\alpha^2(m)$. In addition, since

$$\begin{aligned} \chi_\alpha^2(m) &> \chi_\alpha^2(\beta), \\ \chi_\alpha^2(m) &> \chi_\alpha^2(m-\beta), \end{aligned}$$

the combined index has lower fault sensitivity than the separate use of $T^2$. The similar analysis can be applied on the fault occurred in the residual subspace that delivers the same result.

On the other hand, it always holds

$$\chi_\alpha^2(m) < \chi_\alpha^2(m-\beta) + \chi_\alpha^2(\beta).$$

Thus, there must exist a fault which leads to

$$T_c^2 > \chi_\alpha^2 (m)$$

under the following conditions

$$\begin{aligned} T^2 &< \chi_\alpha^2 (\beta), \\ T_{res}^2 &< \chi_\alpha^2 (m - \beta). \end{aligned}$$

In this case, the combined index may be more sensitive to the fault than using the separate indices.

The previous discussion reveals that

- if the fault $f$ has significantly different influences on the both subspaces, i.e. one of the following two conditions is satisfied

  $$\begin{aligned} f^T P_{pc} P_{pc}^T f &\ll f^T P_{res} P_{res}^T f, \\ f^T P_{pc} P_{pc}^T f &\gg f^T P_{res} P_{res}^T f. \end{aligned}$$

  The separate use of the two test statistics, $T^2$ and $T_{res}^2$, will improve the fault sensitivity compared with the combined index, and

- the use of a combined index is of advantage when the distribution of $\Lambda^{-1} f$ is nearly uniform in the measurement subspace.

According to these observations, each index, i.e. $T^2$, $T_{res}^2$ or $T_c^2$, can be sensitive to a certain kind of faults. Therefore, the joint use of the related test statistics is recommended to improve the fault detection performance.

## 3.4 Fault identification

The fault sensitivity analysis of related test statistic has been discussed so far. In this framework, the issues of identification of off-set and scaling faults will be respectively considered.

### 3.4.1 Identification of off-set fault

As aforementioned, the off-set fault is given by

$$z_f = z + f, \ f \neq 0$$

where $z \sim \mathcal{N}(0, \Phi)$, $\Phi$ is a known matrix and $f$ is an unknown constant vector. It is well known that

$$\bar{z}_f = \frac{1}{N} \sum_{i=1}^{N} z_{f,i}$$

delivers a GLR estimate for $f$, where $z_{f,i}$ $(i = 1, \cdots, N)$ is the $i$-th sample of $z_f$. Suppose that a fault is detected with sample $k$, the off-set fault identification procedure can be briefly summarized as follows: Collect $M$ faulty samples and compute the estimate of $f$, denoted by $\hat{f}$, as

$$\hat{f} = \frac{1}{M+1} \sum_{i=k}^{k+M} z_{f,i}. \tag{3.19}$$

In case that the nominal measurement vector is not zero mean, the $M$ faulty samples shall be firstly centered by the mean value achieved from the training data. Based on the re-centered samples, Eq.(3.19) can be utilized to estimate the off-set fault. It is worth to mention that the above algorithm can also be realized in a recursive manner.

### 3.4.2 Identification of scaling fault

Consider a scaling fault

$$z_F = Fz, \ F \neq I,$$

and suppose that the fault has been detected by standard PCA method with sample $k$. Let $z_{F,k}, \cdots, z_{F,k+M}$ be $M+1$ samples collected after fault detection. Then, it follows that

$$\frac{1}{M} \begin{bmatrix} z_{F,k} & \cdots & z_{F,k+M} \end{bmatrix} \begin{bmatrix} z_{F,k}^T \\ \vdots \\ z_{F,k+M}^T \end{bmatrix} \approx F\Phi F^T = FP\Lambda P^T F^T. \tag{3.20}$$

An SVD on Eq.(3.20) leads to

$$\frac{1}{M} \begin{bmatrix} z_{F,k} & \cdots & z_{F,k+M} \end{bmatrix} \begin{bmatrix} z_{F,k}^T \\ \vdots \\ z_{F,k+M}^T \end{bmatrix} = V\Pi V^T \tag{3.21}$$

with $\Pi = diag\left(\bar{\lambda}_1, \cdots, \bar{\lambda}_m\right)$. Straightforwardly, it follows

$$V\Pi^{1/2} = FP\Lambda^{1/2}.$$

In case that $\Lambda_{res} \approx 0$, the pseudo inverse of $P\Lambda^{1/2}$ is given by

$$\left(P\Lambda^{1/2}\right)^{\dagger} \approx \begin{bmatrix} \Lambda_{pc}^{-1/2} & 0 \\ 0 & 0 \end{bmatrix} \begin{bmatrix} P_{pc}^T \\ P_{res}^T \end{bmatrix}.$$

The estimate of $F$, denoted by $\hat{F}$, can be calculated by

$$\hat{F} = V_1 \Pi_{pc}^{1/2} \Lambda_{pc}^{-1/2} P_{pc}^T \tag{3.22}$$

where

$$\Pi_{pc} = diag\left(\bar{\lambda}_1, \cdots, \bar{\lambda}_\beta\right),$$

$\Pi_{pc}$ contains $\beta$ significant singular values in $\Pi$ and $V_1$ are the corresponding singular vectors.

### 3.4.3 A fault identification algorithm

Assume that a fault has been detected by using $T^2$, $T_{res}^2$ or $T_c^2$ at sample $k$. The major results achieved in this section can be summarized into the following algorithm.

**Fault identification algorithm:**

- Collect $M+1$ faulty samples and center them by the mean value achieved from training data
- Estimate the off-set fault using Eq.(3.19)
- Re-center the samples by $\hat{f}$
- Perform the SVD on Eq.(3.21) based on the re-centered samples
- Compute $\hat{F}$ according to Eq.(3.22).

## 3.5 Concluding remarks

This chapter mainly focuses on the modifications on standard PCA-based fault diagnosis approach. Based on the review of GLR method, a new test statistic for residual subspace is proposed, which is equivalent to the Hawkin's $T_H^2$ statistic but without numerical drawbacks. In comparison with standard SPE statistic, the threshold calculation associated with the proposed test statistic is remarkably simple and does not need statistical approximation. A modified combined index is also developed based on the new test statistic. The further study is dedicated to evaluating these test statistics according to their sensitivities to the fault. As a result, the joint use of these test statistics is recommended. To complete the fault diagnosis framework, an algorithm is finally proposed to identify the off-set and scaling faults.

Unlike the original idea of PCA, which is to reduce the dimension of data by retaining significant variations, both of the principal component subspace and residual subspace should be utilized to achieve reliable fault detection performance. The core of the PCA-based approach consists in a numerically reliable implementation of the $\chi^2$ test for fault detection, which is mainly achieved using the SVD.

# 4 Modifications on PLS-based approach

Besides PCA, PLS is another popular method in MSPM framework. In contrast to PCA, which gives the same weighting to each process variable without considering any causal relationship in the process, PLS extracts the correlation model between process inputs and outputs that may provide further advantages for prediction and fault diagnosis purposes. Although both methods perform a similar way for fault detection, the main aim of PLS is to detect the changes in input variables that are mostly influential to the process outputs by utilizing the correlation information. The basic concepts and algorithms of PLS can be found in [48], [49]. Several modifications of it, such as recursive PLS [89], multiblock PLS [69], [80], local PLS [65] and dynamic PLS [16] are also proposed and implemented in a variety of industrial applications.

Although PLS-based fault diagnosis technique has been widely used, less attention has been paid to the property of the latent space for fault diagnosis purpose. As shown by Eqs.(2.47)-(2.48), the standard PLS algorithm decomposes the input measurement space into two oblique subspaces which may cause some problems for fault diagnosis. Moreover, the standard PLS algorithm introduced in Subsection 2.4.2 is computationally complicated, and most importantly, the correlation model is difficult to interpret due to many iterative computational steps caused by the large number of latent variables.

Motivated by aforementioned observations, in the present work, a modified approach is firstly proposed in order to overcome these difficulties [129]. Based on it, the complete process monitoring scheme is further designed. To this end, a brief comparison between the proposed method and existing approaches is given. Notice that the similar procedure introduced in Section 3.4 can also be utilized for fault identification.

## 4.1 Problem formulation

It is known that standard PLS algorithm divides input measurement space, $U$, into two subspaces, i.e. $\hat{U}$ and $\tilde{U}$, depending on their correlation with output variables, $Y$. Based on it, the $T^2$ and SPE statistics are typically used for monitoring both subspaces. Al-

though standard PLS algorithm works in many cases, the complexity of algorithm, especially the iterative computation procedures caused by many latent variables, lead to the PLS model to be difficult to explain. In addition, it reveals that the standard PLS approach may result in partial correlation between $\hat{U}$ and $Y$ thus, the orthogonal variations in $\hat{U}$ are useless for outputs prediction. Moreover, $\tilde{U}$ may contain large variability of $U$ and therefore, is not suitable for monitoring as residual subspace by means of SPE statistic. To solve these problems, Zhou et al. [134] proposed the so-called total projection to latent structure (TPLS) approach, which is based on the results from standard PLS algorithm and further performs decomposition on certain subspaces.

The drawback due to orthogonal variations amongst interacting subspaces comes from the nature of the standard PLS algorithm. Hence, a slight modification is necessary in order to achieve better fault diagnosis performance. From the application point of view, a desired modification approach shall be computationally less expensive than the standard one and more importantly, avoid the drawbacks mentioned earlier. As a result, the following two issues must be resolved:

- Perform a complete decomposition on input and output spaces, such that the correlation model becomes

$$U = \hat{U} + \tilde{U}, \tag{4.1}$$

$$Y = \hat{Y} + E_y, \tag{4.2}$$

$$\hat{Y} = UM = \hat{U}M \tag{4.3}$$

  where the subspaces $\hat{Y}$ and $E_y$ are respectively correlated and uncorrelated with the input space. $\hat{U}$ and $\tilde{U}$ denote an orthogonal decomposition on input space such that $\tilde{U}$ has no contribution for outputs prediction, while $\hat{U}$ is fully responsible for predicting $Y$ thus does not contain variations orthogonal to $Y$, and

- Develop suitable test statistics and fault identification algorithm to complete the fault diagnosis scheme.

To deal with the first issue, a modified approach is derived in the next section.

## 4.2 A modified approach

### 4.2.1 A complete decomposition of $Y$ space

Based on the discussion so far, it is possible to write the desired relation as follows

$$Y = UM + E_y = \hat{Y} + E_y \tag{4.4}$$

where $M$ is the coefficient matrix and contains correlation information between $U$ and $Y$. $E_y$ is the residual part of $Y$ which is uncorrelated with the input measurement, i.e.

$$\operatorname{cov}(e_y, u) = 0$$

where $u^T$ and $e_y^T$ are row vectors in $U$ and $E_y$, respectively. Without the loss of generality, $M$ is assumed to be a full column-rank matrix. According to Eq.(4.4), in case of $N \gg max\{l, m\}$, it follows that

$$\frac{1}{N-1}Y^TU = \frac{1}{N-1}M^TU^TU + \frac{1}{N-1}{E_y}^TU \approx M^T\frac{U^TU}{N-1}.$$

Thus, if matrix $U^TU$ is invertible, $M$ can be easily calculated as:

$$M = \left(U^TU\right)^{-1}U^TY. \tag{4.5}$$

Note that, if the product $U^TU$ is not a full rank matrix, it follows that

$$M = \left(U^TU\right)^{\dagger}U^TY. \tag{4.6}$$

The pseudo inverse is calculated as:

$$\left(U^TU\right)^{\dagger} = P_{u,pc}\Lambda_{u,pc}^{-1}P_{u,pc}^T \tag{4.7}$$

where an SVD on $U^TU$ leads to

$$U^TU = P_u\Lambda_uP_u^T = \begin{bmatrix} P_{u,pc} & P_{u,res} \end{bmatrix}\begin{bmatrix} \Lambda_{u,pc} & 0 \\ 0 & \Lambda_{u,res} \end{bmatrix}\begin{bmatrix} P_{u,pc}^T \\ P_{u,res}^T \end{bmatrix} \tag{4.8}$$

with $\Lambda_{u,res} = 0$. It is now easy to show that $Y$ is completely decomposed into two parts as desired in Eq.(4.4) depending on their correlations with input measurement space.

### 4.2.2 Orthogonal decomposition of $U$ space

So far, a desired decomposition on $Y$ has been achieved and based on this result, it is necessary to decompose $U$ into two parts, i.e. $\hat{U}$ and $\tilde{U}$, such that $\hat{U}$ does not contain variations orthogonal to $Y$ and thus has the full contribution in predicting $Y$, while $\tilde{U}$ gives no contribution.

A simple way to perform the aforementioned decomposition is achieved by projecting $U$ orthogonally onto the subspaces $S_{\hat{u}} \equiv span\{M\}$ and $S_{\tilde{u}} \equiv span\{M\}^{\perp}$, respectively. Consequently, it follows that

$$\tilde{U}M = 0, \tag{4.9}$$

$$\hat{Y} = UM = \hat{U}M, \tag{4.10}$$

$$\hat{U} \in S_{\hat{u}},\ \tilde{U} \in S_{\tilde{u}}. \tag{4.11}$$

For orthogonal projection, the following steps are necessary:

- Perform the SVD on matrix $MM^T$

$$MM^T = \begin{bmatrix} P_M & \tilde{P}_M \end{bmatrix} \begin{bmatrix} \Lambda_M & 0 \\ 0 & 0 \end{bmatrix} \begin{bmatrix} P_M^T \\ \tilde{P}_M^T \end{bmatrix} \tag{4.12}$$

  with $P_M \in \mathcal{R}^{l\times m}$, $\tilde{P}_M \in \mathcal{R}^{l\times(l-m)}$, $\Lambda_M \in \mathcal{R}^{m\times m}$.

- Construct $\Pi_M$, $\Pi_M^\perp$, which are the orthogonal projectors of the subspaces $S_{\hat{u}}$ and $S_{\tilde{u}}$ respectively, i.e.

$$\Pi_M = P_M P_M^T, \tag{4.13}$$
$$\Pi_M^\perp = \tilde{P}_M \tilde{P}_M^T. \tag{4.14}$$

- Project $U$ onto subspaces $S_{\hat{u}} \equiv span\{M\}$ and $S_{\tilde{u}} \equiv span\{M\}^\perp$, which are mutually orthogonal. Hence, $U$ is decomposed into two parts, i.e.

$$U = \hat{U} + \tilde{U} \tag{4.15}$$

  such that

$$\hat{U} = U\Pi_M = UP_M P_M^T \in S_{\hat{u}} \equiv span\{M\}, \tag{4.16}$$
$$\tilde{U} = U\Pi_M^\perp = U\tilde{P}_M \tilde{P}_M^T \in S_{\tilde{u}} \equiv span\{M\}^\perp. \tag{4.17}$$

The major results achieved in this section can be summarized as the following algorithm. Table 4.1 provides the descriptions of related subspaces.

**Algorithm of the modified approach**

- Calculate the coefficient matrix $M$ according to Eq.(4.5) or Eq.(4.6)
- Do an SVD on $MM^T$, see Eq.(4.12)
- Calculate the orthogonal projectors by Eqs.(4.13)-(4.14)
- (optional) Decompose $U$ according to Eqs.(4.15)-(4.17)
- (optional) Decompose $Y$ as $\hat{Y} = UM$, $E_y = Y - \hat{Y}$.

**Table 4.1:** Description of subspaces

| Subspace | Description |
|---|---|
| $\hat{U}$ | subspace of $U$ that is fully responsible for predicting $Y$ |
| $\tilde{U}$ | subspace of $U$ that is orthogonal to $\hat{U}$ and has no contribution for prediction of $Y$ |
| $\hat{Y}$ | subspace of $Y$ that is correlated to $U$ and represents the prediction of outputs |
| $E_y$ | subspace of $Y$ that is uncorrelated to $U$ |

It is worth to point out that

- the proposed approach calculates the coefficient matrix $M$ in a least square manner and based on it, the orthogonal decomposition on the input space is performed,
- compared to the standard PLS algorithm, the proposed approach provides a desired decomposition on input and output spaces as shown in Eqs.(4.1)-(4.3), and thus avoids the drawbacks of standard PLS algorithm, and
- the proposed approach provides a more clear interpretation of the correlation model and has much less computational overload than the standard PLS algorithm.

## 4.3 The fault defection scheme

Based on the proposed approach, in this section, the fault detection scheme will be discussed in detail.

### 4.3.1 Monitoring subspace $\hat{U}$

Since $\hat{U}$ and $\hat{Y}$ are mutually correlated, it is easy to prove that they are equivalent in the sense of change detection. Thus, in this subsection, the issue of monitoring on subspace $\hat{U}$ is mainly studied, which enables detecting the fault in the input space that has influence on the outputs. To this end, consider the quadratic form of vector $\hat{u}$, which is recommended

to design the test statistic:

$$\hat{u}^T\hat{u} = u^T P_M P_M^T P_M P_M^T u = u^T P_M P_M^T u. \tag{4.18}$$

Since

$$rank\left\{P_M^T U^T\right\} = m,$$

$P_M^T u \in \mathcal{R}^m$ is a suitable candidate for $T^2$ statistic for monitoring $\hat{U}$. Thus, the $T^2$ statistic follows

$$T_{\hat{u}}^2 = u^T P_M \left(\frac{P_M^T U^T U P_M}{N-1}\right)^{-1} P_M^T u. \tag{4.19}$$

The threshold for $T_{\hat{u}}^2$ is given by

$$J_{th,T_{\hat{u}}^2} = \frac{m\left(N^2-1\right)}{N\left(N-m\right)} F_\alpha\left(m, N-m\right) \tag{4.20}$$

where $F\left(m, N-m\right)$ is $F$-distribution with $m$ and $N-m$ degrees of freedom and $\alpha$ is user-specified confidence level. Recalling the GLR technique, in case of large enough $N$, the threshold for $T_{\hat{u}}^2$ can be determined by $\chi^2$ test instead of $F$-distribution as shown in Eq.(4.20), i.e.

$$J_{th,T_{\hat{u}}^2} = \chi_\alpha^2(m). \tag{4.21}$$

The fault detection logic is:

$$T_{\hat{u}}^2 > J_{th,T_{\hat{u}}^2} \Longrightarrow \text{a fault in inputs is detected that is influential on outputs.}$$

### 4.3.2 Monitoring subspace $\tilde{U}$

As mentioned in the previous section, $\tilde{U}$ represents a subspace in $U$ that is not correlated to $Y$ and has no contribution for output prediction. Therefore, similar to Eq.(4.18), the quadratic form of $\tilde{u}$ can be written as:

$$\tilde{u}^T\tilde{u} = u^T \tilde{P}_M \tilde{P}_M^T \tilde{P}_M \tilde{P}_M^T u = u^T \tilde{P}_M \tilde{P}_M^T u. \tag{4.22}$$

Noting that

$$rank\left\{\tilde{P}_M^T U^T\right\} = l - m,$$

hence, $\tilde{P}_M^T u \in \mathcal{R}^{n-m}$ can be used as $T^2$ statistic for monitoring $\tilde{U}$. Thus, it follows

$$T_{\tilde{u}}^2 = u^T \tilde{P}_M \left(\frac{\tilde{P}_M^T U^T U \tilde{P}_M}{N-1}\right)^{-1} \tilde{P}_M^T u. \tag{4.23}$$

The threshold for $T_{\tilde{u}}^2$ is

$$J_{th,T_{\tilde{u}}^2} = \frac{(l-m)\left(N^2-1\right)}{N\left(N-l+m\right)} F_\alpha\left(l-m, N-l+m\right) \tag{4.24}$$

where $F(l-m, N-l+m)$ is $F$-distribution with $l-m$ and $N-l+m$ degrees of freedom under confidence level $\alpha$. Similarly, the threshold can be determined by $J_{th,T_{\tilde{u}}^2} = \chi_\alpha^2(l-m)$. The fault detection logic is

$$T_{\tilde{u}}^2 > J_{th,T_{\tilde{u}}^2} \Longrightarrow \text{a fault in inputs is detected without influence on outputs.}$$

### 4.3.3 Monitoring subspace $E_y$

In this subsection, monitoring and change detection based on $E_y$ is investigated. It is known that $E_y$ is not correlated to input space and can be represented by

$$E_y = Y - \hat{Y} = \left(\hat{U} + \tilde{U}\right) M + E_y - \hat{U}M \tag{4.25}$$

which shows that $E_y$ is not influenced by any change in input measurement. In other words, only the faults occurred in $Y$, e.g. sensor failures, can be detected by monitoring $E_y$. Generally, $e_y$ is assumed small in magnitude and contains insignificant variability information. Based on the available measurement $y$, an SPE statistic can be designed as

$$\text{SPE}_y = \|e_y\|^2 = \|y - \hat{y}\|^2 = \left\|y - M^T u\right\|^2. \tag{4.26}$$

The related threshold is

$$J_{th,SPE_y} = g_y \chi_\alpha^2(h_y) \tag{4.27}$$

where $g_y\chi^2(h_y)$ is $\chi^2$-distribution with scaling factor $g_y = S/2\mu$ and $h_y = 2\mu^2/S$ under given confidence level $\alpha$. $\mu$ and $S$ are sample mean and variance of $\text{SPE}_y$ statistic in Eq.(4.26). In case that input measurement is fault free, the fault detection logic is given as:

$$\text{SPE}_y \leq J_{th,SPE_y} \Longrightarrow \text{fault free, otherwise a fault in } y \text{ is detected.}$$

Note that, in Subsection 3.2.2, a new test statistic, which is similar to Hawkin's $T_H^2$ statistic but without the numerical drawback, has been proposed instead of SPE. Moreover, if $e_y$ is large and retains significant variability information, the new statistic can be simply extended to a combined index to ensure high fault detectability. In this case, the test statistic for $E_y$ becomes

$$T_{\tilde{y}}^2 = e_y^T P_{\tilde{y}} \Xi P_{\tilde{y}}^T e_y \tag{4.28}$$

**Table 4.2:** Subspaces and related test statistics

| Subspace | Test statistics | Threshold |
|---|---|---|
| $\hat{U}$ | $T_{\hat{u}}^2$ | $\frac{m\left(N^2-1\right)}{N(N-m)}F_\alpha\left(m, N-m\right)$ |
| $\tilde{U}$ | $T_{\tilde{u}}^2$ | $\frac{(l-m)\left(N^2-1\right)}{N(N-l+m)}F_\alpha\left(l-m, N-l+m\right)$ |
| $E_y$ | $T_{\tilde{y}}^2$ | $\lambda_m\chi_\alpha^2\left(m\right)$ |

where

$$\Xi = diag\left(\frac{\lambda_m}{\lambda_1}, \cdots, \frac{\lambda_m}{\lambda_{m-1}}, 1\right),$$
$$\lambda_1 \geq \cdots \geq \lambda_{\bar{\beta}} \gg \lambda_{\bar{\beta}+1} \geq \cdots \geq \lambda_m > 0,$$
$$\Lambda_{\tilde{y},pc} = diag(\lambda_1, \cdots, \lambda_{\bar{\beta}}),\ \Lambda_{\tilde{y},res} = diag(\lambda_{\bar{\beta}+1}, \cdots, \lambda_m),$$
$$\frac{1}{N-1}E_y^T E_y = P_{\tilde{y}}\Lambda_{\tilde{y}}P_{\tilde{y}}^T,\ \Lambda_{\tilde{y}} = \begin{bmatrix} \Lambda_{\tilde{y},pc} & 0 \\ 0 & \Lambda_{\tilde{y},res} \end{bmatrix}.$$

Notice that $\Lambda_{\tilde{y},pc}$ and $\Lambda_{\tilde{y},res}$ are calculated by the SVD of $\frac{1}{N-1}E_y^T E_y$ in the off-line design phase. The corresponding threshold is

$$J_{th,T_{\tilde{y}}^2} = \lambda_m\chi_\alpha^2\left(m\right). \tag{4.29}$$

The test statistics related to different subspaces are listed in Table 4.2. To this end, it is necessary to point out that

- the proposed approach employs two $T^2$ indices to monitor input measurement space. As against four test statistics proposed in [134], the proposed monitoring scheme works more efficiently, and
- in practice, the output vector $y$, e.g. the one serves as product quality variable, is not always available on-line. In this case, monitoring subspace $E_y$ by means of $\text{SPE}_y$ or $T_{\tilde{y}}^2$ will induce time delay and it is usually used in off-line analysis.

## 4.4 A brief comparison

Table 4.3 offers a brief comparison among the proposed approach, PLS and TPLS [134], in which the computation complexity of the off-line algorithm, the number of on-line test statistics as well as design parameters are mainly taken into consideration.

**Table 4.3:** Comparison among PLS, TPLS, modified approach

| Method | Computation complexity | Statistics | Parameter |
|---|---|---|---|
| PLS | $\gamma$ times SVD on $l \times l$ matrix | 2 | No. of LVs |
| TPLS | $\gamma + 1$ SVD on $l \times l$ + 1 SVD on $m \times m$ matrices | 4 | No. of LVs |
| Modified approach | 2 times SVD on $l \times l$ matrix | 2 | no |

The computational complexities of these approaches mainly come from the SVD on covariance matrices with different dimensions. Standard PLS needs $\gamma$ times SVD on $l \times l$ matrix. TPLS is based on the results from standard PLS algorithm and additionally needs 2 times SVD on $m \times m$ matrix and an SVD on $l \times l$ matrix. The computation cost of the proposed approach mainly comes from 2 times SVD on $l \times l$ matrix that shows relative lower computation cost compared to PLS and TPLS in case of $\gamma > 2$.

As aforementioned, for on-line implementation, the PLS and modified approach employ 2 test statistics to monitor the input measurement space, while TPLS has 4 test statistics for the same purpose. Moreover, it is worth mentioning that the number of LVs, $\gamma$, is an important design parameter in standard PLS to achieve successful process monitoring. The leave-N-out cross validation is mostly referred in the literature for selecting the number of LVs. Although it is a widely used criterion in practice, different results can be obtained according to the choice of $N$, which may finally influence the performance of the overall fault diagnosis system. Based on this observation, the approach without such a design parameter will show much more advantages from the application point of view.

## 4.5 On fault identification issue

Assume that a fault of input measurement has been detected using $T^2_{\hat{u}}$ or $T^2_{\tilde{u}}$. The fault identification on the input space can be similarly achieved according to the algorithm presented in Subsection 3.4.3. It is known that, the fault detected by $T^2_{\tilde{u}}$ will finally influence the output measurement $y$. Thus, if test statistic $T^2_{\tilde{y}}$ indicates a fault occurred on $y$, the influence of faulty input measurement shall be firstly subtracted in order to reflect the real fault information occurred in outputs. Based on it, the similar fault identification procedure can be applied to identify the faults in output measurement space. To this end,

a brief algorithm can be summarized as follows.

**Fault identification algorithm:**

- Assume that a fault on input measurement is detected by $T^2_{\hat{u}}$ or $T^2_{\tilde{u}}$ at time sample $k$
- Utilize the fault identification procedure presented in Subsection 3.4.3 to identify the fault in input measurement space
- Suppose a fault on output measurement is also detected by $T^2_{\tilde{y}}$. Subtract the influence of the faulty input measurement from the available output measurement. Thus, the data reflecting the real faulty information occurred in $y$ are obtained.
- Utilize similar fault identification procedure to identify the fault in output space.

## 4.6 Simulation examples

In this section, the results obtained with an academic example are presented to illustrate the performance of the modified approach. Consider the following numerical example [134]:

$$u_k = Az_k + e_k, \tag{4.30}$$

$$y_k = Cu_k + v_k \tag{4.31}$$

where

$$A = \begin{bmatrix} 1 & 3 & 4 & 4 & 0 \\ 3 & 0 & 1 & 4 & 1 \\ 1 & 1 & 3 & 0 & 0 \end{bmatrix}^T, C = \begin{bmatrix} 2 & 2 & 1 & 1 & 0 \end{bmatrix},$$

and the noise terms $v_k \sim \mathcal{N}(0, 0.01)$, $e_{k,j} \sim \mathcal{U}([0\ 0.05])$ and $z_{k,i} \sim \mathcal{U}([0\ 1])$ for $i = 1, \cdots, 3$ and $j = 1, \cdots, 5$. $\mathcal{U}$ denotes the uniform distribution.

An additive fault is considered in the following form:

$$u_f = u + \Xi f \tag{4.32}$$

where $u$ is the fault free process vector, $\Xi \in \mathcal{R}^{l \times 1}$ denotes fault direction vector and scalar $f$ is the magnitude of fault.

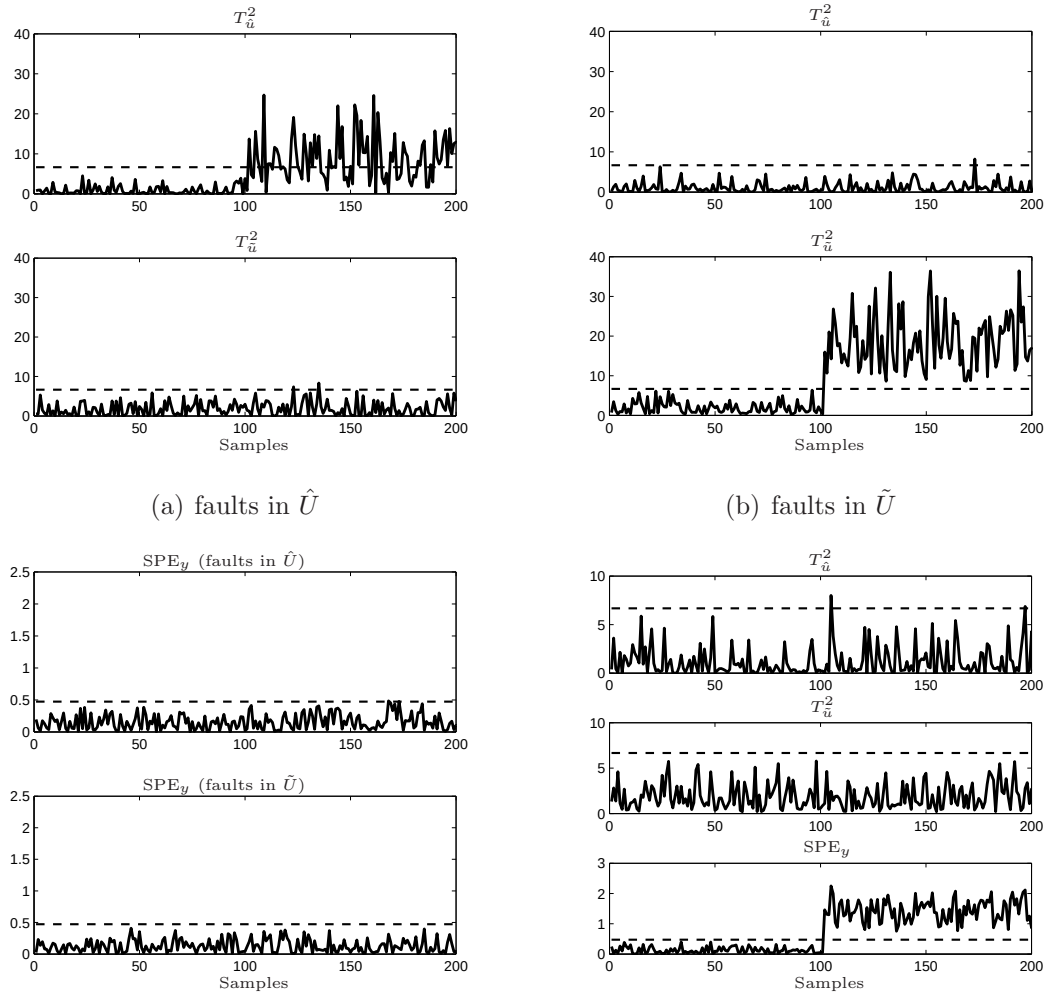


(a) faults in $\hat{U}$

(b) faults in $\tilde{U}$

(c) SPE$_y$ for faults in $\hat{U}$ and $\tilde{U}$

(d) $T^2_{\hat{u}}$, $T^2_{\tilde{u}}$ and SPE$_y$ statistic for faults in output

**Figure 4.1:** Modified approach based process monitoring

For the experiments, following design steps are carried out:

- *Off-line training phase:* Collect training data consisting of 1000 samples and perform the modified approach to calculate $M$, $P_M$ and $\tilde{P}_M$.

- *Threshold computation:* Compute thresholds for $J_{th,T^2_{\hat{u}}}$ and $J_{th,T^2_{\tilde{u}}}$ with $N = 1000$, $l = 5$, $m = 1$, confidence level $\alpha = 0.99$. Optionally, compute $J_{th,SPE_y}$.

- *On-line fault detection:* Simulate the example given by Eqs.(4.30)-(4.31) for 200 samples with fault occurrence after the 100-th time sample. Three different faults are considered as follows.
  **Fault in $\hat{U}$:** As shown in Eq.(4.32), $\Xi$ is selected as the first column of $P_M$ and

**Table 4.4:** Fault detection rate (%): faults in $\hat{U}$

| Magnitude of $f$ | Modified ($T^2_{\hat{u}}$) | Modified ($T^2_{\tilde{u}}$) | PLS ($T^2$) | PLS (SPE) |
|---|---|---|---|---|
| 2 | 8 | 2 | 3 | 5 |
| 4 | 39 | 2 | 12 | 6 |
| 6 | 60 | 2 | 24 | 9 |
| 8 | 75 | 2 | 33 | 15 |
| 10 | 96 | 2 | 57 | 39 |

**Table 4.5:** Fault detection rate (%): faults in $\tilde{U}$

| Magnitude of $f$ | Modified ($T^2_{\hat{u}}$) | Modified ($T^2_{\tilde{u}}$) | PLS ($T^2$) | PLS (SPE) |
|---|---|---|---|---|
| 2 | 1 | 21 | 1 | 9 |
| 4 | 1 | 89 | 1 | 44 |
| 6 | 1 | 100 | 1 | 97 |
| 8 | 1 | 100 | 1 | 100 |
| 10 | 1 | 100 | 1 | 100 |

$f = 6$
**Fault in $\tilde{U}$:** Similar to fault in $\hat{U}$, $\Xi$ is selected as the first column of $\tilde{P}_M$, $f = 6$
**Fault in $Y$:** Additive fault on output.
Compute $T^2_{\hat{u}}$ and $T^2_{\tilde{u}}$. Optionally, calculate $\text{SPE}_y$.

Fig. 4.1(a) shows the result when fault occurs in $\hat{U}$, which can be successfully detected by $T^2_{\hat{u}}$ without significant influence on $T^2_{\tilde{u}}$. On the other hand, Fig. 4.1(b) indicates that if a fault occurs in $\tilde{U}$, $T^2_{\tilde{u}}$ crosses the threshold without significant change in $T^2_{\hat{u}}$. Moreover, as seen from Table 4.4, compared to the standard PLS, the proposed approach not only offers correct fault location information but also provides significant improvement on fault detection rate. $T^2_{\hat{u}}$ gives higher fault detection rate than $T^2$ and $T^2_{\tilde{u}}$ gives lower false alarm rate than SPE statistic of standard PLS approach. Similar results are obtained for fault occurred in $\tilde{U}$ as shown by Table 4.5. In addition, if the fault occurred in input measurement space, $\text{SPE}_y$ statistic gives no alarm, see Fig. 4.1(c). Fig. 4.1(d) illustrates $T^2_{\hat{u}}$, $T^2_{\tilde{u}}$ and $\text{SPE}_y$ statistics if faults occurred in output. It can be seen that only $\text{SPE}_y$ exceeds the threshold that delivers useful information of the location of the fault.

## 4.7 Concluding remarks

In this chapter, a new approach is proposed to overcome the drawbacks of standard PLS-based fault diagnosis technique. This approach firstly calculates the coefficient matrix in a least square manner and then based on it, divides the input measurement into two orthogonal subspaces according to their correlation with outputs. The proposed approach is considerably simpler than the standard technique, and most importantly, avoids the drawbacks and provides a clear interpretation for the correlation model. Based on the proposed approach, the fault detection scheme is designed, in which only two $T^2$ statistics are used for monitoring the overall input space. An algorithm for fault identification is also included in this study.

# 5 Subspace aided data-driven approach

PCA- and PLS-based fault diagnosis methods are powerful tools to deal with the applications under the ideal stationary operating conditions. However, in the industrial applications, we often meet situations that the operating conditions are significantly different from those conditions assumed for the application of the basic MSPM methods. This issue can be illustrated, e.g. by the schematic description of a typical industrial batch process presented in Fig. 5.1. It is evident that the basic MSPM methods like PCA and PLS are not able to construct a reliable fault diagnosis scheme, since

- the process dynamics has not been taken into consideration in the basic MSPM approaches,
- an explicit model for the internal relations between the process variables and operating conditions is always not available in practice and,
- the normalization procedure, which serves as a basic step for MSPM methods, is not suitable for such a process due to wide operation region of process variables.

Although more sophisticated extensions of basic MSPM approaches have been proposed to deal with such dynamic processes [10], [29], [57], [71], [94], [123], a simple method

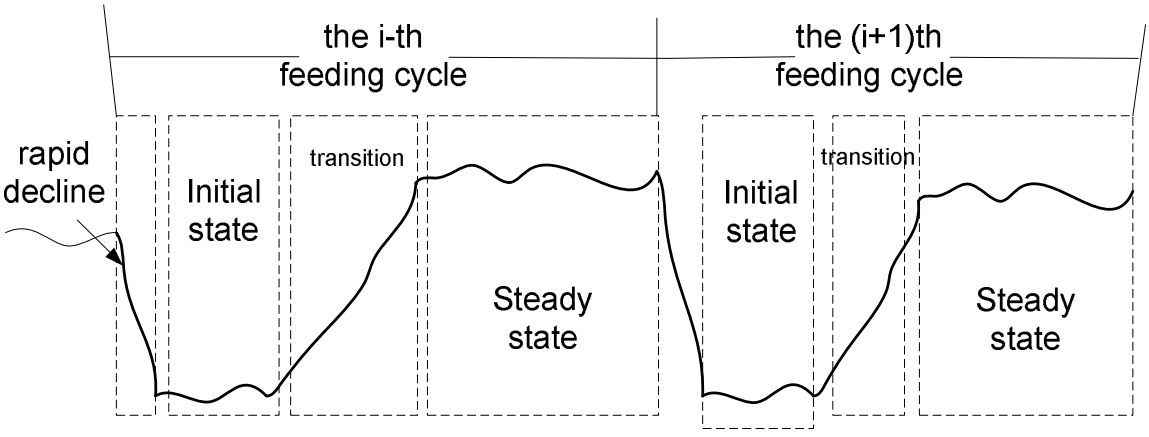


**Figure 5.1:** Schematic description of an industrial batch process

without complicated algorithm is still of great interest from the application viewpoint to reduce the design and engineering efforts.

On the other hand, it is known that the main advantages of the model-based fault diagnosis methods lie in their abilities to deal with aforementioned problems that ensure most efficient way for dynamic process monitoring. Unfortunately, their applications are often unrealistic due to the sophisticated modeling procedure from the first principles, especially for large-scale industrial process.

An alternative way, which is more simple than construction of process model from the first principles, is identification of the process model from operation data. For this purpose, SIM techniques that directly identify the complete state space matrices have gained tremendous attention in the last two decades and have been successfully implemented in many industrial applications [36], [87], [91]. Provided the identified process model, observer and parity space based FDI schemes can be designed [50], [106], [131]. The block diagram in Fig.5.2 describes the classic subspace identification aided design for observer-based fault diagnosis system, in which the state space matrices are identified from the estimated state sequence and the residual generator based on DO or parity relation is then designed according to the model-based FDI schemes described in Section 2.2.

In the present work, an alternative procedure is proposed [24]. As illustrated in Fig. 5.2, the central idea behind the new method is the design of the parameters of DO based on the primary form of residual generators, whose parameters can be directly identified from the process data. In this way, the system identification becomes a part of the fault diagnosis system that leads to a shorter, easier and faster design procedure. A basic assumption in the proposed design scheme is that the mathematical model of the process under consideration is not available. This new approach is of significant practical interest due to the following features:

- The proposed approach is suitable for the application under industrial operating conditions.
- The design procedure is intuitive yet simple and only based on the measured data from the process under consideration.
- Primary fault detection can be realized with the minimal set of identified parameters that is very important and valuable for the application engineers in early project phase to check the realizability of an FDI scheme.
- No special knowledge of modern control theory is needed for design of observer-based residual generators.

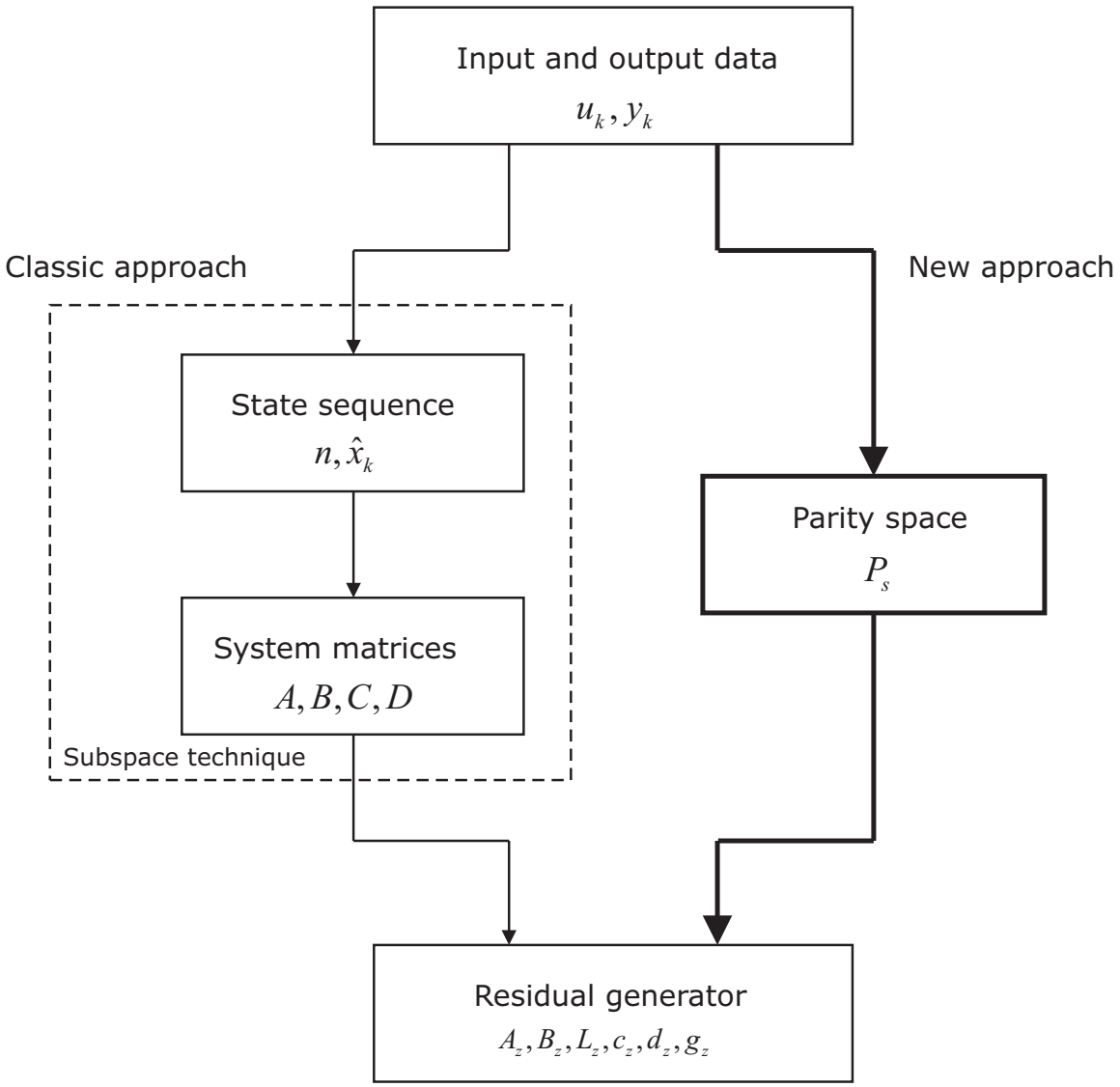


**Figure 5.2:** SIM and new approach

The proposed work is strongly motivated by the successful application of basic MSPM techniques in process industry but also by the intimate relationship between the SIM and parity vectors, which has been studied in [3], [41], [75], [93], [110], [111].

## 5.1 Preliminaries on subspace aided approach

### 5.1.1 Mathematical notations

Assume that the process under consideration can be modeled as an LTI system described by

$$\begin{aligned} x(k+1) &= Ax(k) + Bu(k) + w(k), && (5.1)\\ y(k) &= Cx(k) + Du(k) + v(k). && (5.2) \end{aligned}$$

The model equations are introduced in Eqs.(2.1)-(2.2) in Chapter 2 with $w(k) \in \mathcal{R}^n$, $v(k) \in \mathcal{R}^m$, which are assumed to be zero-mean Gaussian distributed white noise satisfying

$$\mathcal{E}\left( \begin{bmatrix} w(i) \\ v(i) \end{bmatrix} \begin{bmatrix} w(j)^T & v(j)^T \end{bmatrix} \right) = \begin{bmatrix} Q & S \\ S^T & R \end{bmatrix} \delta_{ij} \tag{5.3}$$

where $\delta_{ij}$ is the Kronecker delta function. It is assumed that the system matrices $A, B, C$ and $D$, model order $n$ and matrices $Q$, $R$ and $S$ are unknown *a priori*.

Introduce the following data structure:

$$\begin{aligned} y_s(k) &= \begin{bmatrix} y(k-s+1) \\ y(k-s+2) \\ \vdots \\ y(k) \end{bmatrix} \in \mathcal{R}^{sm},\ u_s(k) = \begin{bmatrix} u(k-s+1) \\ u(k-s+2) \\ \vdots \\ u(k) \end{bmatrix} \in \mathcal{R}^{sl},\\ v_s(k) &= \begin{bmatrix} v(k-s+1) \\ v(k-s+2) \\ \vdots \\ v(k) \end{bmatrix} \in \mathcal{R}^{sm},\ w_s(k) = \begin{bmatrix} w(k-s+1) \\ w(k-s+2) \\ \vdots \\ w(k) \end{bmatrix} \in \mathcal{R}^{sn} \end{aligned}$$

where the integer $s$ is user-defined parameter that determines the number of lagged measurements and, generally, $s > n$. The input, output and state variables can be further congregated as the so-called block Hankel structures:

$$\begin{aligned} X_i &= \begin{bmatrix} x(k+1) & x(k+2) & \cdots & x(k+N) \end{bmatrix} \in \mathcal{R}^{n\times N},\\ Y_p &= \begin{bmatrix} y_s(k) & y_s(k+1) & \cdots & y_s(k+N-1) \end{bmatrix} \in \mathcal{R}^{sm\times N},\\ U_p &= \begin{bmatrix} u_s(k) & u_s(k+1) & \cdots & u_s(k+N-1) \end{bmatrix} \in \mathcal{R}^{sl\times N},\\ Y_f &= \begin{bmatrix} y_s(k+s) & y_s(k+s+1) & \cdots & y_s(k+N+s-1) \end{bmatrix} \in \mathcal{R}^{sm\times N},\\ U_f &= \begin{bmatrix} u_s(k+s) & u_s(k+s+1) & \cdots & u_s(k+N+s-1) \end{bmatrix} \in \mathcal{R}^{sl\times N} \end{aligned}$$

where $N$ is the length of available data samples. Similarly, the noise variables are also gathered in Hankel structures:

$$\begin{aligned} W_p &= \left[ \begin{array}{cccc} w_s(k) & w_s(k+1) & \cdots & w_s(k+N-1) \end{array} \right] \in \mathcal{R}^{sn\times N}, \\ V_p &= \left[ \begin{array}{cccc} v_s(k) & v_s(k+1) & \cdots & v_s(k+N-1) \end{array} \right] \in \mathcal{R}^{sm\times N}, \\ W_f &= \left[ \begin{array}{cccc} w_s(k+s) & w_s(k+s+1) & \cdots & w_s(k+N+s-1) \end{array} \right] \in \mathcal{R}^{sn\times N}, \\ V_f &= \left[ \begin{array}{cccc} v_s(k+s) & v_s(k+s+1) & \cdots & v_s(k+N+s-1) \end{array} \right] \in \mathcal{R}^{sm\times N}. \end{aligned}$$

The subscripts $p$, $f$ denote the past and future data, respectively. Construct inputs and outputs block Hankel structures into:

$$Z_p = \left[ \begin{array}{c} Y_p \\ U_p \end{array} \right] \in \mathcal{R}^{s(l+m)\times N}, \tag{5.4}$$

$$Z_f = \left[ \begin{array}{c} Y_f \\ U_f \end{array} \right] \in \mathcal{R}^{s(l+m)\times N}. \tag{5.5}$$

Therefore, Eqs.(5.1)-(5.2) can be brought into an extended model structure, similar as Eq.(2.29):

$$Y_f = \Gamma_s X_i + H_{u,s} U_f + H_{w,s} W_f + V_f \tag{5.6}$$

where

$$\Gamma_s = \left[ \begin{array}{c} C \\ CA \\ \vdots \\ CA^{s-1} \end{array} \right], \; H_{u,s} = \left[ \begin{array}{cccc} D & 0 & \cdots & 0 \\ CB & D & \ddots & 0 \\ \vdots & \ddots & \ddots & \vdots \\ CA^{s-2}B & CA^{s-1}B & \cdots & D \end{array} \right],$$

$$H_{w,s} = \left[ \begin{array}{cccc} 0 & 0 & \cdots & 0 \\ C & 0 & \ddots & 0 \\ \vdots & \ddots & \ddots & \vdots \\ CA^{s-2} & \cdots & C & 0 \end{array} \right].$$

The extended model structure given by Eq.(5.6) is the core of the SIM. Recall the definition of parity vector and parity space in Eqs.(2.23)-(2.24) and denote them as

$$\upsilon_s = \left[ \begin{array}{cccc} \upsilon_{s,0} & \upsilon_{s,1} & \cdots & \upsilon_{s,s-1} \end{array} \right], \tag{5.7}$$

$$\beta_s = \left[ \begin{array}{cccc} \beta_{s,0} & \beta_{s,1} & \cdots & \beta_{s,s-1} \end{array} \right] \tag{5.8}$$

where $\upsilon_s \in \Gamma_s^{\perp}$, $\beta_s \in \Gamma_s^{\perp} H_{u,s}$ and $\upsilon_{s,i} \in \mathcal{R}^{1\times m}$, $\beta_{s,i} \in \mathcal{R}^{1\times l}$ for $i = 1, \cdots, s-1$.

### 5.1.2 Relations between SIM and PCA

Recall that the core of the PCA-based fault diagnosis technique consists in a numerical reliable implementation of the $\chi^2$ test, which is mainly achieved based on the SVD of data matrix. On the other hand, SIM aims to extract state space model by performing the SVD on the training data matrix described in Eq.(5.5), which can be treated as a time-lagged extension of Eq.(2.34) in the standard PCA algorithm.

The PCA method decomposes the data matrix $Z_f^T$ into two parts, i.e.

$$Z_f^T = TP^T + \tilde{T}\tilde{P}^T \tag{5.9}$$

where $T \in \mathcal{R}^{N\times\beta}$, $\tilde{T} \in \mathcal{R}^{N\times(s(l+m)-\beta)}$ are score matrices and $P \in \mathcal{R}^{s(l+m)\times\beta}$, $\tilde{P} \in \mathcal{R}^{s(l+m)\times(s(l+m)-\beta)}$ are loading matrices. The residual score follows $\tilde{T} = 0$ in the noise free case. It can be shown that the number of PCs, i.e. $\beta$, depends on the model order $n$. Since the score and loading matrices are computed with the help of SVD over $Z_f^T$, it is possible to rewrite Eq.(5.9) as

$$Z_f = \begin{bmatrix} U_{z,pc} & U_{z,res} \end{bmatrix} \begin{bmatrix} \Lambda_{z,pc} & 0 \\ 0 & \Lambda_{z,res} \end{bmatrix} \begin{bmatrix} V_{z,pc}^T \\ V_{z,res}^T \end{bmatrix} \tag{5.10}$$

from which, the score and loading matrices can be directly calculated by the following relations

$$P = U_{z,pc}, \quad T = V_{z,pc}\Lambda_{z,pc}, \tag{5.11}$$

$$\tilde{P} = U_{z,res}, \quad \tilde{T} = V_{z,res}\Lambda_{z,res}. \tag{5.12}$$

Notice that all the model parameters are contained in the matrix $\tilde{P}$ in the deterministic case. For the purpose of system identification, it follows that

$$\begin{bmatrix} \Gamma_s^\perp & -\Gamma_s^\perp H_{u,s} \end{bmatrix} = M\tilde{P}^T = M \begin{bmatrix} \tilde{P}_y \\ \tilde{P}_u \end{bmatrix}^T \tag{5.13}$$

where $M$ is a non-singular matrix. Therefore,

$$\Gamma_s^\perp = M\tilde{P}_y^T, \tag{5.14}$$

$$-\Gamma_s^\perp H_{u,s} = M\tilde{P}_u^T. \tag{5.15}$$

According to Eqs.(5.14)-(5.15), the extended observability matrix $\Gamma_s$ and the block triangular Toeplitz matrix $H_{u,s}$ can be simply extracted by performing PCA on $Z_f$. The system matrices $A, B, C$ and $D$ are then identified with the help of e.g. least squares method.

### 5.1.3 Identification of parity space

In deterministic case, the parity space can be extracted according to Eqs.(5.14)-(5.15). More generally, when the process is corrupted by measurement noise and process noise simultaneously, the data matrix $Z_f$ becomes

$$Z_f = \begin{bmatrix} \Gamma_s & H_{u,s} \\ 0 & I \end{bmatrix} \begin{bmatrix} X_i \\ U_f \end{bmatrix} + \begin{bmatrix} H_{w,s}W_f + V_f \\ 0 \end{bmatrix}. \tag{5.16}$$

In order to remove the effect of the noise, the so-called instrumental variables can be utilized, which should be sufficiently correlated with the informative part of data but uncorrelated with the future noise. A possible choice for the instrumental variables is the past data matrix $Z_p$, which satisfies, for large $N$,

$$\lim_{N\to\infty} \frac{1}{N} \left(H_{w,s}W_f + V_f\right) Z_p^T = 0.$$

Therefore,

$$Z_f Z_p^T \approx \begin{bmatrix} \Gamma_s & H_{u,s} \\ 0 & I \end{bmatrix} \begin{bmatrix} X_i \\ U_f \end{bmatrix} Z_p^T. \tag{5.17}$$

In case that the process is persistently excited, i.e.

$$rank(\begin{bmatrix} X_i \\ U_f \end{bmatrix} Z_p^T) = n + sl, \tag{5.18}$$

the following rank condition also holds:

$$\begin{aligned} rank\left(Z_f Z_p^T\right) &= rank\left(\begin{bmatrix} \Gamma_s & H_{u,s} \\ 0 & I \end{bmatrix}\right) \\ &= sl + n \end{aligned} \tag{5.19}$$

which ensures successful identification of $\Gamma_s^\perp$ and $\Gamma_s^\perp H_{u,s}$. Since $rank\left(\Gamma_s^\perp\right) = sm - n$, according to Eq.(5.18), it turns out

$$\begin{aligned} Z_f^\perp \begin{bmatrix} \Gamma_s & H_{u,s} \\ 0 & I \end{bmatrix} &= 0, \\ rank\left(Z_f^\perp\right) &= sm - n. \end{aligned}$$

In addition, the model order can also be determined by performing SVD on $\frac{1}{N} Z_f Z_p^T$, i.e.

$$\frac{1}{N} Z_f Z_p^T = U_z \begin{bmatrix} \Lambda_{z,1} & 0 \\ 0 & \Lambda_{z,2} \end{bmatrix} V_z^T \tag{5.20}$$

where $U_z \in \mathcal{R}^{s(l+m)\times s(l+m)}$, $V_z \in \mathcal{R}^{s(l+m)\times s(l+m)}$. According to the condition of Eq.(5.18), $\Lambda_{z,1}$ is a diagonal matrix which contains $sl+n$ non-zero singular values, i.e.

$$\begin{aligned} rank\left(\Lambda_{z,1}\right) &= rank\left(\begin{bmatrix} \Gamma_s & H_{u,s} \\ 0 & I \end{bmatrix}\right) \\ &= sl+n, \end{aligned} \tag{5.21}$$

and the diagonal matrix $\Lambda_{z,2}$ has exactly $sm-n$ zero singular values. Thus, divide $U_z$ as follows:

$$U_z = \begin{bmatrix} U_{z,11} & U_{z,12} \\ U_{z,21} & U_{z,22} \end{bmatrix}$$

where $U_{z,11} \in \mathcal{R}^{sm\times(sl+n)}$, $U_{z,12} \in \mathcal{R}^{sm\times(sm-n)}$, $U_{z,22} \in \mathcal{R}^{sl\times(sm-n)}$. Finally, $\Gamma_s^\perp$ and $\Gamma_s^\perp H_{u,s}$ can be calculated by

$$\Gamma_s^\perp = U_{z,12}^T, \tag{5.22}$$

$$\Gamma_s^\perp H_{u,s} = -U_{z,22}^T. \tag{5.23}$$

The algorithm to identify the parity space can be summarized as the following steps.

**Algorithm D2PS (from data to parity space)**

- Generate $Z_f$ and $Z_p$ and construct $\frac{1}{N}Z_f Z_p^T$
- Perform SVD on $\frac{1}{N}Z_f Z_p^T$
- Calculate $\Gamma_s^\perp$ and $\Gamma_s^\perp H_{u,s}$ by Eqs.(5.22)-(5.23)
- (optional) Select $\upsilon_s \in \Gamma_s^\perp$ and $\beta_s \in \Gamma_s^\perp H_{u,s}$.

Notice that the above algorithm identifies the parity space only based on the training data sets $Z_f$ and $Z_p$. The algorithm to design reduced order parity vectors has been presented by Ding et al. [24]. Based on the available $\Gamma_s^\perp$ and $\Gamma_s^\perp H_{u,s}$, the residual generator design will be proposed in the next section.

## 5.2 Residual generator design

### 5.2.1 Single residual generation

It is well-known that, based on the vectors $\upsilon_s \in \Gamma_s^\perp$ and $\beta_s \in \Gamma_s^\perp H_{u,s}$, the primary form of parity space based residual generator is constructed as

$$r(k) = \upsilon_s y_s(k) - \beta_s u_s(k). \tag{5.24}$$

According to the discussion in Subsection 2.2.4, the parity space based residual generator has a one-to-one relationship with the DO-based residual generator. From the application point of view, DO leads to an efficient recursive form for residual generation with less on-line computation and more degrees of design freedom. The strategy of *parity space design, observer-based implementation* has been widely applied in industry to ensure a numerical stable and less complicated on-line fault diagnosis. Therefore, based on the identified vectors $\upsilon_s$ and $\beta_s$, DO-based residual generator ca be constructed in the following form:

$$z(k+1) = A_z z(k) + B_z u(k) + L_z y(k), \tag{5.25}$$

$$r(k) = g_z y(k) - c_z z(k) - d_z u(k) \tag{5.26}$$

where

$$A_z = \begin{bmatrix} 0 & 0 & \cdots & 0 & 0 \\ 1 & 0 & \ddots & \vdots & 0 \\ \vdots & \ddots & \ddots & 0 & \vdots \\ 0 & 0 & \cdots & 1 & 0 \end{bmatrix} \in \mathcal{R}^{(s-1)\times(s-1)},\ L_z = -\begin{bmatrix} \upsilon_{s,0} \\ \upsilon_{s,1} \\ \vdots \\ \upsilon_{s,s-2} \end{bmatrix} \in \mathcal{R}^{(s-1)\times m},$$

$$B_z = \begin{bmatrix} \beta_{s,0} \\ \beta_{s,1} \\ \vdots \\ \beta_{s,s-2} \end{bmatrix} \in \mathcal{R}^{(s-1)\times l},\quad c_z = \begin{bmatrix} 0 & \cdots & 0 & 1 \end{bmatrix} \in \mathcal{R}^{1\times(s-1)},$$

$$g_z = \upsilon_{s,s-1} \in \mathcal{R}^{1\times m},\ d_z = \beta_{s,s-1} \in \mathcal{R}^{1\times l}.$$

It is evident that the residual generator given by Eqs.(5.25)-(5.26) has the poles at the origin. To achieve additional design freedom, the residual generator can be extended to

$$z(k+1) = \bar{A}_z z(k) + \bar{B}_z u(k) + \bar{L}_z y(k), \tag{5.27}$$

$$r(k) = g_z y(k) - c_z z(k) - d_z u(k) \tag{5.28}$$

where

$$L_o = \begin{bmatrix} l_1 \\ l_2 \\ \vdots \\ l_{s-1} \end{bmatrix},\ \bar{A}_z = A_z - L_o c_z = \begin{bmatrix} 0 & 0 & \cdots & -l_1 \\ 1 & 0 & \ddots & -l_2 \\ \vdots & \ddots & \ddots & \vdots \\ 0 & \cdots & 1 & -l_{s-1} \end{bmatrix},$$

$$\bar{B}_z = B_z - L_o d_z,\ \bar{L}_z = L_z + L_o g.$$

$L_o$ determines the eigenvalues of system matrix $\bar{A}_z$ and should be selected so that all the eigenvalues of $\bar{A}_z$ lie in the unit circle.

With combination of Algorithm D2PS, a data-driven scheme for the design of a DO, which delivers a single residual signal, can be summarized as the following algorithm.

**Algorithm PS2DO (from parity space to DO)**

- Select $\upsilon_s \in \Gamma_s^\perp$ and $\beta_s \in \Gamma_s^\perp H_{u,s}$
- Calculate $A_z$, $B_z$, $L_z$, $c_z$, $g_z$ and $d_z$
- Construct a DO-based residual generator according to Eqs.(5.25)-(5.26)
- (optional) Calculate $\bar{A}_z$, $\bar{B}_z$, $\bar{L}_z$ and construct a DO-based residual generator as shown in Eqs.(5.27)-(5.28).

### 5.2.2 Multiple residual generations

In the FDI framework, the fault sensitivity plays an important role in the system design. In order to ensure the high sensitivity to faults, it is the state of the art in the FDI research that a residual vector, instead of a single residual signal, is generated [26]. For instance, the standard Kalman filter or the FDF scheme can be used to design an observer, which delivers an $m$-dimensional residual vector. Hence, it is necessary to extend the data-driven design approach proposed in the last subsection to the multiple residuals case to achieve better fault diagnosis performance.

Suppose that $\Gamma_s^\perp$ and $\Gamma_s^\perp H_{u,s}$ are identified using Algorithm D2PS given in Subsection 5.1.3. The main objective in this section is to generate $m$ linearly independent residual signals using $m$ DOs based on $\Gamma_s^\perp$ and $\Gamma_s^\perp H_{u,s}$. These $m$ DOs should span the overall $n$-dimensional state space. Consider a single DO constructed using a parity vector $\upsilon_s \in \Gamma_s^\perp$ and the corresponding vector $\beta_s \in \Gamma_s^\perp H_{u,s}$. Let

$$e(k) = Tx(k) - z(k)$$

with

$$e(k) = \begin{bmatrix} e_1(k) \\ \vdots \\ e_{s-1}(k) \end{bmatrix},\ z(k) = \begin{bmatrix} z_1(k) \\ \vdots \\ z_{s-1}(k) \end{bmatrix},\ T = \begin{bmatrix} t_1 \\ \vdots \\ t_{s-1} \end{bmatrix}.$$

In case that the influence of the noises is not taken into account, it holds

$$\begin{aligned} e(k+1) &= A_z e(k), \\ r(k) &= c_z e(k) = e_{s-1}(k). \end{aligned}$$

where $(c_z, A_z)$ is an observable pair. In addition, it follows from Eqs.(5.25)-(5.26) that

$$e_s(k) = \upsilon_{s,s-1} Cx(k) - z_{s-1}(k)$$

which implies $z_{s-1}(k)$ is an estimate of a linear combination of the system state variables. Recall that the primary objective is to construct $m$ linearly independent residual signals which span the whole state space. The above observation motivates us to select $m$ parity vectors, $\upsilon_{s_i} \in \Gamma_s^{\perp}$, $i = 1, \cdots, m$, where

$$\upsilon_{s_i} = \begin{bmatrix} \upsilon_{s_i,0} & \upsilon_{s_i,1} & \cdots & \upsilon_{s_i,s-1} \end{bmatrix}$$

satisfying

$$rank \left( \begin{bmatrix} \upsilon_{s_1,s-1} \\ \vdots \\ \upsilon_{s_m,s-1} \end{bmatrix} \right) = m. \tag{5.29}$$

Based on them, construct $m$ DOs, in which the $i$-th DO is presented by

$$z^i(k+1) = A_{z_i} z^i(k) + B_{z_i} u(k) + L_{z_i} y(k), \tag{5.30}$$

$$r_i(k) = g_i y(k) - c_{z_i} z^i(k) - d_{z_i} u(k). \tag{5.31}$$

It is important to notice that the condition in Eq.(5.29) ensures that the $m$ variables, $z_{s-1}^i(k)$, $i = 1, \cdots, m$, are linearly independent. Since

$$\begin{bmatrix} z^1(k) \\ \vdots \\ z^m(k) \end{bmatrix} = \begin{bmatrix} T_1 \\ \vdots \\ T_m \end{bmatrix} x(k),$$

it is expected to have

$$rank\,(T) = n,\ T = \begin{bmatrix} T_1 \\ \vdots \\ T_m \end{bmatrix} \tag{5.32}$$

where $T_1, \cdots, T_m$ are the transformation matrices solving Luenberger equations with respect to each DO. In order to prove Eq.(5.32), it is necessary to introduce the following lemma given by [28].

**Lemma 5.1.** *Given the observable pair $(C, A)$ with $A \in \mathcal{R}^{n\times n}$, $C \in \mathcal{R}^{m\times n}$, then the minimum order of a parity vector is equal to the minimum observability index of the observable pair.*

It follows immediately from Lemma 5.1 that

- for $m = 1$ the minimum order of a parity vector is equal to $n$, and

- for a not fully observable pair $(C, A)$ with $m = 1$ and the dimension of the observable subspace being equal to $\theta < n$, the minimum order of a parity vector is equal to $\theta$.

To this end, the proof of Eq.(5.32) is summarized in the following theorem.

**Theorem 5.1.** *Given $\Gamma_s^\perp$ identified from the observable system Eqs.(5.1)-(5.2), $\upsilon_{s_i} \in \Gamma_s^\perp$, $i = 1, \cdots, m$, satisfying Eq.(5.29) and $m$ DOs Eqs.(5.30)-(5.31) constructed using Algorithm PS2DO, then Eq.(5.32) holds.*

*Proof.* Let $G$ be

$$G = \begin{bmatrix} \upsilon_{s_1,s-1} \\ \vdots \\ \upsilon_{s_m,s-1} \end{bmatrix} = \begin{bmatrix} g_1 \\ \vdots \\ g_m \end{bmatrix}. \tag{5.33}$$

Due to Eq.(5.29), $(GC, A)$ is observable, since

$$\begin{aligned} rank \begin{bmatrix} GC \\ GCA \\ \vdots \\ GCA^{n-1} \end{bmatrix} &= rank\left(diag(G, \cdots, G)\Gamma_{n-1}\right) \\ &= rank\left(\Gamma_{n-1}\right). \end{aligned}$$

Let $\sigma_1, \cdots, \sigma_m$ be the observability indices of observable pair $(GC, A)$. Note that

$$rank \begin{bmatrix} \upsilon_{s_1,s-1}C \\ \vdots \\ \upsilon_{s_1,s-1}CA^{\sigma_1-1} \\ \vdots \\ \upsilon_{s_m,s-1}C \\ \vdots \\ \upsilon_{s_m,s-1}CA^{\sigma_m-1} \end{bmatrix} = n \tag{5.34}$$

where $\sigma_i \leq \vartheta_i$ with $\vartheta_i$ denote the dimension of the observable subspace of pair $(\upsilon_{s_i,s-1}C, A)$, $i = 1, \cdots, m$. Moreover, according to Lemma 5.1 and the associated claim, it follows that

$$\sigma_i \leq \vartheta_i \leq s_i, \ \sum_{i=1}^{m} s_i = s.$$

Denote

$$z^i(k) = \begin{bmatrix} z_{i,1}(k) \\ \vdots \\ z_{i,s_i}(k) \end{bmatrix}, \ T_i = \begin{bmatrix} t_{i,1} \\ \vdots \\ t_{i,s_i} \end{bmatrix}.$$

It turns out for $z^i(0) = T_i x(0)$, $u(k) = 0$, $w(k) = 0$, $v(k) = 0$

$$\begin{aligned}
\begin{bmatrix} z_{i,s_i}(k) \\ \vdots \\ z_{i,s_i-\sigma_i+1}(k) \end{bmatrix} &= \begin{bmatrix} \upsilon_{s_i,s-1}C \\ \vdots \\ \upsilon_{s_i,s-1}CA^{\sigma_i-1} \end{bmatrix} x(k) \\
&= \begin{bmatrix} c_{z_i} \\ \vdots \\ c_{z_i}A_{z_i}^{\sigma_i-1} \end{bmatrix} z^i(k), \\
\begin{bmatrix} \upsilon_{s_i,s-1}C \\ \vdots \\ \upsilon_{s_i,s-1}CA^{\sigma_i-1} \end{bmatrix} &= \begin{bmatrix} c_{z_i} \\ \vdots \\ c_{z_i}A_{z_i}^{\sigma_i-1} \end{bmatrix} T_i.
\end{aligned}$$

Hence, Eq.(5.34) has the same rank as

$$rank\left(diag\left(\begin{bmatrix} c_{z_1} \\ \vdots \\ c_{z_1}A_{z_1}^{\sigma_1-1} \end{bmatrix}, \cdots, \begin{bmatrix} c_{z_m} \\ \vdots \\ c_{z_m}A_{z_m}^{\sigma_m-1} \end{bmatrix}\right)\begin{bmatrix} T_1 \\ \vdots \\ T_m \end{bmatrix}\right)$$

and finally Eq.(5.32) is proved. □

Theorem 5.1 ensures that the $m$ DOs span the whole state space and thus can be used for detecting and isolating all faults occurring in it. The above design procedure is summarized as the following algorithm.

**Algorithm PS2MDO (from parity space to multiple DOs)**

- Identify $\Gamma_s^\perp$ and $\Gamma_s^\perp H_{u,s}$ using Algorithm D2PS
- Select $m$ parity vectors from $\Gamma_s^\perp$, which satisfy Eq.(5.29), and then select the corresponding vectors from $\Gamma_s^\perp H_{u,s}$
- Construct $m$ DOs using Algorithm PS2DO.

It follows from Eqs.(5.30)-(5.31) that each DO is a deadbeat observer. In the practice, it is often necessary to design the observer-based FDI systems to meet special performance demands. For this purpose, the residual signal is fed back to the estimation as follows:

$$z^i(k+1) = A_{z_i}z^i(k) + B_{z_i}u(k) + L_{z_i}y(k) + L_{r_i}r_i(k), \tag{5.35}$$

$$r_i(k) = g_i y(k) - c_{z_i}z^i(k) - d_{z_i}u(k). \tag{5.36}$$

It is straightforward that

$$\begin{aligned} e^i(k+1) &= (A_{z_i} - L_{r_i}c_{z_i})e^i(k), \\ e^i(k) &= T_i x(k) - z^i(k), \\ r_i(k) &= c_{z_i}e^i(k). \end{aligned}$$

In case that the process is corrupted by noise, it follows that

$$\begin{aligned} e^i(k+1) &= (A_{z_i} - L_{r_i}c_{z_i})e^i(k) + \bar{w}^i(k), \\ \bar{w}^i(k) &= T_i w(k) - L_{r_i}g_i v(k), \\ r_i(k) &= c_{z_i}e^i(k) + g_i v(k). \end{aligned}$$

Thus, each DO can be designed by selecting $L_{r_i}$ using the known observer design approaches like Kalman filter or pole assignment scheme.

### 5.2.3 A PCA-like approach

It is known that the instrument variable $Z_p$ is utilized to eliminate the influence of noise. However, for FDI purpose, this step is not always necessary. In this subsection, a PCA-like multiple residual generation scheme is introduced.

Without introducing instrument variable $Z_p$, for a large $N$ it turns out from Eq.(5.16) that

$$\begin{aligned} \frac{Z_f Z_f^T}{N} &= \frac{1}{N}\begin{bmatrix} \Gamma_s & H_{u,s} \\ 0 & I \end{bmatrix}\begin{bmatrix} X_i \\ U \end{bmatrix} Z_f^T + \frac{1}{N}\begin{bmatrix} \Phi_n \\ 0 \end{bmatrix} Z_f^T \\ &\approx \frac{1}{N}\begin{bmatrix} \Gamma_s & H_{u,s} \\ 0 & I \end{bmatrix}\begin{bmatrix} X_i \\ U \end{bmatrix} Z_f^T + \frac{1}{N}\begin{bmatrix} \Phi_n\Phi_n^T & 0 \\ 0 & 0 \end{bmatrix} \end{aligned} \tag{5.37}$$

where $\Phi_n = H_{w,s}W_f + V_f$ represents the noise information. The first term in Eq.(5.37) describes the system dynamics, which responds to the input signal. Since the noise information $\Phi_n$ is generally small in magnitude and contains insignificant variability information, it is possible to separate it by performing SVD on Eq.(5.37). Consequently, it follows that

$$\frac{1}{N}Z_f Z_f^T = U_z \begin{bmatrix} \Lambda_{X,U} & 0 \\ 0 & \Lambda_{\Phi_n} \end{bmatrix} U_z^T \tag{5.38}$$

where $\Lambda_{X,U}$ includes all the singular values corresponding to the influence of input data set $U_f$ on the process variables and hence being significantly larger than the singular values included in $\Lambda_{\Phi_n}$. $U_z$ can be divided according to $\Lambda_{X,U}$ and $\Lambda_{\Phi_n}$ as

$$U_z = \begin{bmatrix} U_{z,X,U} & U_{z,res} \end{bmatrix}.$$

As a result,

$$U_{z,res}^T \begin{bmatrix} \Gamma_s & H_{u,s} \\ 0 & I \end{bmatrix} = \begin{bmatrix} U_{z,res,1} \\ U_{z,res,2} \end{bmatrix}^T \begin{bmatrix} \Gamma_s & H_{u,s} \\ 0 & I \end{bmatrix} = 0, \tag{5.39}$$

$$U_{z,res}^T \left( \frac{Z_f Z_f^T}{N} \right) U_{z,res} = \Lambda_{\Phi_n}. \tag{5.40}$$

Similar to PCA, it is reasonable to construct the test statistic and threshold as follows:

$$T_z^2 = z^T(k)\, U_{z,res} \Lambda_{\Phi_n}^{-1} U_{z,res}^T z(k), \tag{5.41}$$

$$J_{th,T_z^2} = \chi_\alpha^2 (sm - n) \tag{5.42}$$

with $z^T(k) = \begin{bmatrix} y_s^T(k) & u_s^T(k) \end{bmatrix}$.

Note that the statistic presented in Eq.(5.41) contains considerably redundant information and may be too conservative to perform an effective fault detection. According to Eq.(5.39), $U_{z,res,1}^T$ and $U_{z,res,2}^T$ respectively span the parity space and $\Gamma_s^\perp H_{u,s}$. Therefore, it is able to construct $m$ DOs with the help of Algorithm PS2MDO, which delivers $m$ residual signals

$$r(k) = \begin{bmatrix} r_1(k) \\ \vdots \\ r_m(k) \end{bmatrix} \sim \mathcal{N}\left(0, \bar{\Lambda}_{\Phi_n}\right)$$

where $\bar{\Lambda}_{\Phi_n}$ includes $m$ singular values in $\Lambda_{\Phi_n}$. Thus, for fault detection purpose, the following test statistic and threshold can be used

$$T^2 = r^T(k) \bar{\Lambda}_{\Phi_n}^{-1} r(k), \tag{5.43}$$

$$J_{th} = \chi_\alpha^2(m) \tag{5.44}$$

which is less conservative than Eqs.(5.41)-(5.42). The corresponding decision logic is

$$T^2 \leq J_{th} \Longrightarrow \text{fault free, otherwise a fault is detected.}$$

This proposed method is comparable with the standard PCA [127], [128], in which the normalization step is replaced by the SVD that serves to remove the deterministic part in the system dynamics. For a dynamic system with order $n$, the dimension of parity vector $v_s$, being equal to $ms > mn$, may become very high. Therefore, it is advisable to use a recursive computation given in the form of DOs.

## 5.3 State Estimator design

Recall that $T$ is a transformation matrix connecting $z(k)$ and the process state vector $x(k)$, i.e. $z(k) = Tx(k)$. Thus, if a regular matrix $T$ is constructed, the whole process state variables can be estimated based on $z(k)$. In this way, the DOs can be used not only for the process monitoring but also control purpose. Based on a regular matrix $T$, the main objective of this section is to present a procedure to construct the corresponding state estimator.

Suppose that $m$ DOs are constructed according to Algorithm PS2MDO. As a result, Eq.(5.32) holds and there exists a pseudo inverse $T^\dagger$ such that $T^\dagger T = I$. Given a regular matrix $T$, $T^\dagger$ can be calculated as

$$T^\dagger = V_T \Lambda_T^{-1} U_{T,1}^T \tag{5.45}$$

where $V_T \in \mathcal{R}^{n\times n}$ and $\Lambda_T \in \mathcal{R}^{n\times n}$ come from an SVD on matrix $T$, i.e.

$$T = U_T \begin{bmatrix} \Lambda_T \\ 0 \end{bmatrix} V_T^T, \tag{5.46}$$

$$U_T = \begin{bmatrix} U_{T,1} & U_{T,2} \end{bmatrix}. \tag{5.47}$$

Eq.(5.45) allows to estimate $x(k)$ using

$$\hat{x}(k) = T^\dagger z(k) \tag{5.48}$$

which ensures that in the noise free case

$$\lim_{k\to\infty} (x(k) - \hat{x}(k)) = \lim_{k\to\infty} \left(T^\dagger e(k)\right) = 0.$$

The Algorithm D2SE summarizes the necessary steps from the test data to the state estimation, it constructs $m$ DOs using Algorithm D2MDO, which is in fact an $s$-dimensional system with $s$ being possibly significantly larger than model order $n$. In order to propose an approach to design an observer of the $n$-th order, rewrite the $m$ DOs into the following compact form

$$z(k+1) = A_z z(k) + B_z u(k) + L_z y(k), \tag{5.49}$$

$$r(k) = Gy(k) - C_z z(k) - D_z u(k) \in \mathcal{R}^m \tag{5.50}$$

with

$$A_z = diag(A_{z_1}, \cdots, A_{z_m}),\ C_z = diag(c_{z_1}, \cdots, c_{z_m}), \tag{5.51}$$

$$B_z = \begin{bmatrix} B_{z_1} \\ \vdots \\ B_{z_m} \end{bmatrix},\ L_z = \begin{bmatrix} L_{z_1} \\ \vdots \\ L_{z_m} \end{bmatrix},\ D_z = \begin{bmatrix} d_{z_1} \\ \vdots \\ d_{z_m} \end{bmatrix},\ G = \begin{bmatrix} g_1 \\ \vdots \\ g_m \end{bmatrix}. \tag{5.52}$$

**Algorithm D2SE (from data to state estimation)**

- Identify $\Gamma_s^{\perp}$ and $\Gamma_s^{\perp} H_{u,s}$ using Algorithm D2PS
- Construct $m$ DOs using Algorithm D2MDO
- Compute $T_i$, $i = 1, \cdots, m$ by

$$T_i = \begin{bmatrix} \upsilon_{s_i,1} & \upsilon_{s_i,2} & \cdots & \upsilon_{s_i,s-3} & \upsilon_{s_i,s-2} \\ \upsilon_{s_i,2} & \cdots & \cdots & \upsilon_{s_i,s-2} & 0 \\ \vdots & \cdots & \cdots & \vdots & \vdots \\ \upsilon_{s_i,s-2} & 0 & \cdots & \cdots & 0 \end{bmatrix} \Gamma_{s_i}$$

  and form

$$T = \begin{bmatrix} T_1^T & \cdots & T_m^T \end{bmatrix}^T$$

- Set $T^{\dagger}$ according to Eq.(5.45)
- Construct state estimation $\hat{x}(k)$ using Eq.(5.48).

Note that the compact form presented by Eqs.(5.49)-(5.50) is a deadbeat observer. Denote

$$T^{\dagger} A_z T = A_x \tag{5.53}$$

where $A_x$ only includes $n$ eigenvalues of $A_z$ that are all located at the origin. Hence, a full order state estimator follows

$$\hat{x}(k+1) = A_x \hat{x}(k) + B_x u(k) + L_x y(k) \tag{5.54}$$

in which

$$\hat{x}(k) = T^{\dagger} z(k),\ B_x = T^{\dagger} B_z,\ L_x = T^{\dagger} L_z. \tag{5.55}$$

Moreover, an $m$-dimensional residual vector is constructed by

$$r(k) = G y(k) - C_x \hat{x}(k) - D_z u(k) \tag{5.56}$$

with

$$C_x = C_z T. \tag{5.57}$$

The dynamics of the estimation error $e_x(k) = x(k) - \hat{x}(k)$ as well as the residual vector are governed by

$$\begin{aligned} e_x(k+1) &= A_x e_x(k) + \bar{w}_x(k), & (5.58) \\ r(k) &= C_x e_x(k) + \bar{v}(k) & (5.59) \end{aligned}$$

where

$$\begin{aligned} \bar{w}_x(k) &= w(k) - L_x v(k), \\ \bar{v}(k) &= Gv(k). \end{aligned}$$

As mentioned in the previous section, in order to improve the system dynamic behaviors, the residual vector can be fed back to the state estimation

$$\hat{x}(k+1) = A_x\hat{x}(k) + B_x u(k) + L_x y(k) + L_r r(k), \tag{5.60}$$

$$r(k) = Gy(k) - C_x\hat{x}(k) - D_z u(k) \tag{5.61}$$

where $L_r$ is the design parameter, and can be, e.g. used for realizing a Kalman filter scheme.

The main results derived in this section are summarized as the following algorithm.

**Algorithm D2SO (from data to state observer)**

- Identify $\Gamma_s^{\perp}$ and $\Gamma_s^{\perp} H_{u,s}$ using Algorithm D2PS
- Compute $A_z$, $B_z$, $C_z$, $D_z$, $L_z$ and $G$ according to Eqs.(5.33), (5.51)-(5.52)
- Compute $T$ and $T^{\dagger}$ as described in Algorithm D2SE
- Compute $A_x, B_x, C_x$ and $L_x$ as defined in Eqs.(5.53), (5.55), (5.57)
- Construct the state observer according to Eq.(5.54)
- (optional) Generate residual vector presented by Eq.(5.56)
- (optional) Design and construct the state observer Eqs.(5.60)-(5.61).

## 5.4 Concluding remarks

In this chapter, a subspace aided data-driven approach is presented to achieve reliable fault detection in dynamic processes under industrial operating conditions. Instead of identifying the complete process model, primary fault detection can be realized with the identified parity space. For the sake of efficient on-line implementation with enhanced performance, a strategy of *parity space design, observer-based implementation* is achieved

according to the one-to-one relationship between parity space and DO. The further study is dedicated to extending the single residual generation scheme to multiple residuals case in order to ensure high sensitivity to the faults. The multiple DOs can also be utilized to construct state estimation observer for process monitoring and control purposes.

Extending this novel approach in the forthcoming chapter, the uncertainty issue in the industrial environment will be discussed with the help of adaptive technique.

# 6 On recursive and adaptive design issues

In the industrial environment, the processes and plants often involve the changes, e.g. in operating regimes or in the manipulated variables, which may lead to significant variations in the mean and covariance of the process variables. Based on the basic idea of subspace aided data-driven approach, the recursive and adaptive techniques can be integrated to cope with such uncertainty issues. Among the existing techniques, the recursive subspace tracking or recursive identification algorithms have been well developed and have served as the standard data-driven methods with reduced on-line computation. Since the early work by Helland et al. [47] and Qin [89], numerous recursive schemes have been reported [45], [76], [78], [82]. The recursive subspace tracking algorithms are also popularly used for signal processing applications, which can be found in [9], [20], [121].

Besides recursive algorithms, the well-established adaptive control and observer theories [1], [5], [100], [132] offer an alternative and powerful solution with consideration of the convergence and stability issues. It is worth mentioning that the existing recursive algorithms paid less attention on stability problem, which, however, plays a central role when a PCA-like diagnostic observer is applied for a dynamic process. Based on this observation, it is promising that the combination of subspace aided approach and adaptive control technique will lead to new successful solutions.

In the present work, two efficient recursive identification algorithms are firstly proposed based on first-order perturbation (FOP) theory and data-projection method (DPM). The design and implementation of adaptive DO-based residual generator is then discussed with analytically provable convergence rate.

## 6.1 Problem formulation

The subspace aided data-driven approach is a powerful tool to deal with dynamic issue with time invariant parameters. Since the residual generation based on this approach implicitly depends on the model parameters, any deviations will lead to significant false alarms even in normal operation scenarios. Therefore, it is necessary to update the process

model on-line to cope with the nominal changes in the process.

From the system theoretic point of view, the process with parameter changes can be modeled in terms of time varying representation. A shift in the operation point or tuning of manipulated parameters may cause the change in one of the system matrices represented in Eqs.(2.1)-(2.2) due to nonlinearities. Since the primary residual signal can be constructed from the singular vectors belonging to the smallest singular values of the product term $Z_f Z_p^T$ or $Z_f Z_f^T$, the main problem of subspace tracking converges to recursive updating singular values and singular vectors based on the process measurements [83], [84], [124]. For a large-scale industrial process, it always poses a series of challenges considering the limited memory and computational resources. Thus, an approximate subspace tracking algorithm is recommended to achieve the trade-off between accuracy and computation cost.

Although the main advantage of subspace tracking algorithm lies in its efficient computation load compared with standard SVD, the stability and convergence properties are difficult to be proved due to numerical approximations. To cope with such problems, the well-established adaptive technique is desired to be integrated into DO-based residual generation scheme [23], [125]. After the nominal changes of process parameters, the proposed adaptive data-driven scheme should

- deliver a residual signal $r(k)$ satisfying

$$\lim_{k\to\infty} r(k) = 0,$$

- if possible, with an exponential convergence rate independent of the changes.

## 6.2 Subspace tracking technique

The core of subspace tracking algorithm is to perform an approximate recursive SVD using the available process measurements at each time step. In this section, two recursive algorithms based on FOP and DPM are briefly introduced, which focus on subspace tracking of $Z_f Z_p^T$ and $Z_f Z_f^T$, respectively.

### 6.2.1 FOP-based subspace tracking

Consider the product between $Z_f$ and $Z_p$ for $N$ samples denoted by $\Phi_z$

$$\Phi_z = \frac{1}{N} Z_f Z_p^T. \tag{6.1}$$

The recursive version of Eq.(6.1) follows

$$\Phi_z(k) = \alpha\Phi_z(k-1) + (1-\alpha)\, z_f(k) z_p^T(k) \tag{6.2}$$

where $\alpha$ is a forgetting factor in the range $[0, 1]$. The SVD of $\Phi_z(k)$ follows

$$\Phi_z(k) = U(k)\Sigma(k)V^T(k) \tag{6.3}$$

where $U(k)$ and $V(k)$ contain left and right singular vectors and $\Sigma(k)$ is a diagonal matrix including all the singular values. Similarly, a recursive form of Eq.(6.3) becomes

$$\begin{aligned} \Phi_z(k) &= \Phi_z(k-1) + E \\ &= U(k-1)\left(\Sigma(k-1) + F\right) V(k-1)^T \end{aligned} \tag{6.4}$$

where $E$ is the first-order perturbation matrix and

$$F = U^T(k-1) E V(k-1).$$

The roots of the FOP-based singular values and singular vectors updating theory can be traced back to the result presented in [99], which is stated in the following lemma [116].

**Lemma 6.1.** *If all the singular values of $\Phi_z(k-1)$ are simple and the perturbation matrix $E$ is small, then the singular vectors and singular values of the updated matrix $\Phi_z(k)$ can be described as*

$$\bar{U}(k) = U(k-1)\left(I + P\right), \tag{6.5}$$

$$\bar{V}(k) = V(k-1)\left(I + Q\right), \tag{6.6}$$

$$\sigma_i(k) = \sigma_i(k-1) + f_{ii} + O\left(\|E\|^2\right) \tag{6.7}$$

*where $f_{ii}$ is the $(i,i)$-th element of $F$. The elements of matrices $P$ and $Q$ follow: $p_{ij} = q_{ij} = 0$ for $i = j$ and $p_{ji} = -p_{ij}^T$, $q_{ji} = -q_{ij}^T$ for $i > j$, otherwise*

$$p_{ji} = \frac{\sigma_{k-1,i} f_{ji} + \sigma_{k-1,j} f_{ij}^*}{\sigma_{k-1,i}^2 - \sigma_{k-1,j}^2} + O\left(\|E\|^2\right), \tag{6.8}$$

$$q_{ji} = \frac{\sigma_{k-1,i} f_{ij}^* + \sigma_{k-1,j} f_{ji}}{\sigma_{k-1,i}^2 - \sigma_{k-1,j}^2} + O\left(\|E\|^2\right). \tag{6.9}$$

*In case that $\sigma_i \gg \sigma_{i+1}$, Eqs.(6.8)-(6.9) can be further reduced to*

$$p_{ji} = \frac{f_{ji}}{\sigma_{k-1,i}}, \tag{6.10}$$

$$q_{ji} = \frac{f_{ij}}{\sigma_{k-1,j}}. \tag{6.11}$$

As a result, at each time step, the parity space can be identified from the left singular vectors corresponding to the smallest $sm - n$ singular values. The DO-based residual generator can be simply constructed by Algorithm PS2DO.

### 6.2.2 DPM-based subspace tracking

The DPM technique [31], [122] for subspace tracking is based on $Z_f Z_f^T$ and serves as an efficient approach to only update the singular values and singular vectors of interests. Based on this feature, DPM becomes the simplest algorithm if only a number of singular vectors are tracked.

Consider the matrix $\bar{\Phi}_z = \frac{1}{N} Z_f Z_f^T$ and its recursive calculation form as

$$\bar{\Phi}_z(k) = \alpha \bar{\Phi}_z(k-1) + (1-\alpha)\, z_f(k) z_f^T(k). \tag{6.12}$$

The core of DPM algorithm can be explained with the help of the following lemma [30].

**Lemma 6.2.** *Let $\bar{\Phi}_z$ be a symmetric, nonnegative matrix with the singular values $\sigma_i$ and the corresponding singular vectors $u_i$, where $i = 1, \cdots, s(m+l)$ and*

$$\sigma_1 \geq \cdots \sigma_{sl+n} > \sigma_{sl+n+1} \geq \cdots \geq \sigma_{s(m+l)} \geq 0.$$

*Consider the sequence of matrices $U_j \in \mathcal{R}^{(sl+n)\times l}$ defined by the iteration*

$$U_j = orthnorm\left\{\bar{\Phi}_z U_{j-1}\right\}, j = 1, 2, \cdots, \tag{6.13}$$

*where "orthnorm" denotes the orthonormalization procedure using QR decomposition or Gram-Schmidt procedure. Then, we have*

$$\lim_{j\to\infty} U_j = \left[\begin{array}{ccc} u_1 & \cdots & u_{s(m+l)} \end{array}\right].$$

Thus, for the recursive form presented in Eq.(6.12), the sequence of matrices $U_j$ composed of singular vectors corresponding to either the dominant or the smallest eigenvalues can be represented as:

$$U_j = orthnorm\left\{\left(I \pm \mu \bar{\Phi}_z(k)\right) U_{j-1}\right\} \tag{6.14}$$

where "+" and "-" give estimates of *signal* space and *noise* subspace, respectively. $\mu$ is chosen as a small positive number such that the matrix $I_N \pm \mu \Phi_z(k)$ is nonnegative definite.

For the purpose of construction of DO-based residual generator, it is not necessary to update the overall SVD structure but only the *noise* subspace, which is equivalent to the parity space. In fact, in case of construction of a single residual signal, the primary form of residual generator can be established based on any row of the parity space. In this case, it is only required to update the left singular vector related to smallest singular value that again decreases the computational complexity of the algorithm.

### 6.2.3 Recursive updating algorithm

The main steps of recursive subspace tracking algorithm based on FOP and DPM techniques are briefly summarized as follows.

**Recursive updating Algorithm:**

- Collect the new measurements $z_f(k)$ and in addition, $z_p(k)$ only for FOP-based method
- Calculate the correlation structure shown in Eqs.(6.2), (6.12) for FOP or DPM method, respectively.
- Update the complete SVD structure according to Eqs.(6.5)-(6.11) for FOP or update only the noise subspace presented in Eq.(6.14)
- Extract the parity space and associated matrix
- Construct DO-based residual generator with the help of Algorithm PS2DO.

It is worth pointing out that the above recursive subspace tracking algorithm provides an approximate result. The choice of such an algorithm always depends upon the trade-off between accuracy and on-line computation cost. It can be demonstrated that the DPM is the simplest algorithm due to its ability of identifying only a number of required parity vectors for DOs construction.

## 6.3 Adaptive DO-based residual generator

Although recursive subspace tracking techniques provide efficient on-line computation compared to standard SVD, the convergence and stability issues have not been paid enough attention in the research study. In particular, the latter plays a central role especially when a dynamic process is under consideration and a DO-based residual generator is applied. To overcome this difficulty, an adaptive DO-based residual generation scheme is proposed in this section with stability analysis.

### 6.3.1 Mathematical notations

It follows from system model described by Eqs.(2.1)-(2.2) and the transformation $z(k) = Tx(k)$ that the system can be written as

$$\begin{aligned} z(k+1) &= A_z z(k) + B_z u(k) + L_z y(k), && (6.15)\\ g_z y(k) &= c_z z(k) && (6.16) \end{aligned}$$

in which $D = 0$ for sake of simplicity. Hence, parameter changes in the original system matrices are now represented by the changes in $B_z$, $L_z$ and $g_z$. Define new parameter

$$\bar{\theta} = \begin{bmatrix} col\,(B_z) \\ col\,(L) \end{bmatrix} \in \mathcal{R}^{(s-1)(m+l)}$$

with $col\,(\cdot)$ denoting a column-wise re-ordering of a matrix, i.e.

$$\text{for } P = \begin{bmatrix} p_1 & \cdots & p_\alpha \end{bmatrix} \in \mathcal{R}^{\beta\times\alpha},\ col\,(P) = \begin{bmatrix} p_1 \\ \vdots \\ p_\alpha \end{bmatrix} \in \mathcal{R}^{\beta\alpha}.$$

Thus, Eq.(6.15) can be rewritten into

$$z(k+1) = A_z z(k) + \bar{Q}\,(u(k), y(k))\,\bar{\theta} \qquad (6.17)$$

where

$$\begin{aligned} \bar{Q}(u(k), y(k)) &= \begin{bmatrix} \mathcal{U}(k) & \mathcal{Y}(k) \end{bmatrix} \in \mathcal{R}^{(s-1)\times(s-1)(m+l)},\\ \mathcal{U}(k) &= \begin{bmatrix} u_1(k)\times I_{(s-1)\times(s-1)} & \cdots & u_l(k)\times I_{(s-1)\times(s-1)} \end{bmatrix},\\ \mathcal{Y}(k) &= \begin{bmatrix} y_1(k)\times I_{(s-1)\times(s-1)} & \cdots & y_m(k)\times I_{(s-1)\times(s-1)} \end{bmatrix}. \end{aligned}$$

Note that $g_z$ is included in the output equation (6.16). To simplify the notations, define

$$\theta = \begin{bmatrix} \bar{\theta} \\ g_z^T \end{bmatrix} \in \mathcal{R}^{(s-1)(m+l)+m}.$$

### 6.3.2 The adaptive residual generator scheme

Note that Eq.(6.17) is a standard form, based on which several methods are available for designing adaptive observers for the continuous time systems. Moreover, note that

the unknown parameter vector $g_z$ is included in the output presented in Eq.(6.16). From Eqs.(6.16)-(6.17), it follows that

$$z(k+1) = A_z z(k) + \bar{Q}\left(u(k), y(k)\right)\bar{\theta} + L_0\left(g_z y(k) - c_z z(k)\right) \tag{6.18}$$

which can be written into

$$z(k+1) = \bar{A}_z z(k) + Q\left(u(k), y(k)\right)\theta$$

with $\bar{A}_z = A_z - L_0 c_z$ and

$$Q\left(u(k), y(k)\right) = \left[\begin{array}{cc} \bar{Q}(u(k), y(k)) & L_0 y^T(k) \end{array}\right] \in \mathcal{R}^{(s-1)\times((s-1)(m+l)+m)}.$$

Based on Eq.(6.18), an adaptive residual generation scheme is proposed which consists of the following three subsystems:

*Residual generator*

$$\begin{aligned} \hat{z}(k+1) = {} & \bar{A}_z \hat{z}(k) + Q\left(u(k), y(k)\right)\hat{\theta}(k) \\ & + V(k+1)\left(\hat{\theta}(k+1) - \hat{\theta}(k)\right), \end{aligned} \tag{6.19}$$

$$r(k) = \hat{g}_z(k) y(k) - c_z \hat{z}(k) \tag{6.20}$$

where $L_0$ is design parameter vector to ensure that the eigenvalues of $\bar{A}_z$ lie in the unit circle. $\hat{\theta}(k)$ and $V(k+1)$ are generated by the parameter estimator and auxiliary filter given below.

*Auxiliary filter*

$$V(k+1) = \bar{A}_z V(k) + Q(u(k), y(k)), \tag{6.21}$$

$$\varphi(k) = c_z V(k) - \left[\begin{array}{ccccc} 0 & \cdots & 0 & y^T(k) \end{array}\right]. \tag{6.22}$$

*Parameter estimator*

$$\hat{\theta}(k+1) = \gamma(k)\varphi^T(k) r(k) + \hat{\theta}(k), \tag{6.23}$$

$$\gamma(k) = \frac{\mu}{\delta + \varphi(k)\varphi^T(k)},\ \delta \geq 0,\ 0 < \mu < 2. \tag{6.24}$$

The on-line implementation of the adaptive residual generator follows the algorithm given below.

**On-line implementation of the adaptive residual generator**

- *Step 0:* Set the initial values for $k = 0$, $\hat{z}(0)$, $\hat{\theta}(0)$, $V(0) = 0$, $\varphi(0) = 0$, $r(0) = y(0) - c_z\hat{z}(0)$
- *Step 1:* Compute $V(k+1)$ according to Eq.(6.21)
- *Step 2:* Compute $\hat{\theta}(k+1)$ according to Eq.(6.23)
- *Step 3:* Compute $\hat{z}(k+1)$ according to Eq.(6.19)
- *Step 4:* Increase $k$ by one and receive new measurements $y(k)$ and $u(k)$
- *Step 5:* Compute $r(k)$, $\varphi(k)$ according to Eqs.(6.20), (6.22), respectively, and go to *Step 1*.

### 6.3.3 Stability and exponential convergence

The stability of the proposed adaptive residual generator and the convergence issue will be studied in this subsection. For this purpose, the useful results on the gradient algorithm are given in the following two lemmas [1].

**Lemma 6.3.** *Given*

$$y(k) = \varphi(k)\theta,$$

*let*

$$\begin{aligned} \hat{\theta}(k+1) &= \frac{\mu}{\delta + \varphi(k)\varphi^T(k)}\varphi^T(k)e(k) + \hat{\theta}(k), \\ e(k) &= y(k) - \varphi(k)\hat{\theta}(k),\ \delta \geq 0,\ 0 < \mu < 2. \end{aligned}$$

*It then follows*

$$\lim_{k\to\infty} \frac{e(k)}{\sqrt{\delta + \varphi(k)\varphi^T(k)}} = 0. \tag{6.25}$$

**Lemma 6.4.** *The difference equation*

$$\tilde{\theta}(k+1) = \left(I - \frac{\mu\varphi^T(k)\varphi(k)}{\delta + \varphi(k)\varphi^T(k)}\right)\tilde{\theta}(k)$$

*is globally exponentially stable if there exist positive constants $\beta_1, \beta_2$, and integer $\Pi$ such that, for all $k$*

$$0 < \beta_1 I \leq \sum_{i=k}^{k+\Pi-1} \varphi^T(i)\varphi(i) \leq \beta_2 I < \infty.$$

To begin with the stability proof, define

$$\begin{aligned}\eta(k) &= \tilde{z}(k) - V(k)\tilde{\theta}(k),\\ \tilde{z}(k) &= z(k) - \hat{z}(k),\\ \tilde{\theta}(k) &= \theta - \hat{\theta}(k).\end{aligned}$$

Notice that residual signal can be rewritten into

$$\begin{aligned}r(k) &= g_z y(k) - c_z\hat{z}(k) - (g_z - \hat{g}_z(k))\, y(k)\\ &= c_z\tilde{z}(k) - y^T(k)\tilde{g}_z^T(k)\end{aligned}$$

which leads to

$$\begin{aligned}\tilde{z}(k+1) = A_z z(k) + \bar{Q}\left(u(k), y(k)\right)\bar{\theta} - A_z\hat{z}(k) - \bar{Q}\left(u(k), y(k)\right)\hat{\bar{\theta}}(k)\\ - L_0 r(k) - V(k+1)\left(\hat{\theta}(k+1) - \hat{\theta}(k)\right)\\ = \bar{A}_z\tilde{z}(k) + Q\left(u(k), y(k)\right)\tilde{\theta}(k) - V(k+1)\left(\hat{\theta}(k+1) - \hat{\theta}(k)\right).\end{aligned}$$

Moreover, it holds

$$\begin{aligned}V(k+1)\tilde{\theta}(k+1) &= V(k+1)\left(\tilde{\theta}(k+1) - \hat{\theta}(k+1) + \hat{\theta}(k)\right),\\ \tilde{\theta}(k+1) &= -\gamma(k)\varphi^T(k)r(k) + \tilde{\theta}(k)\\ &= \tilde{\theta}(k) - \gamma(k)\varphi^T(k)\left(c_z\tilde{z}(k) - y^T(k)\tilde{g}^T(k)\right)\\ &= \left(I - \gamma(k)\varphi^T(k)\varphi(k)\right)\tilde{\theta}(k) + \Theta(k)\eta(k)\end{aligned}$$

with $\Theta(k) = -\gamma(k)\varphi^T(k)c_z$.
Hence, after a straightforward calculation, it turns out

$$\begin{bmatrix}\eta(k+1)\\ \tilde{\theta}(k+1)\end{bmatrix} = \begin{bmatrix}\bar{A}_z & 0\\ \Theta(k) & I - \gamma(k)\varphi^T(k)\varphi(k)\end{bmatrix}\begin{bmatrix}\eta(k)\\ \tilde{\theta}(k)\end{bmatrix}. \tag{6.26}$$

Based on Eq.(6.26) and Lemmas 6.3-6.4, the following result can be achieved.

**Theorem 6.1.** *Given adaptive residual generator presented by Eqs.(6.19)-(6.24), then*

$$\lim_{k\to\infty} r(k) = 0. \tag{6.27}$$

*Proof.* It follows from Eq.(6.26) that $\eta(k)$ goes to zero with exponential convergence rate. Hence, it is only needed to consider

$$r(k) = c_z\tilde{z}(k) - y^T(k)\tilde{g}^T(k) = \varphi(k)\tilde{\theta}(k), \tag{6.28}$$

$$\tilde{\theta}(k+1) = \left(I - \gamma(k)\varphi^T(k)\varphi(k)\right)\tilde{\theta}(k) \tag{6.29}$$

which, according to Lemma 6.3, leads to

$$\lim_{k\to\infty} \frac{r(k)}{\sqrt{\delta + \varphi(k)\varphi^T(k)}} = 0.$$

Considering that the auxiliary filter given by Eqs.(6.21)-(6.22) is exponentially stable and the inputs and outputs of the system are bounded, it turns out

$$\begin{aligned} \left|\varphi(k)\varphi^T(k)\right| &< \infty, \\ \lim_{k\to\infty} \left\|\gamma(k)\varphi^T(k)c_z\eta(k)\right\| &= 0 \end{aligned}$$

which finally results in Eq.(6.27). □

It follows from Theorem 6.1 that

- the adaptive residual generation scheme presented by Eqs.(6.19)-(6.24) is stable and,
- the residual signal satisfies the basic requirement on residuals, i.e. $\lim_{k\to\infty} r(k) = 0$ in the fault free case.

On the other hand, it is well-known that an early fault detection requires a quick convergence of $r(k)$. However, Theorem 6.1 does not provide the knowledge of the convergence rate. For this purpose, additional condition is required, which is given in the following theorem.

**Theorem 6.2.** *Given adaptive residual generator Eqs.(6.19)-(6.24) and assume that there exist positive constants $\beta_1$, $\beta_2$ and integer $\Pi$ such that $\forall k$*

$$0 < \beta_1 I \leq \sum_{i=k}^{k+\Pi-1} \varphi^T(i)\varphi(i) \leq \beta_2 I < \infty, \tag{6.30}$$

*then system given by Eq.(6.26) is globally exponentially stable.*

*Proof.* The proof is similar to the one of Theorem 6.1. It follows from Lemma 6.4 that the residual signal presented by Eq.(6.28) is exponentially stable. Moreover, considering that $\eta(k)$ exponentially converges to zero and $\Theta(k)$ is bounded, it can be concluded that Eq.(6.26) is exponentially stable. □

The condition shown in Eq.(6.30) is known as the existence condition for persistent excitation which is needed for a successful parameter identification. In other words, the adaptive residual generator Eqs.(6.19)-(6.24) is exponentially stable if the system under consideration is persistently excited. Note that in this case

$$\lim_{k\to\infty} \hat{\theta}(k) = \theta$$

with an exponential convergence rate.

## 6.4 Simulation examples

Since the convergence and stability issues play an important role in the proposed approach, a simulation example is considered to research the tracking performance of the proposed adaptive DO-based scheme in parameter variation case. A mathematic model, which is used to generate the simulation data, can be described in the following state space form.

$$x(k+1) = Ax(k) + Bu(k) + w(k), \tag{6.31}$$

$$y(k) = Cx(k) + v(k) \tag{6.32}$$

where

$$A = \begin{bmatrix} 0 & 0.3 \\ -0.2 & 0.3 + 0.25\rho(k) \end{bmatrix},\ B = \begin{bmatrix} 0.5 \\ -0.3 \end{bmatrix},\ C = \begin{bmatrix} 1 & -0.2 \\ 0.5 & -0.6 \end{bmatrix},$$

and $w$ and $v$ are process and measurement noises, respectively. The parameter variation is presented by $\rho_k = sin\,(0.8 + 0.001k)$. The input signal selected for the experiments is a mixture of sinusoidal signals of different frequencies:

$$u(k) = \sum_{j=1}^{10} \sin\,(0.3898\pi jk).$$

To demonstrate the tracking performance of proposed adaptive scheme, an experiment including the following steps is performed:

- Identify the initial value of $\theta$, denoted by $\theta_0$, using the process data generated in time invariant case, i.e. $\rho(k) = sin(0.8)$, with order reduction $s = 2$, see [24]. Then it follows that

$$B_z = 0.56,\ L = \begin{bmatrix} 0.2521 & -0.2423 \end{bmatrix},\ g_z = \begin{bmatrix} 1 & 0 \end{bmatrix},$$
$$\theta_0^T = \begin{bmatrix} 0.56 & 0.2521 & -0.2423 & 1 & 0 \end{bmatrix}.$$

- The adaptive DO runs for 9500 data samples with time varying parameter $\rho(k)$. For sake of simplicity, $g_z$ is kept as a constant throughout the process in order to illustrate the tracking performance of the adaptive scheme.

Fig. 6.1 shows the tracking performance of adaptive DO scheme for the first three elements of $\theta$, denoted as $\theta_1$, $\theta_2$ and $\theta_3$. It can be evidently seen that, if the process data satisfy the persistent excitation condition, the proposed scheme has a good tracking property even with time varying parameter.

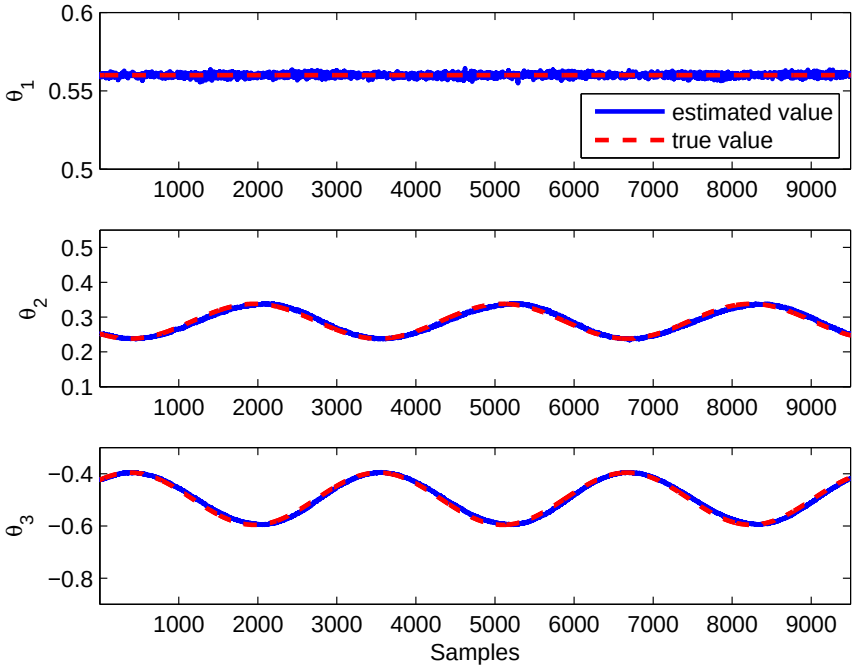


**Figure 6.1:** Tracking performance of adaptive DO scheme

## 6.5 Concluding remarks

In this chapter, two recursive algorithms for subspace tracking are firstly proposed. Both the algorithms avoid to computing complicated SVD at each step and provide approximate recursive estimate of the matrix decomposition with less computation cost. The DO-based residual generator designed with the help of these algorithms deal efficiently with the processes that vary around stable operating point or contain uncertain parameter variations. Despite the recursive subspace tracking algorithms are widely used in practice, the stability and convergence issues are difficult to prove due to their numerical approximations. Based on the well-established adaptive control theory, a data-driven adaptive residual generation scheme is further proposed, whose stability and convergence rate can be analytically proven. In addition, the proposed scheme does not involve any computation of matrix inverse and produces consistent estimate of the parameters. Thus, it is extremely suitable for process monitoring in large-scale process under industrial operating conditions with uncertainty issue.

# 7 Benchmark study

The data-driven design approaches proposed in this thesis will be applied on industrial benchmark processes to illustrate their effectiveness. Three industrial benchmarks are utilized corresponding to the previous study in each chapter.

- Tennessee Eastman (TE) chemical process [32]: The simulation of TE process is a realistic representation of a chemical plant with 50 internal states, 11 manipulated and 40 measured variables. Since the mathematical equations of the process are extremely complex to derive, TE process serves as a preferred benchmark to test data-driven algorithms for control, process monitoring and fault diagnosis. The basic operation mode of TE process is utilized to evaluate the basic MSPM methods under ideal stationary operating conditions.
- Fed-batch fermentation penicillin (FBFP) process [7]: The simulation of FBFP process is developed by using a realistic dynamic model of penicillin fermentation [7]. The FBFP process is a typical dynamic, multi-stage batch process and thus utilized to demonstrate the effectiveness of the subspace aided data-driven approach.
- Continuous stirred tank heater (CSTH) [101]: The model plant of CSTH is developed by [101] which is a hybrid one, derived from real data and rigorous modeling. The data-driven design of adaptive residual generator is applied on CSTH process under variation operating regimes.

A brief introduction of the aforementioned benchmarks will be firstly provided in the next section. The proposed data-driven schemes are then applied and the representative results are presented in detail.

## 7.1 Benchmark description

### 7.1.1 TE process

TE process model is a realistic simulation program of a chemical plant which is widely accepted as a benchmark for control and monitoring studies. The process is described in

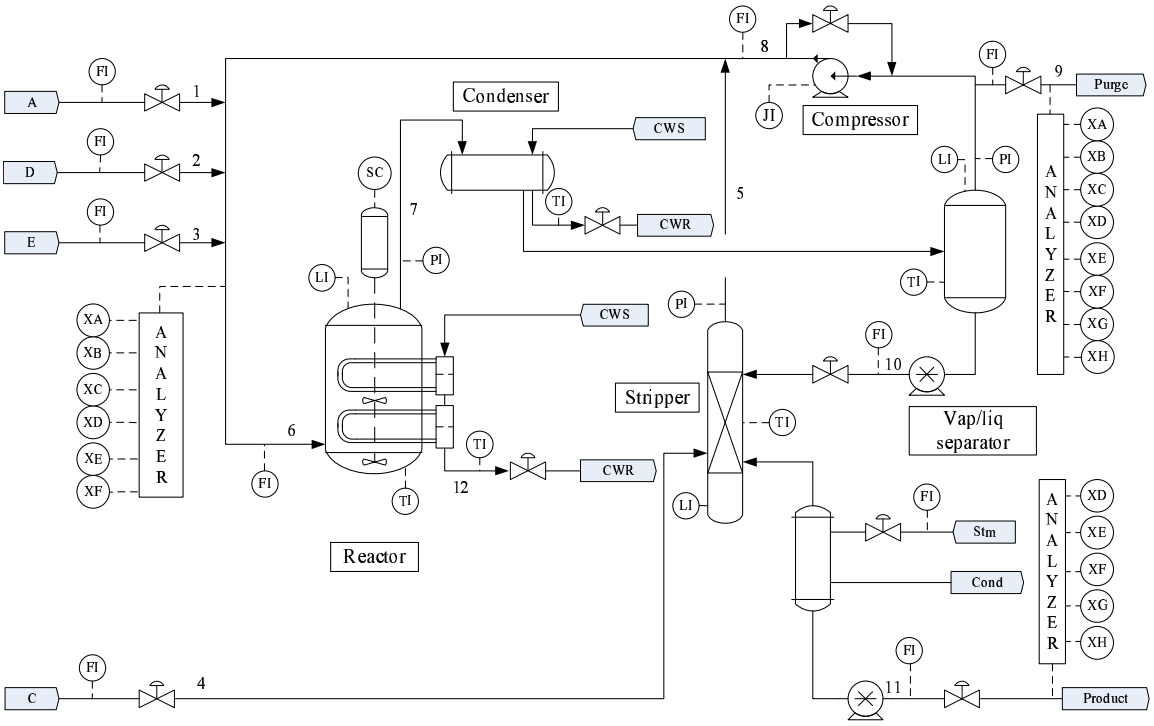


**Figure 7.1:** The Tennessee Eastman process

[32] and the FORTRAN code of the process is available over internet. Fig. 7.1 shows the flow diagram of the process with five major units, i.e. reactor, condenser, compressor, separator and stripper. The process has two products from four reactants. Additionally, an inert and a by-product are also produced making a total of 8 components denoted as A, B, C, D, E, F, G and H. The process allows total 52 measurements out of which 41 are process variables and 11 are manipulated variables listed in Table 7.1 and Table 7.2.

Downs and Fogel initially defined 20 process faults and an additional valve fault was further introduced in [12], see Table 7.3. Since no prior knowledge about the mathematical model of TE process is available, the PM-FD system shall be designed only based on the process data. The data sets given in [12] are widely accepted for PM-FD study, in which 22 training sets (including normal operating condition) were collected to record the process measurements for 24 operation hours. Correspondingly, 22 (on-line) test data sets including 48 hours plant operation time were generated, where the faults were introduced after 8 simulation hours. By considering the time constants of the process in closed loop, the sampling time was selected as 3 minutes. These data sets can be downloaded from `http://brahms.scs.uiuc.edu`. According to the original TE code, a Simulink code provided by [95] is available to simulate the plants closed-loop behavior. Based on the simulator, the operation modes, measurement noise, sampling time and magnitudes of the faults can be easily modified and thus its generated data sets are more helpful for PM-FD

**Table 7.1:** Process variables

| Block name | Variable name | Number |
|---|---|---|
| Input feed | A feed (stream 1) | XMEAS(1) |
| | D feed (stream 2) | XMEAS(2) |
| | E feed (stream 3) | XMEAS(3) |
| | A and C feed | XMEAS(4) |
| Reactor | Reactor feed rate | XMEAS(6) |
| | Reactor pressure | XMEAS(7) |
| | Reactor level | XMEAS(8) |
| | Reactor temperature | XMEAS(9) |
| Separator | Separator temperature | XMEAS(11) |
| | Separator level | XMEAS(12) |
| | Separator pressure | XMEAS(13) |
| | Separator underflow | XMEAS(14) |
| Stripper | Stripper level | XMEAS(15) |
| | Stripper pressure | XMEAS(16) |
| | Stripper underflow | XMEAS(17) |
| | Stripper temperature | XMEAS(18) |
| | Stripper steam flow | XMEAS(19) |
| Miscellaneous | Recycle flow | XMEAS(5) |
| | Purge rate | XMEAS(10) |
| | Compressor work | XMEAS(20) |
| | Reactor water temperature | XMEAS(21) |
| | Separator water temperature | XMEAS(22) |
| Reactor feed analysis | Component A | XMEAS(23) |
| | Component B | XMEAS(24) |
| | Component C | XMEAS(25) |
| | Component D | XMEAS(26) |
| | Component E | XMEAS(27) |
| | Component F | XMEAS(28) |
| Purge gas analysis | Component A | XMEAS(29) |
| | Component B | XMEAS(30) |
| | Component C | XMEAS(31) |
| | Component D | XMEAS(32) |
| | Component E | XMEAS(33) |
| | Component F | XMEAS(34) |
| | Component G | XMEAS(35) |
| | Component H | XMEAS(36) |
| Product analysis | Component D | XMEAS(37) |
| | Component E | XMEAS(38) |
| | Component F | XMEAS(39) |
| | Component G | XMEAS(40) |
| | Component H | XMEAS(41) |

comparison study. Note that the control structure utilized in [12] is different from the one in [95], which may lead to some differences in later simulation study. In the analysis, the base operating mode of TE process is considered to be identical with the case in [12] to simulate the process behavior under stationary operating conditions. The simulator can be downloaded from `http://depts.washington.edu/control/LARRY/TE/download.html`.

**Table 7.2:** Process manipulated variables

| Variable name | Number | Base value(%) | Units |
|---|---|---|---|
| D feed flow | XMV(1) | 63.053 | kg$h^{-1}$ |
| E feed flow | XMV(2) | 53.980 | kg$h^{-1}$ |
| A feed flow | XMV(3) | 24.644 | kscmh |
| A and C feed flow | XMV(4) | 61.302 | kscmh |
| Compressor recycle valve | XMV(5) | 22.210 | % |
| Purge valve | XMV(6) | 40.064 | % |
| Separator pot liquid flow | XMV(7) | 38.100 | $m^3h^{-1}$ |
| Stripper liquid product flow | XMV(8) | 46.534 | $m^3h^{-1}$ |
| Stripper steam valve | XMV(9) | 47.446 | % |
| Reactor cooling water flow | XMV(10) | 41.106 | $m^3h^{-1}$ |
| Condenser cooling water flow | XMV(11) | 18.114 | $m^3h^{-1}$ |

**Table 7.3:** Descriptions of process faults in TE process

| Fault number | Process variable | Type |
|---|---|---|
| IDV(1) | A/C feed ratio, B composition constant | Step |
| IDV(2) | B composition, A/C ration constant | Step |
| IDV(3) | D feed temperature | Step |
| IDV(4) | Reactor cooling water inlet temperature | Step |
| IDV(5) | Condenser cooling water inlet temperature | Step |
| IDV(6) | A feed loss | Step |
| IDV(7) | C header pressure loss-reduced availability | Step |
| IDV(8) | A,B,C feed composition | Random variation |
| IDV(9) | D feed temperature | Random variation |
| IDV(10) | C feed temperature | Random variation |
| IDV(11) | Reactor cooling water inlet temperature | Random variation |
| IDV(12) | Condenser cooling water inlet temperature | Random variation |
| IDV(13) | Reaction kinetics | Slow Drift |
| IDV(14) | Reactor cooling water valve | Sticking |
| IDV(15) | Condenser cooling water valve | Sticking |
| IDV(16) | Unknown | Unknown |
| IDV(17) | Unknown | Unknown |
| IDV(18) | Unknown | Unknown |
| IDV(19) | Unknown | Unknown |
| IDV(20) | Unknown | Unknown |
| IDV(21) | The valve fixed at steady state position | Constant position |

### 7.1.2 FBFP process

The FBFP process is a typical dynamic, multi-stage batch process that is utilized to demonstrate the effectiveness of the subspace aided data-driven approach. A flow diagram of this benchmark is shown in Fig. 7.2. The fed-batch penicillin fermentation can be divided into two operation stages, i.e. the pre-culture stage with biomass growth and the fed-batch stage. In the pre-culture stage, the initial substrate is consumed by microorganisms and the glucose is depleted. In case that glucose concentration reaches a pre-defined value, the fed-batch stage begins with continuous substrate feed, which is an

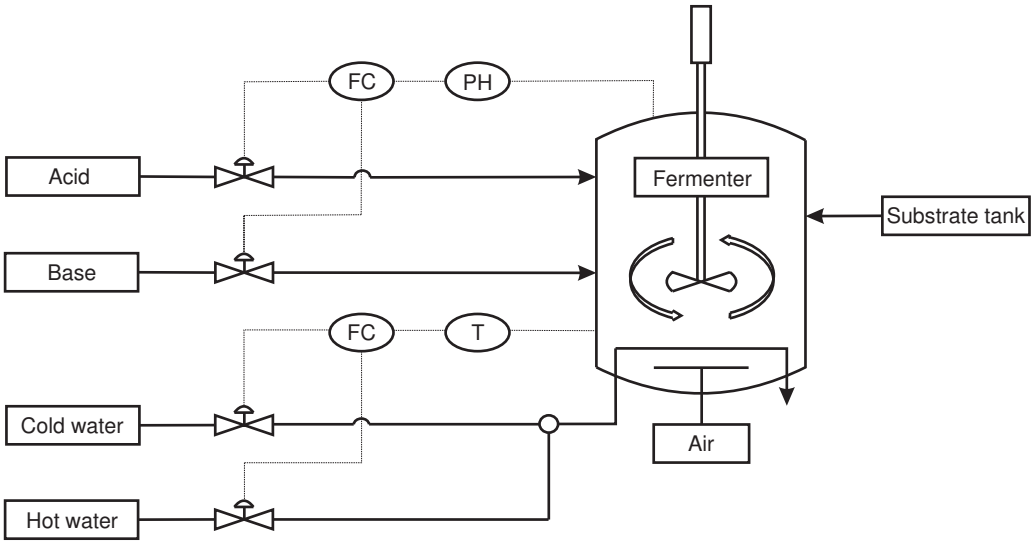


**Figure 7.2:** Fed-batch fermentation penicillin process

open-loop operation procedure. Two PID controllers are installed to control the pH and the temperature in fermenter through manipulating the acid/base solution and hot/cold water flow rate.

The data sets generated from PenSim v2.0 [7], including 12 process variables, are listed in Table 7.4. The entire duration of each batch is 400h and consists pre-culture phase about 44h and fed-batch stage of 356h. The sampling interval for off-line design and on-line implementation is chosen as 0.5h. The initial conditions and set points for normal operations are listed in Table 7.5. The simulator PenSim v2.0. is available at the web site `http://216.47.139.198/pensim/simul.html`.

**Table 7.4:** Descriptions of process variables

| Number | Process variable | Unit |
|---|---|---|
| 1 | Aeration rate | $L/h$ |
| 2 | Agitator power | $W$ |
| 3 | Substrate feed temperature | $K$ |
| 4 | Substrate concentration | $g/L$ |
| 5 | Dissolved oxygen concentration | $g/L$ |
| 6 | Culture volume | $L$ |
| 7 | Carbon dioxide concentration | $g/L$ |
| 8 | pH | |
| 9 | Fermenter temperature | $K$ |
| 10 | Cooling water flow rate | $L/h$ |
| 11 | Biomass concentration | $g/L$ |
| 12 | Penicillin concentration | $g/L$ |

**Table 7.5:** Initial conditions and set points

| | |
|---|---|
| **Initial conditions** | |
| Substrate concentration | 14-16 $g/h$ |
| Dissolved oxygen concentration | 1.16 $mmol/L$ |
| Biomass concentration | 0.09-0.11 $g/L$ |
| Penicillin concentration | 0 $g/L$ |
| Culture volume | 100-104 $L$ |
| Carbon dioxide concentration | 0.5-0.55 $mmol/L$ |
| Carbon dioxide concentration | 0.5-0.55 $mmol/L$ |
| Carbon dioxide concentration | 0.5-0.55 $mmol/L$ |
| pH | 4.9-5.1 |
| Bioreactor temperature | 298-299 $K$ |
| Generated heat | 0 $kcal$ |
| **Set points** | |
| Aeration rate | 8.5-8.6 $g/h$ |
| Agitator power | 29-31 $W$ |
| Substrate feed flow rate | 0.040-0.043 $L/h$ |
| Bioreactor temperature | 296-297 $K$ |
| PH | 5.0-5.2 |
| Substrate feed temperature | 298-299 $K$ |

### 7.1.3 CSTH process

The CSTH simulator is developed by Thornhill et al. [101]. The nonlinear behaviors and the physical constraints of the real plant are accurately captured by look-up table in the simulation model. In addition, the hybrid simulator includes more realistic characteristics of noise and disturbances derived from the real measurements. Moreover, the set point of CSTH process can be non-steady that offers challenging task especially for the adaptive process monitoring approaches.

The structure of CSTH process is showed in Fig. 7.3. The cold and hot water are mixed, further heated by a heating coil and then flow out through a long pipe. The temperature in the tank is homogeneous. By integrating three PID controllers, the cold water level and the temperature of the water in tank, which are the manipulated variables, can be controlled according to their related set point values. The process inputs consist of hot water, cold water, and steam valve position. The cold water flow, level and temperature of the tank are measured output signals. The set point variation of manipulated variables results in significant change of system parameters and makes the CSTH a time varying system. Therefore, CSTH is used as a benchmark for illustrate the effectiveness of adaptive DO-based residual generation scheme.

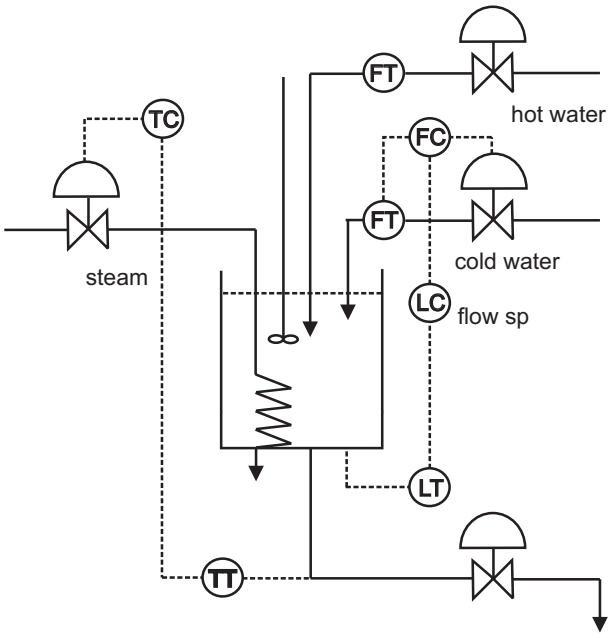


**Figure 7.3:** CSTH process

## 7.2 MSPM methods on TE

The first objective in this section is to implement the modified approach proposed in chapter 4 to detect 21 pre-defined faults listed in Table 7.3. The data sets offered by [13] are utilized, in which 22 process measurements (XMEAS(1-22)) and 11 manipulated variables (XMV(1-11)) are considered as input variables $U$ and the analyzer for component G (XMEAS(35)) is treated as a product quality variable, $y$. Both standard PLS and proposed approach based process monitoring schemes are designed according to 480 samples obtained from the normal process operation. The number of latent variables is selected as 6 based on the cross validation tests. Since the faults in TE may occur in different subspaces, which are generally unknown in practice, a reasonable process monitoring logic is achieved by joint use of the related test statistics, i.e. for the modified approach by means of $T_{\tilde{x}}^2$, $T_{\tilde{x}}^2$ and PLS using $T^2$, SPE indices.

Table 7.6 summarizes the results of the experiments for all the faults in TE process, in which the number printed in bold denotes the highest fault detection rate (FDR) related to the certain type of fault. It can be seen that the modified approach shows significant improvements on FDRs compared with standard PLS method, especially in the case of IDV(5), IDV(16) and IDV(19). According to Table 7.3, IDV(5) represents a step-wise fault in condenser cooling water inlet temperature happened after the 160th time sample. It occurs in both subspaces with significant influence on product quality variable $y$. The process monitoring results of IDV(5) offered by standard PLS and modified approach are

**Table 7.6:** FDR (%): PLS vs. modified approach

| Fault number | PLS ($T^2$ or SPE) | modified ($T^2_{\hat{x}}$ or $T^2_{\tilde{x}}$) |
|---|---|---|
| IDV(1) | 99.88 | **100** |
| IDV(2) | 98.63 | **99.88** |
| IDV(3) | 14.25 | **18.75** |
| IDV(4) | 99.5 | **100** |
| IDV(5) | 33.63 | **100** |
| IDV(6) | **100** | **100** |
| IDV(7) | **100** | **100** |
| IDV(8) | 97.88 | **98.63** |
| IDV(9) | **14.5** | 12.13 |
| IDV(10) | 82.63 | **91.3** |
| IDV(11) | 78.63 | **83.25** |
| IDV(12) | 99.25 | **99.88** |
| IDV(13) | 95.25 | **95.5** |
| IDV(14) | **100** | **100** |
| IDV(15) | 23 | **23.25** |
| IDV(16) | 68.38 | **94.28** |
| IDV(17) | 94.25 | **97.13** |
| IDV(18) | 90.75 | **91.25** |
| IDV(19) | 26 | **94.25** |
| IDV(20) | 62.75 | **91.5** |
| IDV(21) | 59.88 | **72.75** |

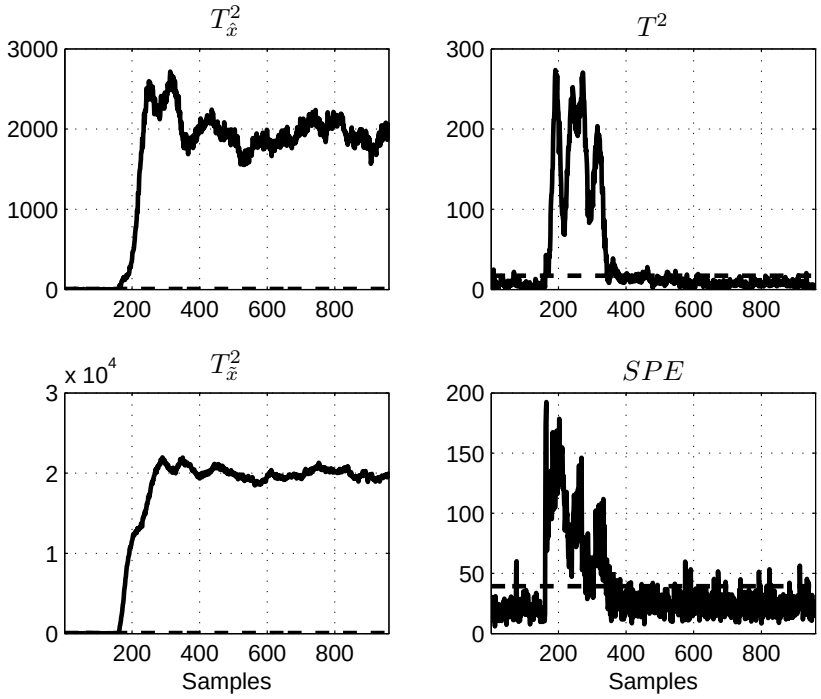


**Figure 7.4:** Process monitoring in case of IDV(5)

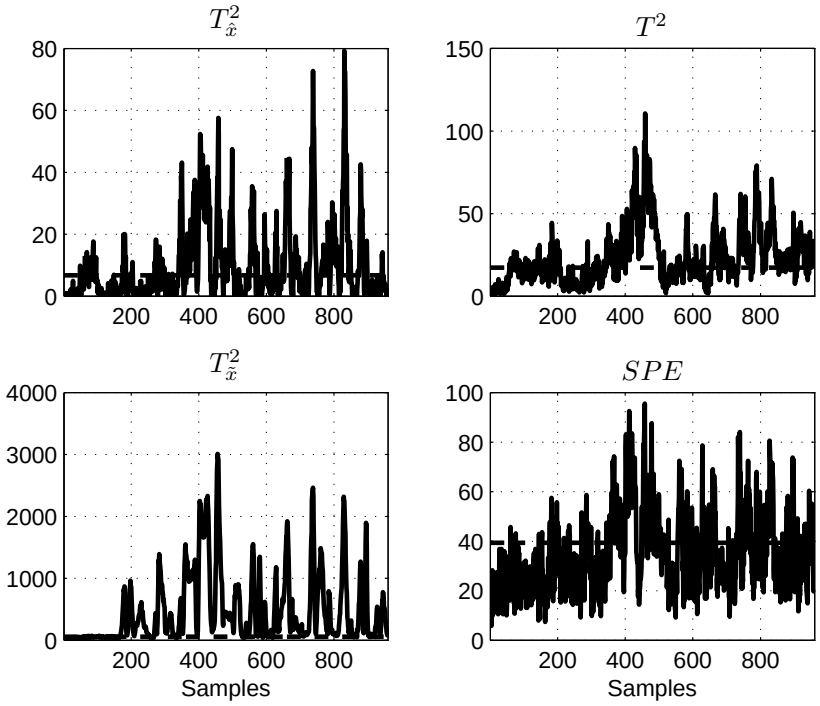


**Figure 7.5:** Process monitoring in case of IDV(16)

presented in Fig. 7.4, from which it can be seen that the modified approach has persistent response to the fault during its occurrence.

Similarly, IDV(16) denotes a fault occurred in the both subspaces as shown in Fig. 7.5, from which the modified approach also provides superior fault detection performance. In addition, IDV(19) represents the fault which almost has no influence on product quality variable. From Fig. 7.6 it is obvious that the $T^2_{\tilde{x}}$ statistic of the modified approach is more sensitive than SPE of standard PLS under the similar FDRs given by $T^2_{\hat{x}}$ and $T^2$ statistics.

If the nature of the fault is known in advance, the false classification rate (FCR) for the fault unrelated to $y$ is another critical index for evaluating the related methods. For this purpose, $T^2_{\hat{x}}$ and $T^2$ are respectively utilized to calculate FCRs for modified approach and standard PLS. To classify the faults, the criterion presented in [134] is used to divide the faults into two categories, i.e. (a) fault affecting $y$ and, (b) fault having no influence on $y$. Particularly, the fault is said to affect $y$, if over 10% samples of $y$ exceed certain threshold after the fault occurs. Otherwise, the faults are assumed to have no influence on $y$. The threshold for $y$ can be determined based on the normal operation data.

Based on this criterion, the process faults IDV(3-4), IDV(9,11), IDV(14-15) and

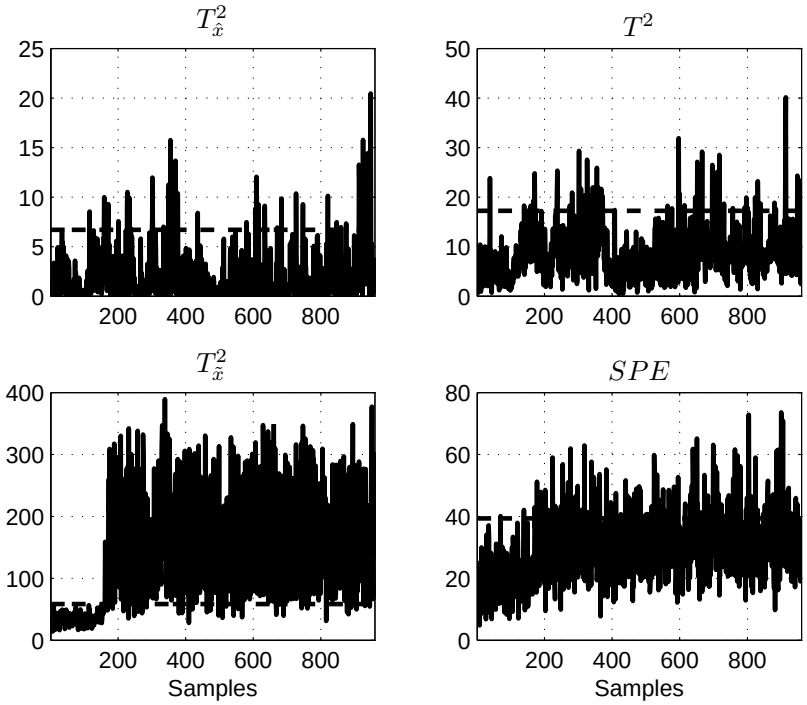


**Figure 7.6:** Process monitoring in case of IDV(19)

IDV(19) have almost no influence on $y$. Table 7.7 gives the FCRs of both methods. It can be shown that except IDV(3) and IDV(19), in which PLS and the modified approach give similar FCRs, the modified approach gives significantly lower FCRs than the other methods which proves an excellent choice.

Another objective of this section is to evaluate the basic MSPM methods as well as subspace aided approach when the process works in constant operating regime. For this purpose, the TE simulator proposed in [95] is utilized to generate the process data for Monte Carlo study. For each type of faults, one hundred Monte Carlo simulations are performed to obtain FDRs of all the discussed methods. The measurement noises are

**Table 7.7:** FCR (%): PLS vs. modified approach

| Fault number | PLS ($T^2$) | modified ($T^2_{\hat{x}}$) |
|---|---|---|
| IDV(3) | **11.5** | 13.63 |
| IDV(4) | 63.13 | **11** |
| IDV(9) | 11.38 | **7.63** |
| IDV(11) | 64.75 | **10.25** |
| IDV(14) | 99.88 | **10** |
| IDV(15) | 20.88 | **10.5** |
| IDV(19) | **6.63** | 7 |

**Table 7.8:** FDRs (%) based on simulator

| Fault | PCA | PLS | Modified | Subspace |
|---|---|---|---|---|
| IDV(1) | 99.64 | **99.77** | 99.63 | 99.3 |
| IDV(2) | 99.65 | **99.76** | 99.63 | 99.25 |
| IDV(8) | **100** | **100** | **100** | **100** |
| IDV(9) | **99.99** | **99.99** | **99.99** | **99.99** |
| IDV(10) | **100** | **100** | **100** | **100** |
| IDV(11) | **99.63** | **99.63** | **99.63** | **99.63** |
| IDV(12) | **99.88** | **99.88** | **99.88** | **99.88** |
| IDV(13) | **99.63** | **99.63** | **99.63** | **99.63** |
| IDV(4) | 58.98 | 57.61 | 56.58 | **61.15** |
| IDV(6) | 78.1 | 77.28 | 93.9 | **99.02** |
| IDV(7) | 94.88 | 95.13 | 96.17 | **98.07** |
| IDV(17) | 75.59 | 76.56 | 78.26 | **92.2** |
| IDV(18) | 31.19 | 31.16 | 36.52 | **73.12** |
| IDV(20) | 50.63 | 52.93 | 65.8 | **80.41** |
| IDV(3) | 1.49 | 2.03 | 1.53 | **3.57** |
| IDV(5) | 1.42 | 1.81 | 1.41 | **2.95** |
| IDV(14) | 1.57 | 1.81 | 1.49 | **3.02** |
| IDV(15) | 1.53 | 1.77 | 1.4 | **3.19** |
| IDV(16) | 1.52 | 1.82 | 1.61 | **3.6** |
| IDV(19) | 1.47 | 1.78 | 1.47 | **3.45** |

added to process variables in each simulation run. Since the magnitudes of faults defined in the simulator are very large, the modified magnitudes, which are less than 40% of original values, are implemented in the simulation study.

Table 7.8 summarizes the detailed FDRs. In the first block of Table 7.8, we can see that all the tested methods give similar FDRs. The evident difference among FDRs can be found in the second block of this Table, where subspace aided approach offers much better FDRs over all the other methods. However, the faults listed in the third block are undetectable by all the given methods.

Based on the observations obtained in this section, it is necessary to point out that (a) the modified approach offers much better FDRs and more accurate fault diagnosis information compared with the standard PLS approach; (b) the basic MSPM methods like PCA and PLS, which have not considered the dynamic properties of the process, shows relatively lower FDRs compared with the subspace aided approach even under stationary operating conditions; and (c) in practice, the large scale industrial plants are generally complex dynamic systems and the process measurements will not strictly follow Gaussian distribution as shown in TE process. Although the process data can not perfectly fulfill the basic assumptions, most of the tested methods show their abilities for process monitoring within constant operating regime. Especially, the subspace aided approach, which has higher FDRs and relatively lower computation cost, will receive more attentions in practice application.

## 7.3 Subspace approach on FBFP

Since FBFP process is a typical dynamic, multi-stage batch process, it is utilized in this section to demonstrate the effectiveness of the proposed data-driven subspace aided approach. The trajectories of 12 process variables from a normal batch operation are depicted in Fig. 7.7.

A total of 20 batches of normal process operation data were generated by PenSim v2.0 for off-line design procedure. The biomass and penicillin concentrations are selected as output variables and the other 9 process variables serve as input variables, see Table 7.4. There are totally 16000 data samples collected from normal operation batches and $s$ is chosen as 10 to build the Hankel matrix. Based on them, diagnostic observers were constructed according to Algorithm D2MDO.

Based on the constructed DO-based residual generators, the abnormal batches, including four typical process faults at different stages of fermentation listed in Table 7.9, are utilized to verify the effectiveness of the proposed approach.

The first fault, presenting 20% step decrease in agitation power, was introduced to the first abnormal batch at 180 $h$ and retaining until to the end of this batch (380 $h$). As pointed by [7], an abnormal decrease of agitation power can lead to a lower dissolved oxygen concentration in the culture medium and will finally cause the undesired decrease of penicillin concentration. The process monitoring result of the proposed approach is shown in Fig. 7.8(a), from which it is obvious that the test statistic significantly exceeds the threshold from 190 $h$ which indicates an occurrence of fault. The abnormal situations related to substrate feed rate were also taken into consideration due to its influence on the final penicillin production. Two types of such faults, which represent linear decrease and step change of substrate feed rate, were introduced in the 2-nd and 3-rd batches at different stage of fermentation. From Fig. 7.8(b) and Fig. 7.8(c) it can be observed that the slow decreasing of substrate feed rate can be detected after 320 $h$, while the step decrease of substrate feed rate can be immediately monitored after its occurrence. In the 4-th abnormal batch, a 20% step fault was imposed to aeration rate after 180 $h$. The monitoring result is shown Fig. 7.8(d), which indicates a fast detection of abnormality after 190 $h$.

**Table 7.9:** Process faults in FBFP process

| Batch No. | Description of faults | Occurrence time ($h$) |
|---|---|---|
| 1 | 20% step decrease in agitation power | 180 |
| 2 | linear decrease of substrate feed rate from 0.042 to 0.032 $L/h$ | 230 |
| 3 | 30% step decrease in substrate feed rate | 50 |
| 4 | 20% step decrease in aeration rate | 180 |

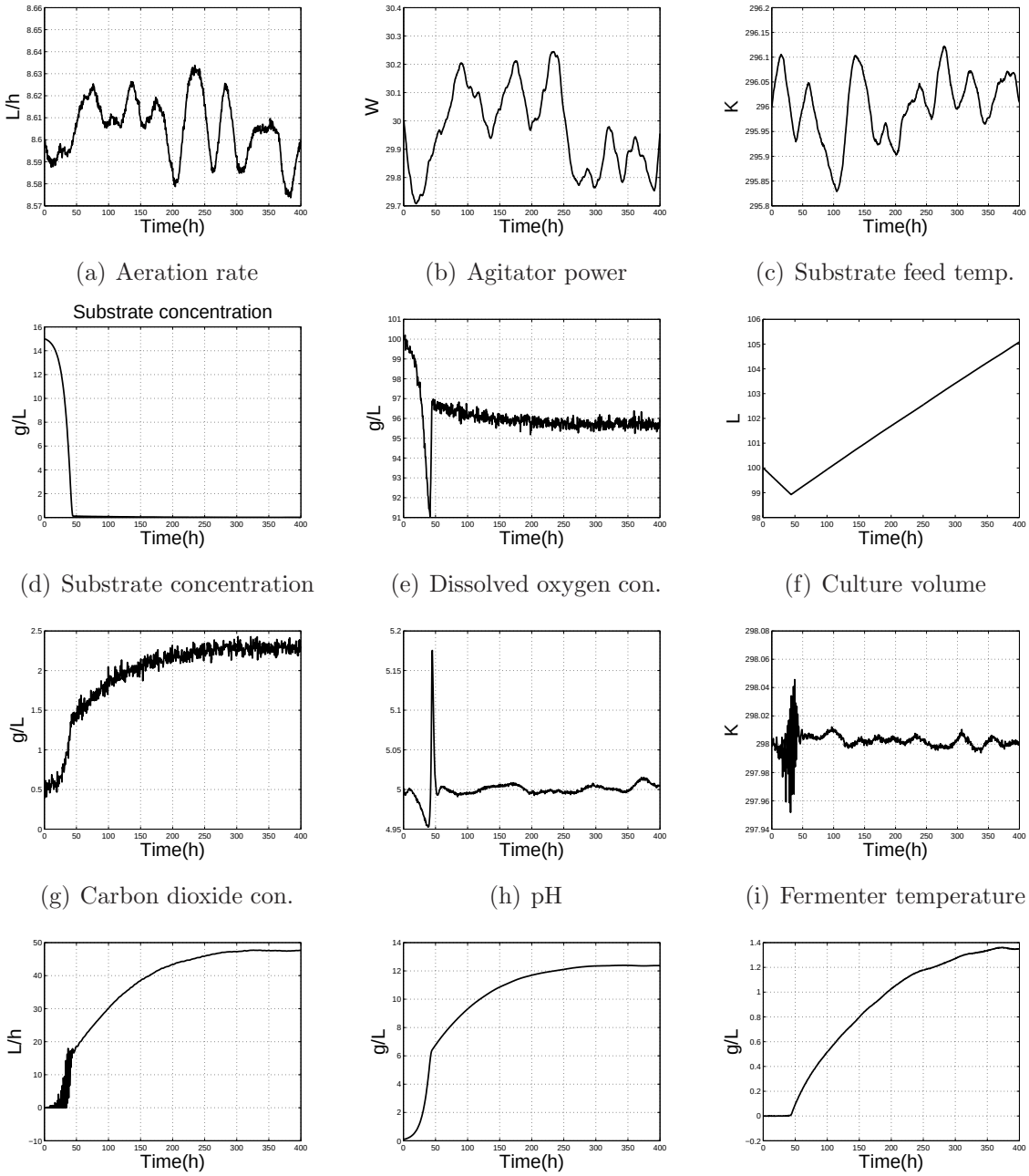


(a) Aeration rate (b) Agitator power (c) Substrate feed temp.

(d) Substrate concentration (e) Dissolved oxygen con. (f) Culture volume

(g) Carbon dioxide con. (h) pH (i) Fermenter temperature

(j) Cooling water flow rate (k) Biomass concentration (l) Penicillin concentration

**Figure 7.7:** Process variables in a normal batch

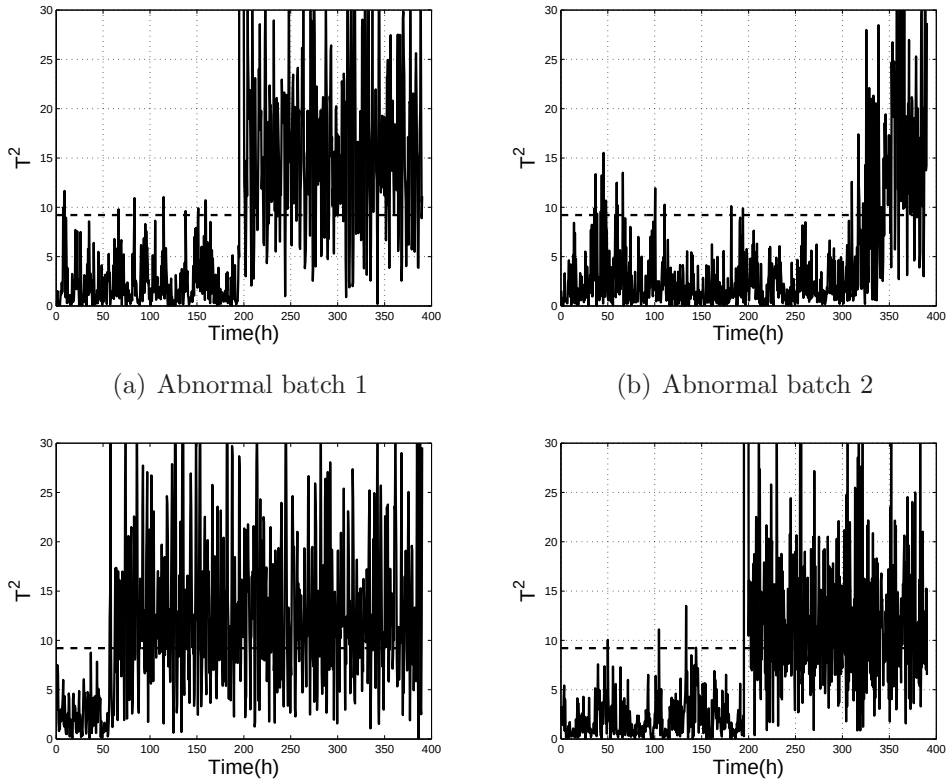


(a) Abnormal batch 1

(b) Abnormal batch 2

(c) Abnormal batch 3

(d) Abnormal batch 4

**Figure 7.8:** On-line process monitoring

## 7.4 Adaptive approach on CSTH

In this section, CSTH process is utilized to check the effectiveness of data-driven adaptive DO-based residual generation scheme. As suggested in [101], the set point variation in CSTH process results in significant change of system parameters and makes the CSTH a time varying system.

The CSTH process is simulated to collect 1800 data samples. During the first and the last 400 data samples, the set points of cold water valve position and steam valve position are unchanged. In the middle 1000 data samples, both set points are consistently changed from $12mA$ and $10.5mA$ to $12.8mA$ and $9.7mA$, respectively, in order to simulate the time varying scenario, which is considered as normal process operation.

The first 300 data samples are used to construct the DO-based residual generator without adaptive scheme. The residual signals of the adaptive scheme and conventional DO-based method are illustrated in Fig. 7.9 with confidence level $\alpha = 0.99$. It is clear that the conventional method is not competent to monitor the process under time varying scenario that can be seen by the numerous false alarms.

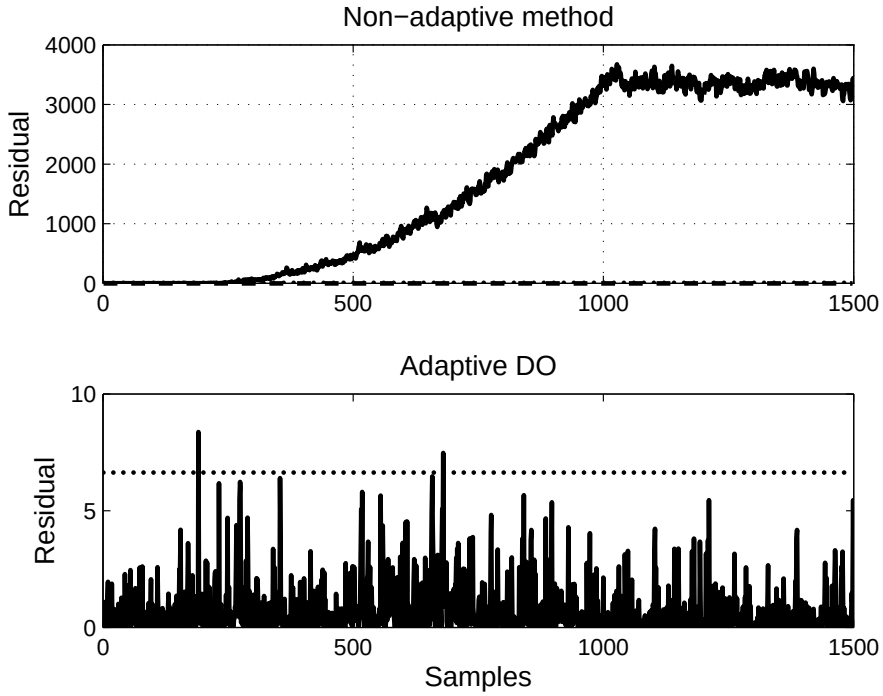


**Figure 7.9:** Conventional vs. Adaptive

In the last experiment, a sensor fault is simulated inside the CSTH process, with all other operating conditions remaining unchanged. The fault occurs between 1300-th and 1400-th samples and is approximately 10% bias to the actual flow measurement. It can be seen in Fig. 7.10 that the adaptive DO-based residual generator comfortably detects the fault after its occurrence. Hence, the proposed adaptive scheme is more suitable for process monitoring under industrial operating conditions with uncertainty issue.

## 7.5 Concluding remarks

In this chapter, all the discussed data-driven methods are implemented on three well-known industrial benchmark processes to show their effectiveness for process monitoring purpose. The basic MSPM methods as well as data-driven subspace aided approach are firstly applied on TE process. Most of these methods illustrate their monitoring abilities for such a large-scale industrial plant under stationary operating conditions. Especially, the proposed modified PLS approach and subspace aided approach offer superior results compared to the other methods. In addition, the subspace aided approach is further tested on FBFP plant and shows satisfactory results for monitoring such a typical dy-

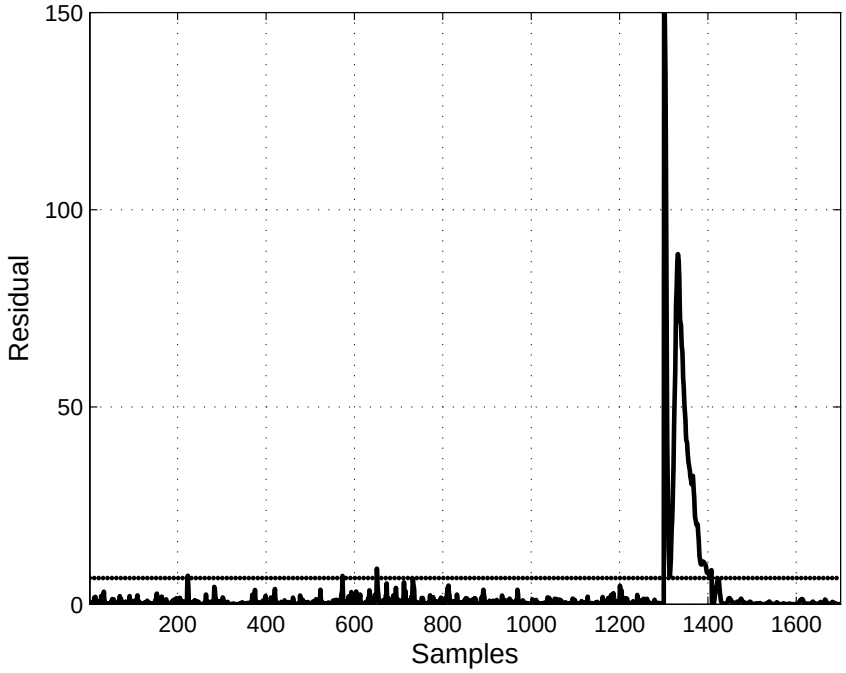


**Figure 7.10:** Adaptive DO-based process monitoring

namic, multi-stage process. The adaptive DO-based residual generation scheme is finally implemented on the CSTH process. The simulation results show that the adaptive design scheme performs better than the conventional non-adaptive approach in handling uncertainty issue, e.g. operating point variations.

# 8 Conclusions and future work

The primary objective of this thesis was to design efficient data-driven fault diagnosis systems according to operating conditions of the underlying process. An overview of major developments and basic concepts of fault diagnosis techniques, which include model-based and MSPM approaches, are firstly presented. Since it is difficult to obtain quantitative model through the first principles in practice, the basic data-driven MSPM approaches like PCA and PLS are then studied due to their easy design and simple operation. The modifications on basic MSPM approaches are helpful to improve the process monitoring performance under stationary operating conditions.

Based on the review of GLR method in Chapter 3, an alternative test statistic is proposed for PCA-based fault diagnosis approach. Compared with standard SPE index, the threshold calculation of the new test statistic is considerably simple without statistical approximation. The fault sensitivity of the associated test statistics is then analyzed. An algorithm is finally proposed to identify the off-set and scaling faults.

In Chapter 4, a new approach is proposed to overcome the drawbacks of standard PLS approach. The core of this approach is to calculate the coefficient matrix in a least square sense and then perform orthogonal decomposition on the input space according to its correlation with outputs. This approach does not only deliver a better fault diagnosis performance but also requires less computation in comparison with the standard PLS scheme. An algorithm for fault identification is also included.

Although the modifications on basic MSPM methods enhance fault diagnosis performance under steady operating conditions, the process dynamic and uncertainty issues can not be directly treated by these approaches. The subspace aided data-driven approach, which combines the advantages of model-based and MSPM techniques, is then proposed in Chapter 5 to achieve fault diagnosis on dynamic processes under industrial operating conditions. The novel approach identifies only key components from the process data instead of identifying the complete process model. According to the one-to-one relationship between parity space and DO, observer-based implementation can be achieved with enhanced performance and less computation cost. To ensure high sensitivity to the faults, the multiple residual generation scheme is further developed. The state estimator design scheme is also included for process monitoring and control purposes.

The uncertainty issues in the industrial environment are discussed in Chapter 6. The DO-based residual generator designed with the help of subspace tracking algorithms is firstly proposed to deal with uncertainty change, e.g. operating point or process parameter variations. A data-driven adaptive residual generation scheme is then proposed with desired performance on stability and convergence issues. This adaptive scheme does not involve complicated computation and produces consistent estimate of the key parameters. Thus, it is extremely suitable for process monitoring in large-scale process under industrial operating conditions with uncertain change.

In Chapter 7, the proposed data-driven methods are finally implemented on industrial benchmark processes to evaluate their effectiveness for process monitoring purpose. All of the aforementioned approaches illustrate their monitoring abilities for a large-scale industrial plant under ideal stationary operating conditions. In particular, the proposed subspace aided approach and modified PLS approach offer superior results over the other methods. Moreover, the subspace aided approach and adaptive DO-based residual generation scheme show their superior performance to deal with process dynamics and uncertainty issues, respectively, and thus are suitable choices for process monitoring under industrial operating conditions.

This work attempts to build a framework for the data-driven design of fault diagnosis systems to deal with different operating conditions. Another issue that requires worthy attention is design of fault-tolerant controller with embedded fault diagnosis schemes. The major objective of future investigation is to establish a framework for the design and construction of the fault tolerant architecture directly from the process data. Realization of advanced FDI/FTC schemes on this fault-tolerant architecture is the overall goal in the future works.

# Bibliography


[1] K.J. Aström and B. Wittenmark. *Adaptive Control*. Addison-Wesley Longman Publishing Co., Inc., Reading, Massachusetts, USA, 1996.

[2] M. Basseville. Detecting changes in signals and systems - a survey. *Automatica*, 24 (3):309–326, 1988.

[3] M. Basseville. On-board component fault detection and isolation using the statistical local approach. *Automatica*, 34(11):1391–1415, 1998.

[4] M. Basseville and I. Nikiforov. *Detection of Abrupt Changes: Theory and Application*. Prentice Hall, 1993.

[5] G. Bastin and M.R. Gevers. Stable adaptive observers for nonlinear time-varying systems. *IEEE Transaction on Automatic Control*, 33(7):650–658, 1988.

[6] R. Beard. *Failure Accommodation in Linear Systems through Self-Reorganization*. PhD dissertation, Massachusetts Institute of Technology, 1971.

[7] G. Birol, C. Ündey, and A. Cinar. A modular simulation package for fed-batch fermentation: penicillin production. *Computers and Chemical Engineering*, 26(11): 1553–1565, 2002.

[8] M. Blanke, M. Kinnaert, J. Lunze, M. Staroswiecki, and J. Schröder. *Diagnosis and Fault-Tolerant Control*. Springer Verlag, Berlin, 2006.

[9] B. Champagne. Adaptive eigendecomposition of data covariance matrices based on first-order perturbations. *IEEE Transactions on Signal Processing*, 42(10):2758–2770, 1994.

[10] J. Chen and K.C. Liu. On-line batch process monitoring using dynamic PCA and dynamic PLS models. *Chemical Engineering Science*, 57(1):63–75, 2002.

[11] J. Chen and R.J. Patton. *Robust Model-Based Fault Diagnosis for Dynamic Systems*. Kluwer Academic Publishers, Norwell, MA, USA, 1999.

[12] L.H. Chiang, E.L. Russell, and R.D. Braatz. Fault diagnosis in chemical processes using fisher discriminant analysis, discriminant partial least squares, and principal component analysis. *Chemometrics and Intelligent Laboratory Systems*, 50(2):243–252, 2000.

[13] L.H. Chiang, E. Russell, and R.D. Braatz. *Fault Detection and Diagnosis in Industrial Systems*. Springer Verlag, London, 2001.

[14] L.H. Chiang, M.E. Kotanchek, and A.K. Kordon. Fault diagnosis based on fisher discriminant analysis and support vector machines. *Computers and Chemical Engineering*, 28(8):1389–1401, 2004.

[15] S.W. Choi and I.-B. Lee. Nonlinear dynamic process monitoring based on dynamic kernel PCA. *Chemical Engineering Science*, 59(24):5897–5908, 2004.

[16] S.W. Choi and I.-B. Lee. Multiblock PLS-based localized process diagnosis. *Journal of Process Control*, 15(3):295–306, 2005.

[17] E. Chow and A. Willsky. Analytical redundancy and the design of robust failure detection systems. *IEEE Transactions on Automatic Control*, 29(7):603–614, 1984.

[18] B.S. Dayal and J.F. MacGregor. Improved PLS algorithms. *Journal of Chemometrics*, 11(1):73–85, 1997.

[19] B. De Moor and P. Van Overschee. Unifying theorem for three subspace system identification algorithms. *Automatica*, 31(12):1853–1864, 1995.

[20] R.D. DeGroat. Noniterative subspace tracking. *IEEE Transactions on Signal Processing*, 40(3):571–577, 1992.

[21] S.X. Ding. *Model-based Fault Diagnosis Techniques*. Springer Verlag, Berlin, 2008.

[22] S.X. Ding, T. Jeinsch, and E.L. Ding. An approach to analysis and design of observer and parity relation based FDI systems. In *Proceedings of the 16th IFAC World Congress*. Beijing, P.R. China, 1999.

[23] S.X. Ding, S. Yin, P. Zhang, E.L. Ding, and A.S. Naik. An approach to data-driven adaptive residual generator design and implementation. In *Proceedings of the 7th IFAC Symposium on Fault Detection and Supervision and Safety of Technical Processes*. Barcelona, Spain, 2009.

[24] S.X. Ding, P. Zhang, A.S. Naik, E.L. Ding, and B. Huang. Subspace method aided data-driven design of fault detection and isolation systems. *Journal of Process Control*, 19(9):1496–1510, 2009.

[25] S.X. Ding, P. Zhang, E.L. Ding, S. Yin, A.S. Naik, P. Deng, and W. Gui. On the application of PCA technique to fault diagnosis. *Tsinghua Science and Technology*, 15(2):138–144, 2010.

[26] S.X. Ding, S. Yin, Y. Wang, Y. Wang, Y. Yang, and B. Ni. Data-driven design of observers and its applications. In *Proceedings of the 18th IFAC World Congress*, Milano, Italy, 2011.

[27] S.X. Ding, P. Zhang, and S. Yin. An integrated design framework of fault tolerant wireless networked control systems for industrial automatic control applications. *Submitted to IEEE Transactions on Industrial Informatics*, 2011.

[28] X. Ding, L. Guo, and T. Jeinsch. A characterization of parity space and its application to robust fault detection. *IEEE Transactions on Automatic Control*, 44(2): 337–343, 1999.

[29] D. Dong and T.J. McAvoy. Batch tracking via nonlinear principal component analysis. *AIChE Journal*, 42(8):2199–2208, 1996.

[30] X.G. Doukopoulos and G. Moustakides. Fast and stable subspace tracking. *IEEE Transactions on Signal Processing*, 56(4):1452–1465, 2008.

[31] X.G. Doukopoulos and G.V. Moustakides. Blind adaptive channel estimation in OFDM systems. *IEEE Transactions on Wireless Communications*, 5(7):1716–1725, 2006.

[32] J. Downs and E. Fogel. A plant-wide industrial process control problem. *Computers and Chemical Engineering*, 17(3):245–255, 1993.

[33] R.O. Duda, P.E. Hart, and D.G. Stork. *Pattern Classification*. Wiley Interscience, New York, 2001.

[34] R. Dunia and S.J. Qin. Joint diagnosis of process and sensor faults using principal component analysis. *Control Engineering Practice*, 6(4):457–469, 1998.

[35] L. Elshenawy, S. Yin, A.S. Naik, and S.X. Ding. Efficient recursive principal component analysis algorithms for process monitoring. *Industrial and Engineering Chemistry Research*, 49(1):252–259, 2010.

[36] W. Favoreel, B. De Moor, and P. Van Overschee. Subspace state space system identification for industrial processes. *Journal of Process Control*, 10(2-3):149–155, 2000.

[37] F. Flehmig and W. Marquardt. Detection of multivariable trends in measured process quantities. *Journal of Process Control*, 16(9):947–957, 2006.

[38] P.M. Frank. Fault diagnosis in dynamic systems using analytical and knowledge-based redundancy: A survey and some new results. *Automatica*, 26(3):459–474, 1990.

[39] P.M. Frank, S.X. Ding, and T. Marcu. Model-based fault diagnosis in technical processes. *Transactions of the Institute of Measurement and Control*, 22(1):57–101, 2000.

[40] J. Gertler. *Fault Detection and Diagnosis in Engineering Systems*. Marcel Dekker Inc., New York, USA, 1998.

[41] J. Gertler and J. Cao. PCA-based fault diagnosis in the presence of control and dynamics. *AIChE Journal*, 50(2):388–402, 2004.

[42] J. Gertler and R. Monajemy. Generating directional residuals with dynamic parity relations. *Automatica*, 31(4):627–635, 1995.

[43] J. Gertler and D. Singer. A new structural framework for parity equation-based failure detection and isolation. *Automatica*, 26(2):381–388, 1990.

[44] M. Girolami. *Self-Organising Neural Networks: Independent Component Analysis and Blind Source Separation*. Springer Verlag, London, 1999.

[45] T. Gustaffson and C. MacInnes. A class of subspace tracking algorithm based on approximation of noise subspace. *IEEE Transaction on Signal Processing*, 48(11): 3231–3235, 2000.

[46] Q.P He, S.J Qin, and J. Wang. A new fault diagnosis method using fault directions in fisher discriminant analysis. *AIChE Journal*, 51(2):555–571, 2005.

[47] D.M. Helland, H.E. Bernstein, O.S. Borgen, and H. Martens. Recursive algorithm for partial least squares regression. *Chemometrics and Intelligent Laboratory Systems*, 14(1-3):129–137, 1992.

[48] I.S. Helland. On the structure of partial least squares regression. *Communications in Statistics-Simulation and Computation*, 17:581–607, 1998.

[49] A. Höskuldsson. PLS regression methods. *Journal of Chemometrics*, 2:211–228, 1988.

[50] I. Hwang, S. Kim, Y. Kim, and C.E. Seah. A survey of fault detection, isolation, and reconfiguration methods. *IEEE transactions on control systems technology*, 18 (3):636–653, 2010.

[51] A. Hyvärinen, J. Karhunen, and E. Oja. *Independent Component Analysis*. Wiley, New York, 2001.

[52] R. Isermann. Fault diagnosis of machines via parameter estimation and knowledge processing: tutorial paper. *Automatica*, 29(4):815–835, 1993.

[53] R. Isermann. *Fault Diagnosis Systems: an introduction from fault detection to fault tolerance*. Springer Verlag, Berlin, 2006.

[54] J.E. Jackson. *A User's Guide to Principal Components*. Wiley Interscience, New York, USA, 1991.

[55] J.E. Jackson and G.S. Mudholkar. Control procedures for residuals associated with principal component analysis. *Technometrics*, 21(3):341–349, 1979.

[56] S.-L. Jämsä-Jounela, M. Vermasvuori, P. Enden, and S. Haavisto. A process monitoring system based on the kohonen self-organizing maps. *Control Engineering Practice*, 11(1):83–92, 2003.

[57] M. Jia, F. Chu, F. Wang, and W. Wang. On-line batch process monitoring using batch dynamic kernel principal component analysis. *Chemometrics and Intelligent Laboratory Systems*, 101(2):110–122, 2010.

[58] I.T. Jolliffe. *Principal Component Analysis*. Springer Verlag, Berlin, 1986.

[59] H.L. Jones. *Failure Detection in Linear Systems*. PhD dissertation, Massachusetts Institute of Technology, 1973.

[60] M. Kano, S. Tanaka, S. Hasebe, and I. Hashimoto. Monitoring independent components for fault detection. *AIChE Journal*, 49(4):969–976, 2003.

[61] A.A. Khan, J.R. Moyne, and D.M. Tilbury. Virtual metrology and feedback control for semiconductor manufacturing processes using recursive partial least squares. *Journal of Process Control*, 18(10):961–974, 2008.

[62] B. Köppen-Seliger. *Fehlerdiagnose mit künstlichen neuronalen Netzen*. PhD dissertation, VDI Verlag, Düsseldorf, Germany, 1997.

[63] T. Kourti and J.F. MacGregor. Process analysis, monitoring and diagnosis, using multivariate projection methods. *Chemometrics and Intelligent Laboratory Systems*, 28(1):3–21, 1995.

[64] J.V. Kresta, J.F. MacGregor, and T.E. Marlin. Multivariate statistical monitoring of process operating performance. *Canadian Journal of Chemical Engineering*, 69 (1):35–47, 1991.

[65] U. Kruger and G. Dimitriadis. Diagnosis of process faults in chemical systems using a local partial least squares approach. *AIChE Journal*, 54(10):2581–2596, 2008.

[66] W. Ku, R.H. Storer, and C. Georgakis. Disturbance detection and isolation by dynamic principal component analysis. *Chemometrics and Intelligent Laboratory Systems*, 30(1):179–196, 1995.

[67] W.E. Larimore. Canonical variate analysis in identification, filtering and adaptive control. In *Proceedings of the 29th IEEE Conference on Decision and Control*. Honolulu, Hawaii, USA, 1990.

[68] M. Laser. Recent safety and environmental legislation. *Transactions IChemE*, 78 (B):36–45, 2000.

[69] G. Lee, C.H. Han, and E.S. Yoon. Multiple-fault diagnosis of the Tennessee Eastman process based on system decomposition and dynamic PLS. *Industrial and Engineering Chemistry Research*, 43(25):8037–8048, 2004.

[70] J.-M. Lee, S.J. Qin, and I.-B. Lee. Fault detection and diagnosis based on modified independent component analysis. *AIChE Journal*, 52(10):3501–3514, 2006.

[71] J.M. Lee, C. Yoo, and I.B. Lee. Fault detection of batch processes using multiway kernel principal component analysis. *Computers and Chemical Engineering*, 28(9): 1837–1847, 2004.

[72] J.M. Lee, C. Yoo, and I.B. Lee. Statistical process monitoring with independent component analysis. *Journal of Process Control*, 14(5):467–485, 2004.

[73] T. Lee. *Independent Component Analysis: Theory and Applications*. Kluwer Academic, Boston, MA, 1998.

[74] G. Li, S.J. Qin, and D.H. Zhou. Geometric properties of partial least squares for process monitoring. *Automatica*, 46(1):204–210, 2010.

[75] W. Li and S.J. Qin. Consistent dynamic PCA based on errors-in-variables subspace identification. *Journal of Process Control*, 11(6):661–678, 2001.

[76] W. Li, H. Yue, S. Valle-Cervantes, and S.J. Qin. Recursive PCA for adaptive process monitoring. *Journal of Process Control*, 10(5):471–486, 2000.

[77] L. Ljung. *System Identification: Theory for the User*. Prentice Hall, Englewood Cliffs, New Jersey, 1987.

[78] M. Lovera, T. Gustaffson, and M. Verhaegen. Recursive subspace identification of linear and non-linear wiener state-space models. *Automatica*, 36(11):1639–1650, 2000.

[79] J.F. MacGregor. Statistical process control of multivariate processes. *Control Engineering Practice*, 3(3):403–414, 1995.

[80] J.F. MacGregor, C. Jaeckle, C. Kiparissides, and M.Koutoudi. Process monitoring and diagnosis by multiblock PLS methods. *AIChE Journal*, 40(5):826–838, 1994.

[81] G.J. McLachlan. *Discriminant Analysis and Statistical Pattern Recognition*. Wiley Interscience, Hoboken, NJ, USA, 2004.

[82] G. Mercere, L. Bako, and S. Lecoeuche. Propagator-based methods for recursive subspace model identification. *Signal Processing*, 88(3):468–491, 2008.

[83] A.S. Naik, S. Yin, and S.X. Ding. Recursive identification algorithm for parity space based fault detection systems. In *Proceedings of the 7th IFAC Symposium on Fault Detection and Supervision and Safety of Technical Processes*, Barcelona, Spain, 2009.

[84] A.S. Naik, S. Yin, S.X. Ding, and P. Zhang. Recursive identification algorithms to design fault detection systems. *Journal of Process Control*, 20(8):957–965, 2010.

[85] I. Nimmo. Adequately address abnormal situation operations. *Chemical Engineering Progress*, 91(9):36–45, 1995.

[86] P. Nomikos and J.F. MacGregor. Multivariate SPC charts for monitoring batch processes. *Technometrics*, 37:41–59, 1995.

[87] P. Van Overschee and B. De Moor. *Subspace Identification for Linear Systems*. Kluwer Academic Press, Dordrecht, 1996.

[88] R.J. Patton, P.M. Frank, and R.N. Clark. *Issues of Fault Diagnosis for Dynamic Systems*. Springer Verlag, Berlin, 2000.

[89] S.J. Qin. Recursive PLS algorithms for adaptive data modeling. *Computers and Chemical Engineering*, 22(4-5):503–514, 1998.

[90] S.J. Qin. Statistical process monitoring: basics and beyond. *Journal of Chemometrics*, 17(8-9):480–502, 2003.

[91] S.J. Qin. An overview of subspace identification. *Computers and Chemical Engineering*, 30(10-12):1502–1513, 2006.

[92] S.J. Qin. Data-driven fault detection and diagnosis for complex industrial processes. In *Proceedings of the 7th IFAC Symposium on Fault Detection and Supervision and Safety of Technical Processes*, Barcelona, Spain, 2009.

[93] S.J. Qin and W. Li. Detection and identification of faulty sensors in dynamic processes. *AIChE Journal*, 47(7):1581–1593, 2001.

[94] S. Rännar, J.F. MacGregor, and S. Wold. Adaptive batch monitoring using hierarchical PCA. *Chemometrics and Intelligent Laboratory Systems*, 41(1):73–81, 1998.

[95] N.L. Ricker. Decentralized control of the Tennessee Eastman challenge process. *Journal of Process Control*, 6(4):205–221, 1996.

[96] E. Russell, L. Chiang, and R.D. Braatz. *Data-driven Methods for Fault Detection and Diagnosis in Chemical Processes*. Springer Verlag, London, 2000.

[97] W. Shewhart. *Statistical Method from the Viewpoint of Quality Control*. Dover Publications, 1986.

[98] S. Simani, C. Fantuzzi, and R.J. Patton. *Model-Based Fault Diagnosis in Dynamic Systems Using Identification Techniques*. Springer Verlag, Secaucus, New Jersey, USA, 2002.

[99] G.W. Steward. *Matrix Perturbation Theory*. Academic Press, San diago, 1990.

[100] G. Tao. *Adaptive Control Design and Analysis*. Wiley Interscience, Hoboken, New Jersey, USA, 2003.

[101] N. Thornhill, S. Patwardhan, and S. Shah. A continuous stirred tank heater simulation model with applications. *Journal of Process Control*, 18(3-4):347–360, 2008.

[102] N.D. Tracy, J.C. Young, and R.L. Mason. Multivariate control charts for individual observations. *Journal of Quality Technology*, 24(2):88–95, 1992.

[103] S. Valle, W. Li, and S.J. Qin. Selection of the number of principal components: the variance of the reconstruction error criterion with a comparison to other methods. *Industrial and Engineering Chemistry Research*, 38(11):4389–4401, 1999.

[104] P. Van Overschee and B. De Moor. N4SID: subspace algorithms for the identification of combined deterministic-stochastic systems. *Automatica*, 30(1):75–93, 1994.

[105] P. Van Overschee and B. De Moor. *Subspace Identification for Linear Systems*. Kluwer Acadamic Publishers, USA, 1996.

[106] V. Venkatasubramanian, R. Rengaswamy, K. Yin, and S.N. Kavuri. A review of process fault detection and diagnosis. Part I: Quantitative model-based methods. *Computers and Chemical Engineering*, 27(3):293–311, 2003.

[107] V. Venkatasubramanian, R. Rengaswamy, K. Yin, and S.N. Kavuri. A review of process fault detection and diagnosis: Part II: Qualitative models and search strategies. *Computers and Chemical Engineering*, 27(3):313–326, 2003.

[108] V. Venkatasubramanian, R. Rengaswamy, K. Yin, and S.N. Kavuri. A review of process fault detection and diagnosis: Part III: Process history based methods. *Computers and Chemical Engineering*, 27(3):327–346, 2003.

[109] M. Verhaegen and P. Dewilde. Subspace model identification. Part I: the output-error state-space model identification class of algorithms. *International Journal of Control*, 56(5):1187–1210, 1992.

[110] J. Wang and S.J. Qin. A new subspace identification approach based on principal component analysis. *Journal of Process Control*, 12(8):841–855, 2002.

[111] J. Wang and S.J. Qin. Closed-loop subspace identification using the parity space. *Automatica*, 42(2):315–320, 2006.

[112] Z. Wang, B. Huang, and K. Burnham. Stochastic reliable control of a class of uncertain time-delay systems with unknown nonlinearities. *IEEE Transactions on Circuits and Systems - Part I*, 48(5):646–650, 2001.

[113] Z. Wang, D.W.C. Ho, and X. Liu. State estimation for delayed neural networks. *IEEE Transactions on Neural Networks*, 16(1):279–284, 2005.

[114] Z. Wang, Y. Liu, M. Li, and X. Liu. Stability analysis for stochastic cohen-grossberg neural networks with mixed time delays. *IEEE Transactions on Neural Networks*, 17(3):814–820, 2006.

[115] Z. Wang, G. Wei, and G. Feng. Reliable H-infinity control for discrete-time piecewise linear systems with infinite distributed delays. *Automatica*, 45(12):2991–2994, 2009.

[116] T. Willink. Efficient adaptive SVD algorithm for MIMO applications. *IEEE Transactions on Signal Processing*, 56(2):615 –622, 2008.

[117] A. Willsky. A survey of design methods for failure detection in dynamic systems. *Automatica*, 12:601–611, 1984.

[118] A. Willsky and H.L. Jones. A generalized likelihood ratio approach to the detection and estimation of jumps in linear systems. *IEEE Transactions on Automatic Control*, 21(1):108–112, 1976.

[119] B.M. Wise and N.B. Gallagher. The process chemometrics approach to process monitoring and fault detection. *Journal of Process Control*, 6(6):329–348, 1996.

[120] S. Wold, M. Sjöström, and L. Eriksson. PLS-regression: a basic tool of chemometrics. *Chemometrics and Intelligent Laboratory Systems*, 58(2):109–130, 2001.

[121] B. Yang. Projection approximation subspace tracking. *IEEE Transactions on Signal Processing*, 43(1):95–107, 1995.

[122] J.-F. Yang and M. Kaveh. Adaptive eigensubspace algorithms for direction or frequency estimation and tracking. *IEEE Transactions on Acoustics, Speech and Signal Processing*, 36(2):241–251, 1988.

[123] Y. Yao, T. Chen, and F. Gao. Multivariate statistical monitoring of two-dimensional dynamic batch processes utilizing non-Gaussian information. *Journal of Process Control*, 20(10):1188–1197, 2010.

[124] S. Yin, A.S. Naik, and S.X. Ding. Adaptive process monitoring based on parity space method. In *Proceedings of the 7th IFAC Symposium on Fault Detection and Supervision and Safety of Technical Processes*, Barcelona, Spain, 2009.

[125] S. Yin, A.S. Naik, and S.X. Ding. Data-driven design of fault diagnosis scheme for periodic systems. In *Proceedings of the 7th Workshop on Advanced Control and Diagnosis*, Zielona Gora, Poland, 2009.

[126] S. Yin, S.X. Ding, A.S. Naik, P. Deng, and A. Haghani. On PCA-based fault diagnosis techniques. In *Proceedings of the Conference on Control and Fault-Tolerant Systems*, Nice, France, 2010.

[127] S. Yin, S.X. Ding, A. Hagahni, and H. Hao. Data-driven monitoring for stochastic systems and its application on batch process. *Accepted by International Journal of System Science*, 2011.

[128] S. Yin, S.X. Ding, A. Hagahni, H. Hao, and P. Zhang. A comparison study of basic data-driven fault diagnosis and process monitoring methods on the benchmark Tennessee Eastman process. *Submitted to Journal of Process Conrol*, 2011.

[129] S. Yin, S.X. Ding, P. Zhang, A. Haghani, and A.S. Naik. Study on modifications of PLS approach for process monitoring. In *Proceedings of the 18th IFAC World Congress*, Milano, Italy, 2011.

[130] S. Yoon and J.F. MacGregor. Statistical and causal model-based approaches to fault detection and isolation. *AIChE Journal*, 46(9):1813–1824, 2000.

[131] P. Zhang and S.X. Ding. On fault detection in linear discrete-time, periodic, and sampled-data systems (survey). *Journal of Control Science and Engineering*, 2008: 1–19, 2008.

[132] Q.H. Zhang. Adaptive observer for multiple-input-multiple-output (MIMO) linear time-varying systems. *IEEE Transaction on Automatic Control*, 47(3):525–529, 2002.

[133] Y.W. Zhang and Y. Zhang. Fault detection of non-Gaussian processes based on modified independent component analysis. *Chemical Engineering Science*, 65(16): 4630–4639, 2010.

[134] D. Zhou, G. Li, and S.J. Qin. Total projection to latent structures for process monitoring. *AIChE Journal*, 56(1):168–178, 2010.